EFFECTS OF RHEOLOGY ON THE SMOOTH ELECTROSPUN NANOFIBER
PRODUCTION FROM PECTIN FOR THE DEVELOPMENT OF PACKAGING
MATERIALS

by
Büşra Akınalan Balık

Submitted to Graduate School of Natural and Applied Sciences
in Partial Fulfillment of the Requirements
for the Doctor of Philosophy in
Biotechnology

Yeditepe University
2019

EFFECTS OF RHEOLOGY ON THE SMOOTH ELECTROSPUN NANOFIBER PRODUCTION FROM PECTIN FOR THE DEVELOPMENT OF PACKAGING MATERIALS

APPROVED BY:

Assist. Prof. Dr. Sanem Argın   ....
(Thesis Supervisor)
(Yeditepe University)

Prof. Dr. Mustafa Özilgen   ....
(Yeditepe University)

Assoc. Prof. Dr. Filiz Altay   ....
(İstanbul Technical University)
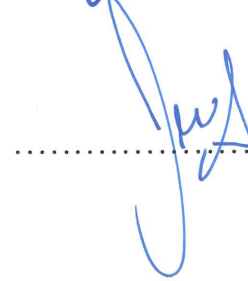
Assist. Prof. Dr. Aslı Can Karaça   ....
(İstanbul Technical University)

Assist. Prof. Dr. Cem Levent Altan   ....
(Yeditepe University)

DATE OF APPROVAL: ..../..../2019

ACKNOWLEDGEMENTS

I would like to extend my deepest gratitude to my dissertation advisor Assist. Prof. Sanem Argın for her endless support in broadening my mind and presenting unlimited source of learning. Her never-ending motivation and energy took me one step further not only for academic life, but also in finding myself. You will always be my role model.

I also would like thank to my dissertation committee for all of their guidance through this process; your suggestions, ideas, and feedback have been absolutely invaluable.

Many thanks to my colleagues, M.Sc. Ceren Uğurlu, M.Sc. Selcen Semerciöz, M.Sc. Dilay Şen, M.Sc. Gizem Özan and Dr. Bahar Hazal Yalçınkaya for those memorable days. It was a great pleasure to work with you all. Thanks should also go to our laboratory technician and my dear friend Selma Aka Dinç.

I would like to express my sincere appreciation to Prof. Lagaron for accepting me to his research group of Novel Materials and Nanotechnology in IATA, CSIC, Spain. Within very short time I gained very valuable experiences. I must also thank to Dr. Sergio Torres-Giner, Dr. Cristina Prieto López, Beatriz Meléndez Rodríguez and Alberto Rodriguez for their help, support and sincere friendship during my visit.

Special thanks should be delivered to my dear parents Nilgün and İsmet Akınalan for supporting me whole of my life and for their profound belief in my studies. I am also very grateful to the existence of rest of my family, we will always be the greatest team of the world!

Finally, I would like to express my deepest appreciation to my dear husband, Erdem Balık, for always loving, protecting and supporting me. I love you to the moon and back.

ABSTRACT

EFFECTS OF RHEOLOGY ON THE SMOOTH ELECTROSPUN NANOFIBER PRODUCTION FROM PECTIN FOR THE DEVELOPMENT OF PACKAGING MATERIALS

Electrospinning is known to be the most convenient, easy and efficient nanofiber production method. Determining the important parameters necessary for the prediction of a successful electrospinning process from solution properties is essential, yet, not easy in the case of biopolymers due to their distinct natures. As the first objective, the effect of rheological parameters, namely zero shear viscosity, tip viscosity, elastic modulus, phase angle, cohesive energy, on the formation of smooth pectin nanofibers was evaluated simultaneously. Low methyl esterified amidated pectin solutions at different concentrations were blended with polyethylene oxide (PEO) at different molecular weights. Non-beaded nanofibers were obtained only when PEO_{2000} was used in the blends. Our results showed that (1) the viscosity of the solution is not an indication of jet formation, but once the jet is formed, high zero shear viscosity and high tip viscosity are required to maintain a dominant whipping instability for smooth nanofiber formation and (2) while evaluating the elasticity of the spinning solutions, comparing only the elastic modulus values would be misleading, since low phase angle values are also necessary for pectin solutions to be electrospun into nonbeaded fibers. As the second objective, obtained pectin nanofibers were used to develop a food packaging material. Plasticizer added fibers were subjected to annealing, to obtain homogenous and transparent films with reduced porosity. The annealing conditions (temperature, time and applied load) were optimized for each electrospun mat. Addition of plasticizer was found to be crucial to accomplish homogenous films. The results showed that the 30 wt. percent glycerol-containing fibers coalesced more easily at $140\ ^{o}C$ and under 12 kN for 1 minute to form films with lower porosity and higher transparency. The optimal pectin-based film was, finally, applied as an inner-layer in a multilayer structure based on two external electrospun layers of poly(3-hydroxybutyrate-co-3-hydroxyvalerate). The barrier properties of the multilayers showed that the resultant biopolymer multilayer films can be considered as promising materials to be utilized for food packaging applications.

ÖZET

AMBALAJ MALZEMELERİNİN GELİŞTİRİLMESİ İÇİN PEKTİNDEN DÜZ ELEKTROSPUN NANOLİF ÜRETİMİNDE REOLOJİNİN ETKİLERİ

Elektro-eğirme, en kolay, verimli ve elverişli nanolif üretim yöntemi olarak bilinmektedir. Çözelti özelliklerinden başarılı bir elektrospinleme işleminin öngörülmesi için gerekli olan önemli parametrelerin belirlenmesi esastır, ancak, biyopolimerlerde, farklı doğaları nedeniyle kolay değildir. İlk amaç olarak, sıfır kayma viskozitesi, uç viskozitesi, elastik modül, faz açısı, yapışma enerjisi gibi reolojik parametrelerin pectin nanoliflerin oluşma üzerine etkisi incelenmiştir. Farklı konsantrasyonlarda düşük metil esterleştirilmiş amidatlanmış pektin, farklı molekül ağırlığında polietilen oksitle (PEO) karıştırıldı. Sonuçlarımız (1) çözeltinin viskozitesinin bir jet oluşumunun göstergesi olmadığını, ancak jet oluşturulduktan sonra, pürüzsüz nanofiber oluşumu için baskın bir çırpma dengesizliğini korumak için yüksek sıfır kesme viskozitesi ve yüksek uç viskozitesinin gerekli olduğunu (2) eğirme çözeltilerinin esnekliğini değerlendirirken, sadece elastik modül değerlerini karşılaştırmanın yanıltıcı olacağını, çünkü düşük faz açısı değerleri de pektin çözeltilerinin boncuksuz lifler halinde elektrostatik hale getirilmesi için gerekli olduğunu göstermiştir. İkinci amaç olarak, elde edilen pektin nano lifleri gıda paketleme malzemesi geliştirmek için kullanıldı. Plastikleştirici eklenmiş lifler, gözenekliliği azaltılmış homojen ve saydam filmler elde etmek için tavlama olarak da adlandırılan bir ısıl işlemden geçirilmiştir. Tavlama şartları (sıcaklık, zaman ve uygulanan yük) her elektro-eğrilmiş yüzey için optimize edilmiştir. Plastikleştirici ilavesinin homojen film elde etmek için belirleyici olduğu görülmüştür. Sonuçlar, yüzde 30 gliserol içeren liflerin, 1 dakika boyunca 140 °C, 12 kN altında daha kolay bir şekilde kaynaştığını ve daha düşük gözeneklilik ve daha yüksek şeffaflığa sahip filmler oluşturduğunu gösterdi. Son olarak, optimize edilmiş şartlarda üretilen pektin temelli filmler, elektro-eğrilmiş poli(3-hidroksibutirat-ko-3-hidroksivalerat) (PHBV) film arasına ara katman olarak uygulanarak çok katmanlı yapıda bir film elde edildi. Ortaya çıkan çok katmanlı biyopolimer filmlerin bariyer özellikleri, gıdaların raf ömrünü uzatmak için gıda ambalajlama uygulamalarında kullanılabileceğini göstermiştir.

TABLE OF CONTENTS

LIST OF FIGURES

LIST OF TABLES

LIST OF SYMBOLS/ABBREVIATIONS

γ_{cr}	Critical strain
Δ	Phase angle
λ_p	Relaxation time
φ_p	Volume fraction
C	Concentration
C_e	Entanglement concentration
C*	Overlap concentration
G'	Elastic modulus
G''	Viscous modulus
N	Flow behavior index
n_e	Entanglement number
Q	Volumetric flow rate
t^*	Characteristic time
w_{max}	Growth rate
DE	Degree of esterification
De	Deborah number
DSC	Differential scanning calorimetry
FT IR	Fourier transform infrared spectroscopy
LM	Low methyl esterified
LVR	Linear viscoelastic region
M_e	Entanglement molecular weight
M_w	Molecular weight
Nm	Nanometer
PEG	Poly(ethylene glycol)
PEO	Poly(ethylene oxide)
PLA	Poly(lactic acid)
PHB	Poly (hydroxybutyrate)

PHBV	Poly (3-hydroxybutyrate-co-3-hydroxyvalerate)
PVOH	Poly(vinyl alcohol)
PVP	Poly(vinylpyrrolidone)
SEM	Scanning electron microscope
SFT	Surface tension
TGA	Thermogravimetric analysis

1. INTRODUCTION

Nanotechnology, which refers to the area of developing or synthesizing materials, objects or structures where at least one of their dimensions is 1-100 nm, has been one of the most important sciences growing rapidly in recent years[1]. The capability of developing novel and advanced materials with functional properties provides a huge attraction to nanotechnology in different engineering and technological fields. Nanomaterials can exist as nanoparticles, nanorods, nanotubes, nanodiscs, nanoplates or nanofibers. While nanoparticles are zero-dimensional structures, existing as the simplest form of nanomaterials, nanotubes, nanorods or nanofibers are more developed assemblies, which are stood as one-dimensional structures[2]. Amongst these structures, nanofibers have been one of the most studied subjects in the recent years owing to their unique properties including large surface-to-volume ratio, flexibility for adapting a variety of sizes and shapes, superior mechanical performances and extremely porous structure. Nanofibers can be applied to different disciplines including textile, health, security, automotive and food industries as seen in Figure 1.1.

Nanofibers can be obtained from both natural based and synthetic polymers. So far, self-assembly[3], phase separation[4], melt blowing[5], spunbond, template synthesis[6] and electrospinning techniques have been utilized for the production of nanofibers. Self-assembled materials suggest a variety of ready-made nanostructures for research and technological applications. In this process, the components assemble themselves and bind building blocks individually into desired structure[4, 7]. Phase separation consists of many steps including dissolution, gelation, isolation, freezing and drying in order to convert polymers into nano-porous foam. So, even it is preferable in some cases, this process is unwanted because of taking a serious time. Melt blowing and spunbond are techniques that are used in industry. Melt blown is considerably old techniques that contain one or more jets of gas, air, to reduce molten polymer streams into nano-scale filaments. However, these processes allow working only with thermoplastics[5, 8]. A nanoporous material is used as a model for obtaining nanofibers in template synthesis method, but the continuity is the main problem for this method.
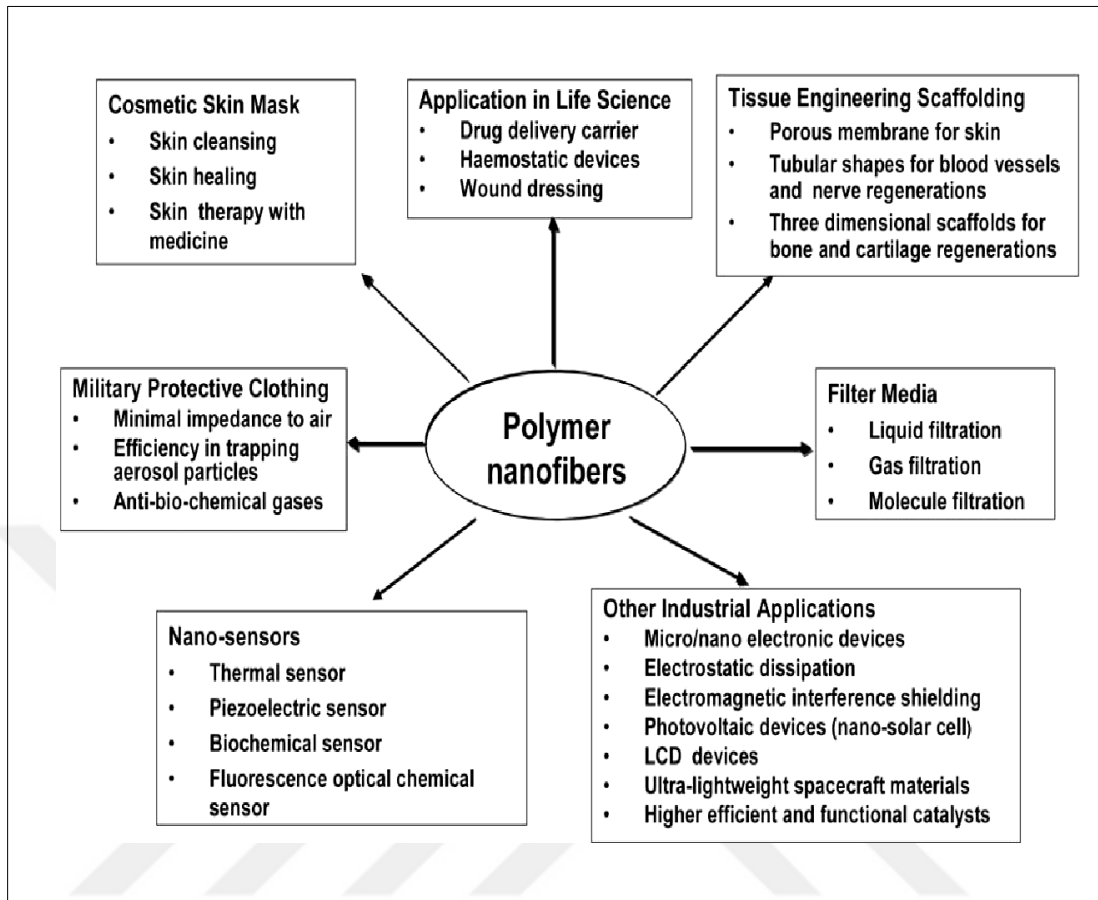
Figure 1.1. The possible applications of nanofibers[12].

1.1. ELECTROSPINNING

Electrostatic spinning, or electrospinning, is a fiber forming technique that uses electrostatic forces to convert polymer solution or melt into fine jets, afterwards to fibers that having diameters of sizes in nano or submicron. This technique provides working with single polymer solutions or melts, emulsions, polymer blends or composites. Nanofibers with different cross sectional morphologies, porosities and varying fiber diameters can be obtained by electrospinning technique[9]. Therefore, electrospinning has been pointed as the most time efficient, straightforward, versatile and economical one compared to other nanofiber production methods[10, 11].

1.1.1. Background of Electrospinning

Electrospinning was firstly introduced at the end of the 19th century by Rayleigh. Then, it was developed more comprehensively by Zeleny[12] in 1914, while patented as a valid technique by Formhals in 1934[13, 14]. In his patent, he introduced a technique that exists a capability of collecting polymer filaments by the help of electrostatic repulsions. Later, Formhals developed his invention and published several more patents which describe the formation of polymer fibers by using electrostatic force until 1944. He succeeded spinning of cellulose acetate filaments from acetone/alcohol solution[15]. He has also published his new work related to composite fiber production in 1940[16]. However, the industrialized usage of electrospinning was firstly seen in 1990's[17]. This technique used to be well known in textile sector in the production of nonwoven fabric for a long time.

While the simplicity, versatility and wide uses of this process were discovered, the number of studies and publications that are related to electrospinning has been increased significantly in the recent years. There has been respectable number of studies regarding to process mechanism, modeling of effecting factors, characterization of fibers in terms of characterization and application. Now, the application of electrospun nanofibers has been prolonged to varying fields including biomedical, military, energy and food applications.

1.1.2. Electrospinning Set up and Principle

Basically, electrospinning is a simple, versatile and easy fiber producing method that utilizes electrical forces. An adjustable voltage supplier, usually until 30 kV and working in DC mode, is used to charge liquid, polymer melt or solution, to create fibers.

Fibers are obtained with a diameter ranging from tens of nanometer to a number of micrometers by drawing polymer solution or melt into fine jets, followed by collecting them on a grounded collector. Different configurations of electrospinning setup exist depending on the structure of desired final product. The system can be set as either horizontal or vertical as seen in Figure 1.2. Typically, there are three main constituents of electrospinning systems:

- A blunt-ended stainless steel capillary that leads polymer to come out. The capillary is attached to a syringe and the flow rate of solution is altered by a syringe pump.

- An adjustable high voltage power supply.

- A ground collector which can be either a rotating drum or a flat surface. Type of collector defines the tailoring of fibers.
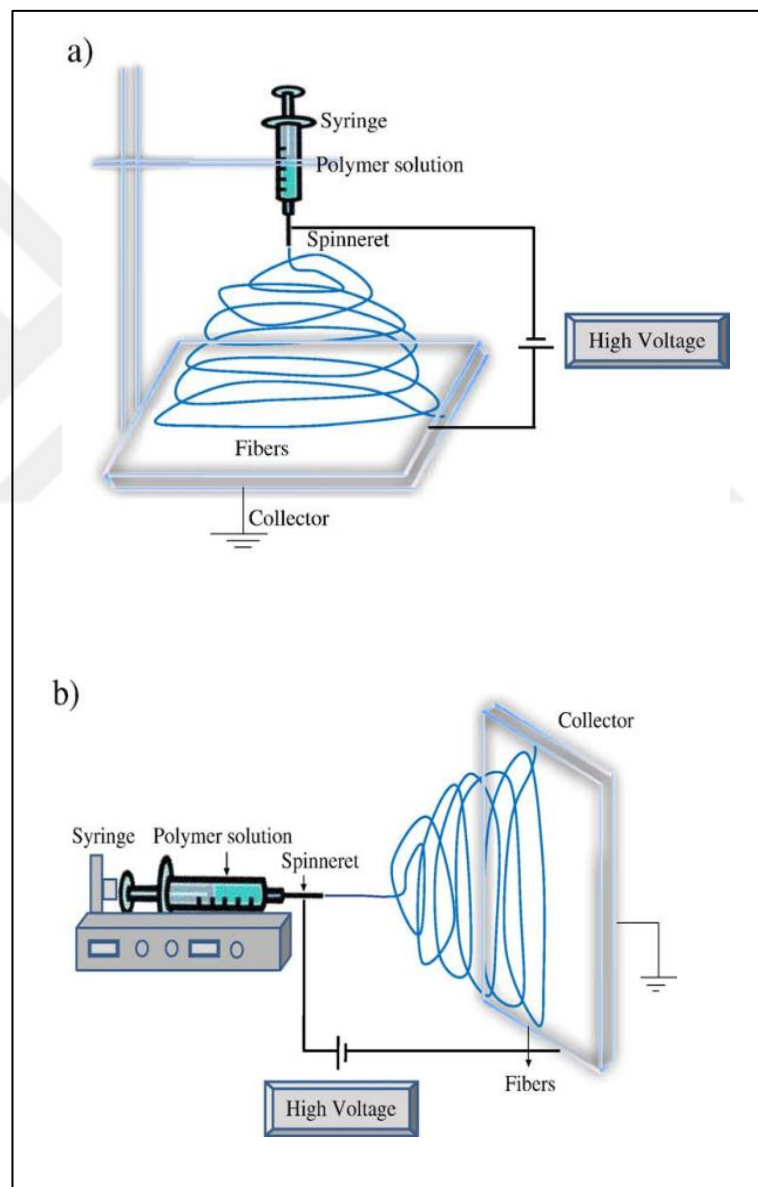
Figure 1.2. A representative illustration of a typical (a) vertical and (b) horizontal set up electrospinning apparatus[18].

Some modifications depending on the needs can be applied to basic electrospinning setup. The conventional electrospinning process includes a single nozzle, or capillary, as the spinneret, which results to a low yield of product in each run of the machine. The limitation of production scales obstructs the industrialization of produced fibers in the commercial market, also the replacement of existing technology with electrospinning. Thus, multi-nozzle spinneret systems have been developed in order to increase the production capacity where a high yield of product is desired[19, 20]. This system comprises side by side arrangement of multiple capillaries, while they offer a facility to obtain physically well mixed nanofibers on the collector. Also, needless electrospinning systems are available, which suggest the technology that the polymer solution is ejected from a free surface. Besides scaling up the production rate, it is possible to overcome clogging issues by using needless electrospinning. Different types of needless electrospinning have been shown up in the literature such as, bubble electrospinning, hollow tube, roller electrospinning, wire electrode and slit surface electrospinning[21].

The coaxial feeding systems have been introduced by several researchers in order to create core and shell fiber structures[22-24]. The production of compound nanofibers from different synthetic polymers was demonstrated by Sun et al. at the first time, where the microscopic visualization of nanofibers were presented too[25]. The basic set up of coaxial electrospinning is given in Figure 1.3[23]. It is very similar with conventional electrospinning system except for having an additional inner capillary. The inner and outer capillaries can be connected to pumps separately in order to set up different flow rates. Although the obtained nanofibers have huge potential to utilize in some areas including medical, pharmaceutical and food applications, there still have been some difficulties of using this technology. For example, the liquids have to be immiscible, since one common Taylor cone is formed at the end of the coaxial tips where the inner one was surrounded by an outer meniscus. Also, the existence of only one voltage supply obstructs the jet initiation, since the need of electrostatic repulsion forces of two solutions may differ.

Although it consists of a simple setup, the mechanism of electrospinning is quite complicated and still needed to discover. It is very crucial to understand and control the effecting parameters such as electrical voltage, solution conductivity, etc. in order to obtain desirable fibers from every different type of polymer solution. Thus, the mechanism of the

process under the sway of electrical field must be well understood. In Figure 1.4, different forces effecting polymer drop influence the jet behaviour during the process were illustrated.
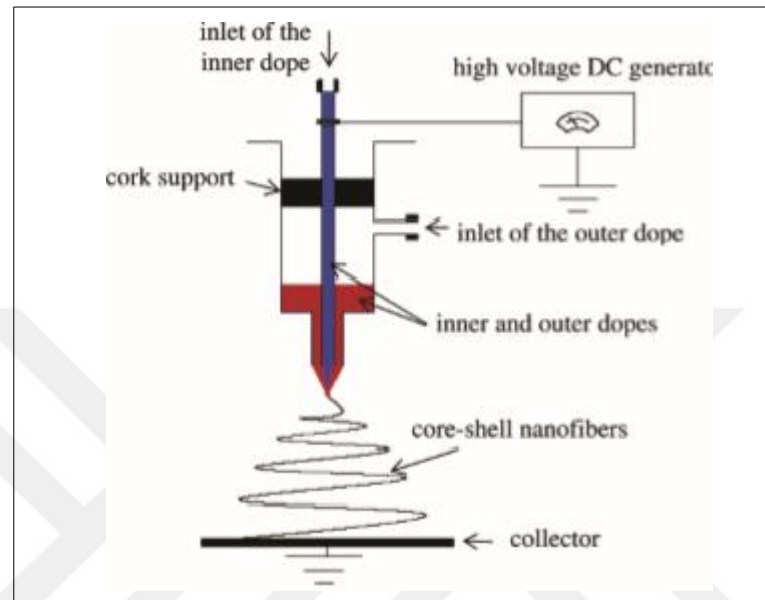
Figure 1.3. The coaxial electrospinning system[23].

Initially, the polymer drop is faced with interfacial forces (surface tension and viscosity drag) and gravitational forces without an electrical field. When the electrical force is applied, an electrical field is created between the charged syringe tip and ground collector. Once the polymer is charged, it stretches and orients in the opposite direction of surface tension because of the Columbic repulsion force. If the electrical field is generated in a critical value, a conical shape known as Taylor cone is formed and jet is ejected from Taylor cone.

The term "Taylor cone" was first suggested in 1969 by Taylor, investigating the behaviour of polymer drops at the end of capillary in which identifies the "cone" shape[27]. When the electrical field is increased, a jet is produced where the Taylor cone ends. The electrical field takes the jet to the surface of the collector by "whipping instability". Polymer chains in the jet are expected to stretch and orient when solvent evaporates rapidly. The jet behaves instable when stretching begins; it is only stable at the tip of the capillary, which is formed in cone shape as seen in Figure 1.5[28]. The formed jet is faced the forces as

mentioned above. By the help of these forces, the jet is thinned up to a point and solvent evaporates. When all the solvent is removed, the jet gathers on the collector surface.
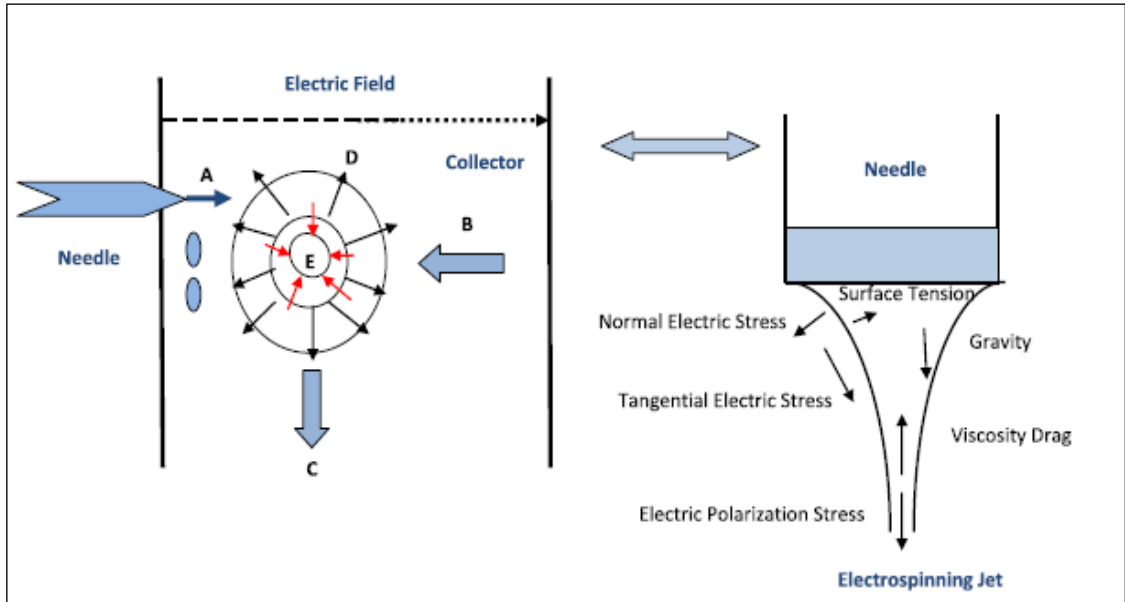
Figure 1.4. Different forces acting on polymer drop during electrospinning[26].
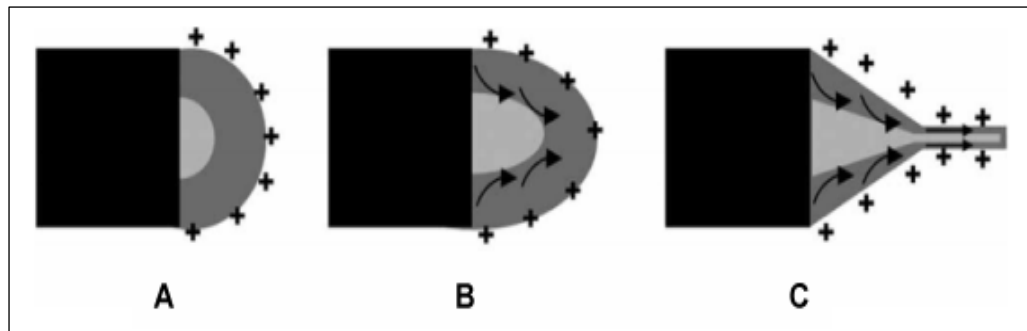
Figure 1.5. Stage by stage Taylor cone formation[28].

According to numerous numbers of studies in the literature, in order to obtain ideal nanofibers, the conditions that are looked for can be listed as[29]:

- ✓ Controllable and stable fiber diameter
- ✓ Defect-free or defect-controllable fiber morphologies

✓ Collectable nanofiber mats.

In order to acquire these requirements, it is very crucial to understand how the solution properties and process factors will effect on the fiber formation, also the morphology of fibers. The viscosity of the fiber forming solution is found to be critical for jet initiation and stabilization[30, 31]. Besides, the conductivity and the surface tension of the solution as well as the solvent volatility are significant solution properties; while the processing factors as the applied voltage, the feeding rate, the distance between the needle and the collector are also important[18,19]. Temperature, humidity and atmospheric pressure should also be considered as environmental factors[17].

1.1.3. Effect of Solution Properties on Fiber Formation and Electrospun Fiber Properties

1.1.3.1. Rheological Properties

Rheology has been described as the science of flow and deformation of matter. It measures the respond of materials under applied force (stress) or deformation (strain). Rheological properties of fluids are very critical in optimizing processing materials and understanding the material behaviour. Wide-ranging studies are available in the literature that aims to understand the effect of the rheological properties, especially the viscosity, of polymer solutions on the resultant fiber formation and fiber morphology by electrospinning[32–37].

Viscosity

Viscosity of the fiber forming solution is one of the main parameter to consider for a successful electrospinning process[30, 33]. Viscosity is described as the resistance of a sample against flow and calculated as the ratio of shear stress to shear rate. The average molecular weight (M_w) and the concentration of the polymer, as well as the solvent type are the prominent factors affecting the viscosity of a polymer solution. Viscosity of the fiber forming solution is one of the factors, which determine whether the solution can be electrospun or not. For example, if the viscosity of the polymer solution is too high, the applied electrical field may not be enough to eject the solution from capillary.

When the same polymer solution is considered, the jet ends up with particles, bead-on-string structure or non-beaded fibers depending on the polymer concentration. If the concentration of polymer is not sufficiently high or the polymer chains are too short (low M_w), jet stability cannot be maintained, so the jets break into droplets as a result of Rayleigh instability mechanism as can be seen in Figure 1.6. This process is called as "electrospraying" and "particles", instead of fibers, are obtained at the end of this process. Electrospinning and electrospraying are mentioned as "sister" systems with having dissimilarity only in the molecular cohesion in feeding polymers, which can be optimized by concentration[1, 26]. Spherical micro-particles can be obtained by electrospraying, while very long nanofibers are obtained in electrospinning. The electrosprayed micro-particles also have found place to utilize in some applications, especially drug delivery, coating and encapsulation or stabilization[38–40].
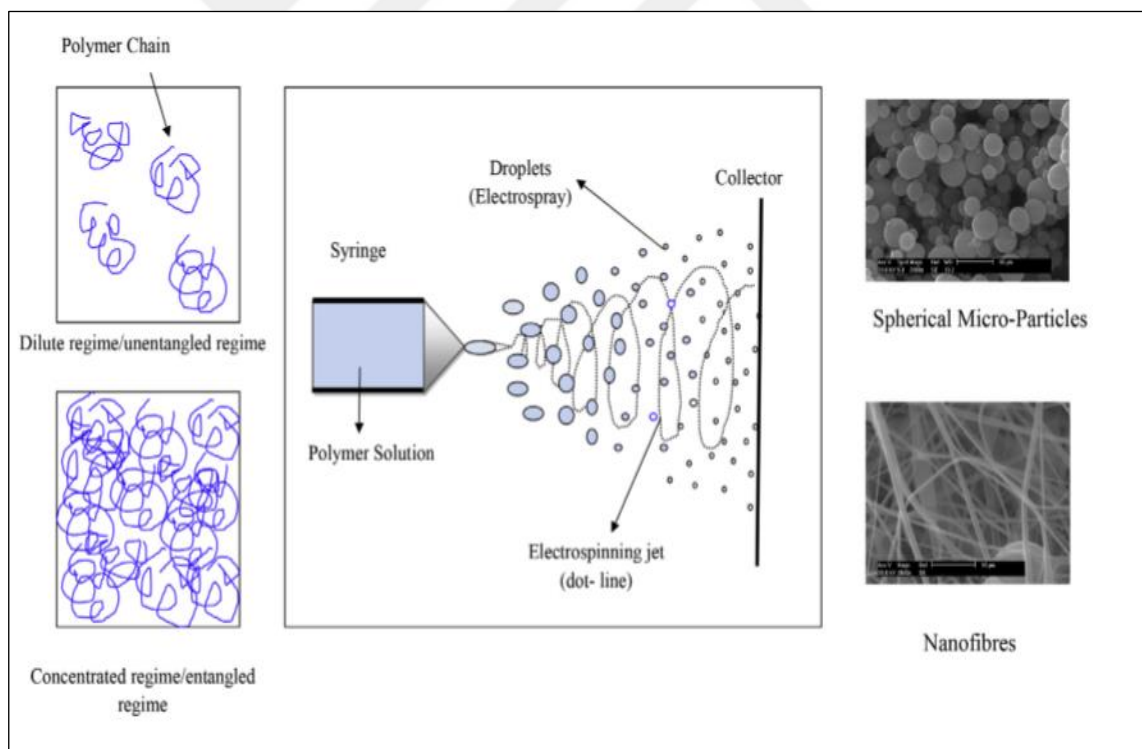
Figure 1.6. Electrospinning (down) and electrospraying (up) processes[26].

The bead-on-string structure is another type of result that comes from the electrospinning process. The term of "bead" signifies the defects on fiber structure and the bead formation

on fiber is a common problem that needs to be solved. The exact reason of obtaining only beads or beads-on-string formation instead of non-beaded and smooth electrospun fiber production is still being researched. According to Kriegel et al.[17], the existence and the amount of entanglements, that changes the viscosity, are important to preserve stability of jet. If flexible random coil chains are long enough, they form bridges by forming loops on themselves (Figure 1.7). Entanglements can be defined as the network of these bridges also the contacts between mean paths of the molecular chains[41, 42].
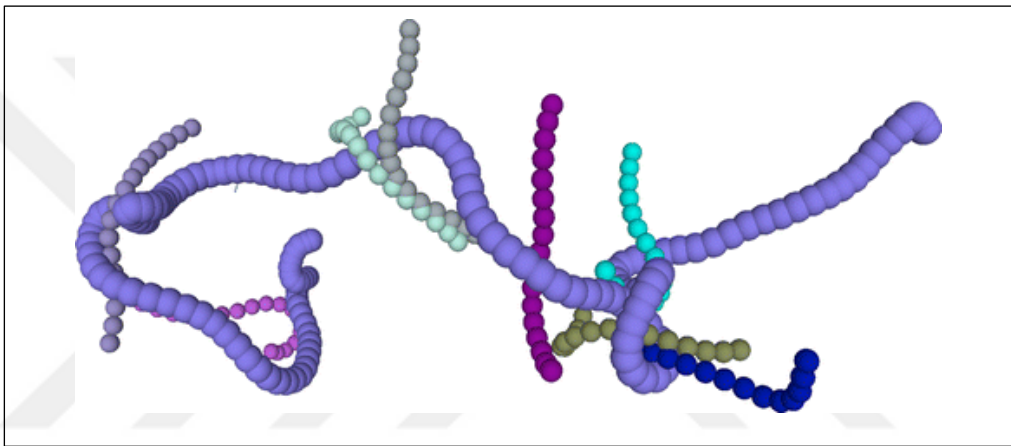
Figure 1.7. The entangled polymer chains[41].

If the polymer chains in the solution are not entangled, the possibility of observing continuous and homogenous fiber formation becomes impossible; instead, droplet falling or beaded fiber formation may be observed[32]. During electrospinning process, a solution jet is expelled from Taylor cone with the aid of high voltage and it reaches to the collector. At this stage, the jet stretches as a result of rapid solvent evaporation, which is called as whipping or bending instability process; eventually, the fibers are aggregated on the collector. So, first, the jet stability should be maintained in order to obtain uniform, no-beaded fibers. Higher viscosities lead to higher viscoelastic forces which balance the counter forces; eventually the polymer jets do not break up and bead formation is prevented.

Chain entanglement is the physical interlocking of polymer chains which arises after chain overlap. McKee et al[34]. indicated polymer solutions are needed to be prepared two to

eight times above their entanglement concentrations to be able to electrospun successfully. The entanglement concentration of different polymers can be found in literature or calculated by different approximations. Zero shear viscosity or specific viscosity might be a measure of chain entanglement since it depends both on the molecular weight (chain length) of polymer and the concentration of solution. Zero shear viscosity gives the viscosity value of a solution in the absence of any shear force. Specific viscosity is calculated by subtracting the solvent viscosity.

Figure 1.8 shows concentration versus specific viscosity graphs of alginate at two different M_w[35]. It can be seen that, the overlap concentration (C^*), which is the first change in the slope, and the entanglement concentration (C_e), which is the second change in the slope, are much smaller for the alginate sample with higher M_w. Bonino et al.[35] reported that below the entanglement concentrations, fiber formation was not observed. Moreover, addition of PEO to the alginate solution helped fiber formation by decreasing the specific viscosity at the same alginate concentration.
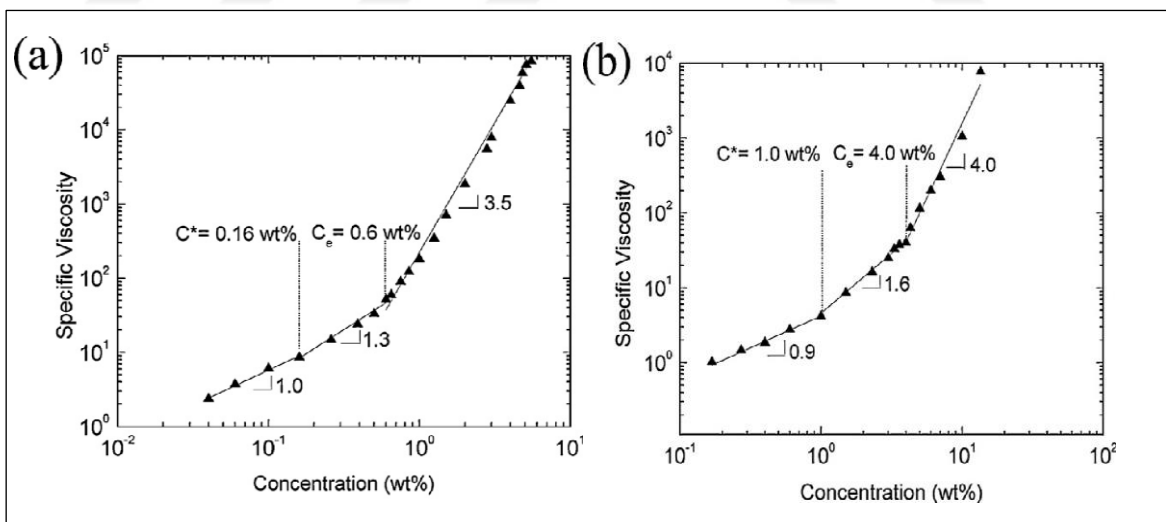
Figure 1.8. The determination of overlap concentration (C*) and entanglement concentration (C_e) for alginate-water solution in molecular weights of (a) 196 kDa (b)37 kDa alginate[35].

Below the overlap concentration (C*), a solution is in dilute regime and critical chain overlapping, thus the chain entanglement, is not present. When concentration is the same

as the overlap concentration (C*), chains start to overlap. However, at concentrations around the overlap concentration, jet stabilization might not be achieved (mixture of beads and fiber instead) if the number of chain entanglement is not sufficient. At concentrations above C*, when the number of chain entanglements is enough, the jet can be stabilized[32]. They showed a correlation between the number of chain entanglements and morphology of fibers in good solvents.

Based on their suggestion, by understanding of M_e and the M_w for a polymer, the polymer concentration that is needed to transit from electrospraying to electrospinning can be determined. While considering both concentration and molecular weight terms together, a model was developed by Shenoy et al. for medium concentrated or concentrated solutions (C>>C*), where n_e is the number of entanglements in solution and ϕ_p, is the volume fraction.

$$(n_e)sln = \frac{M_w}{(M_e)sln} = \frac{(\varphi_p M_w)}{M_e} \tag{1.1}$$

For instance, by using Equation 1, the fiber formation for polyvinylpyrrolidone (PVP) is found to begin at a concentration of 4 wt% and the bead formation is calculated to disappear at concentrations higher than 7.5 wt%. This calculation is supported by the images shown in Figure 1.9a. Later, Munir et al.[43] supported this study and developed different structural configurations for various molecular weights and concentrations of PVP. When plotting polymer concentration versus number of entanglements, the magnitude of slope is increased with molecular weight, which means less concentration is needed for bead free fiber formation as the molecular weight increases (Figure 1.9b).
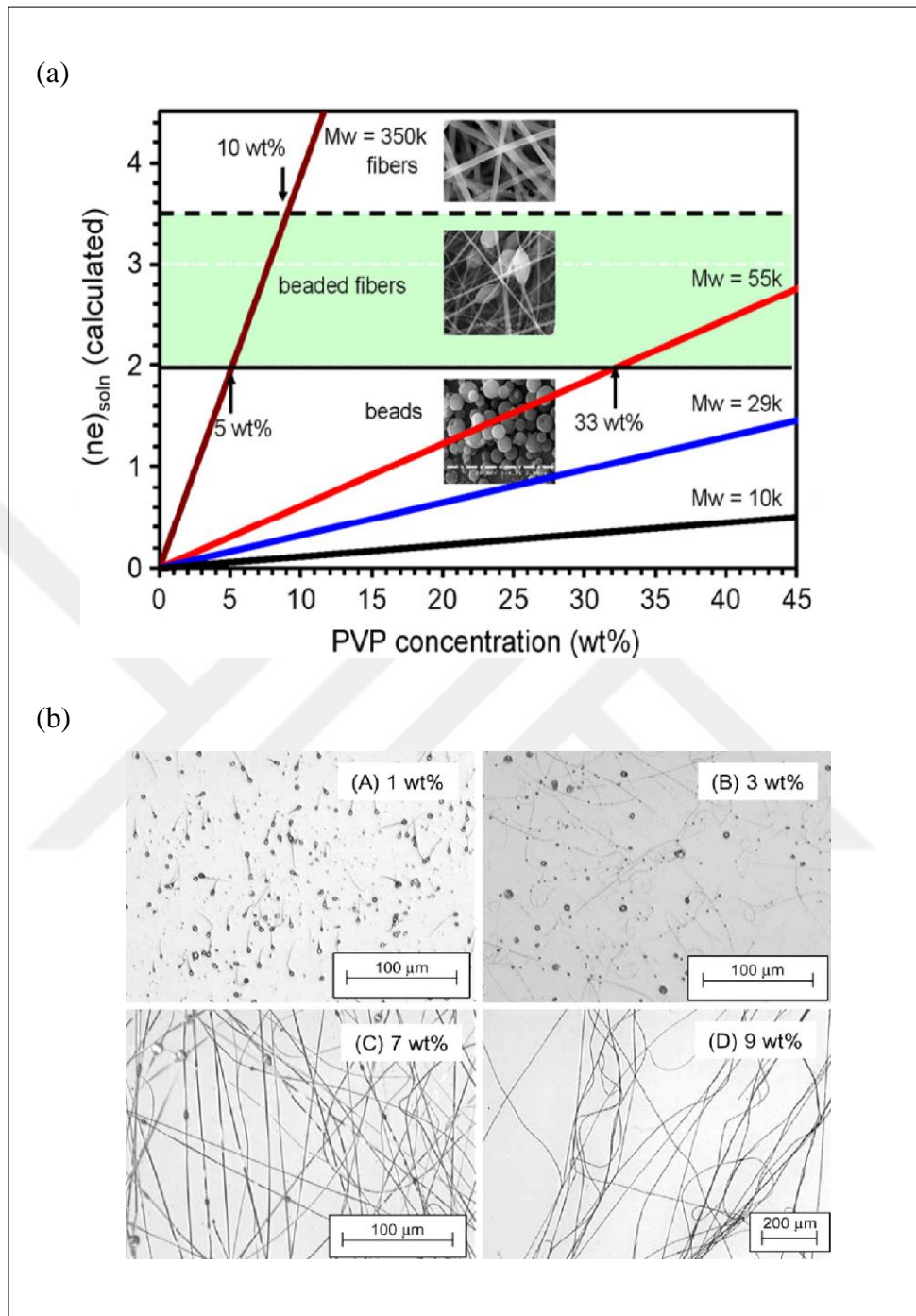
Figure 1.9. (a) Plot of PVP concentration versus entanglement number for different molecular weights of PVP and SEM images[43]. (b) Optical microscopy images of electrospun PVP (M_w=1300 kDa) fibers at concentrations of (A) 1 wt%, (B) 3 wt%, (C) 7%, (D) 9% in ethanol solution[32].

Elasticity

In the literature, it was reported that, the electrospinnable solutions require in certain amount of elasticity[31, 32, 44]. Yu et al.[44] states that uniform fibers are not formed if the polymer solution lacks elasticity, but it is not essential for solution to be entangled. For example, in the case of dilute solutions or if the polymer chains are short or rigid, it will not be possible to form a network of entanglements. However, such a problem can be overcome by adding a second polymer with a higher elasticity into the solution in order to create a network of entanglements which sequentially raises elasticity and the stability of the starting polymer which makes the solution easily spinnable. Moreover, in some fluids such as the Boger fluids, it is possible to show strong elasticity at low concentrations in the absence of entanglements if the solution relaxes in longer time than its extension. In their study, Yu et al.[44] focused on the extensional viscosity (not shear viscosity) and the assistance of fluid elasticity on the electrospinning of low concentrated polymer solutions. They used PEO and PEG at different molecular weights as aiding polymers and measured the extensional viscosity of polymer solutions using extensional rheometer.

They related uniform fiber formation to Deborah Number (D_e) which is calculated as:

$$De = \frac{\lambda_p w_{max}}{t^*} \tag{1.2}$$

where t^* indicates the characteristic time, w_{max} is the growth rate of a viscoelastic jet and λ_p is the relaxation time. If De>>1, which also means relaxation time is higher than time of different developments of instability. Consequently, capillary forces do not break the jet into drops; as an alternative, the result of bead on string is observed. If De>6, than, uniform fibers can be obtained[45].

The elasticity of electrospinning solutions were also investigated by Rosic et al.[31], Regev et al.[46] and Pelipenko et al.[47]. They were also intended to relate the results of elasticity measurements to the fiber formation. Rosic et al.[31], conducted interfacial rheological measurements for alginate and chitosan solutions which are both charged biopolymers. They have added different amounts of PEO as aiding polymer and concluded that

interfacial rheology predicts the spinnability of polyelectrolytes better than bulk rheology. On the contrary to many other studies, they stated that, electrospinnable polymer solutions must exhibit greater plasticity than elasticity to support jet stabilization. Elasticity of solution should be at minimum but it is necessary to initialize jet formation. They stated that, bulk and interface properties should be considered together, since bulk rheology is more important in the region of Taylor cone and jet initialization, on the other hand interfacial rheology is crucial for jet stabilization and continuity. Similarly, in an earlier study by Regev et al. (2010), it was demonstrated that the protein (bovine serum albumin) solution without significant bulk elasticity could be electrospun[46]. Their results suggested that interfacial parameters and adsorption kinetics are important for continuous fiber formation.

1.1.3.2. Surface Tension

Surface tension of polymer solutions is another influencing factor that decides their electrospinnability. It is affected by solvent type and composition. If the polymer solution possesses high surface tension, the bead-on-string or spindle type fibers are obtained instead of continuous fibers[48]. The aqueous solutions of biopolymers are known to have high surface tension which can create difficulties during electrospinning. Surface tension of a solution may be decreased by addition of different kinds of surfactants. Non-ionic (e.g. Tween20, Span20) and zwitterionic (e.g. lecithin) can be used as surfactants to maintain molecular organization of the structures of low M_w carbohydrate polymers[49].

1.1.3.3. Conductivity

Conductivity is a measure of charge carrying capacity for solutions. Most of the polymers are in conductive characteristics except the dielectric materials[18]. The conductivity can be altered by solvent type, polymer type, and presence of salts. Solutions having higher conductivity, exhibit more charge carrying ability compared to other solutions. In this reason, they are exposed to a higher force, thus they behave unstable under electric field, which causes to intense bending instability and a wide diameter distribution[50]. Nevertheless, Stijnman et al.[51] reported that there wasn't a relationship between the conductivities of the polysaccharide solutions and their fiber formation abilities. For

polymers such as PVA, mean fiber diameter and bead formation might be reduced by adding salts (NaCl, KH_2PO_4) due to having a greater electrical conductivity[52].

1.1.4. Effect of Processing Parameters on Fiber Formation and Fiber Properties

1.1.4.1. Applied Voltage

The applied voltage is the most influencing process factor in electrospinning because it alters the edge of electrostatic forces that prompt the emergence of a polymer jet. The amount of voltage is crucial for the initiation of the process. When low electrical voltages are applied, a pendant drop is formed and the Taylor cone is produced at the tip of the pendant drop. But, when the electrical voltage is increased, the size of the drop decreases. After that, Taylor cone is produced at the tip of the capillary (Figure 1.10). More increase in the applied voltage may remove Taylor cone, which will result in bead defects[53]. Briefly, existence and position of Taylor cone, affected by the applied voltage, is related to the formation of beaded electrospun fibers.
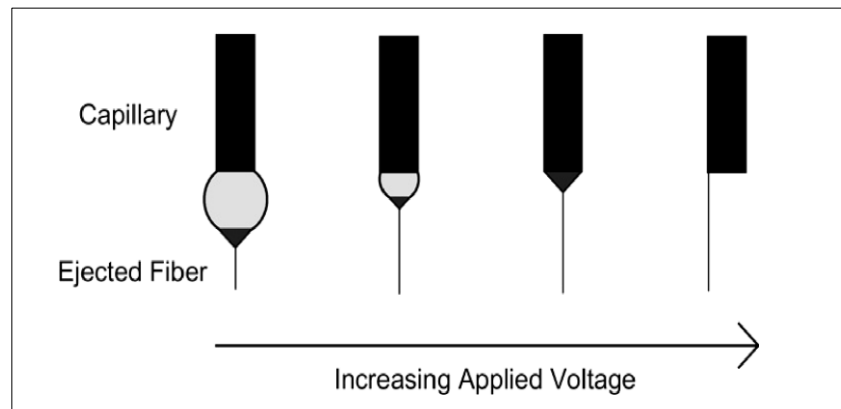
Figure 1.10. From left to right, changes in Taylor cone by the increase of applied voltage[53].

When the electrical voltage is applied at a lower value, a reduction in the fiber diameter could be observed, since a reduced flight speed may allow the division of jet[54]. On the other hand, an increase in electrical voltage can cause a broader diameter distribution[55].

An optimized electrical field should be maintained for a certain polymer solution to achieve continuous fiber formation.

1.1.4.2. Feeding Rate and Tip to Collector Distance

The flow rate of polymer solution and distance from the tip to the collector have importance on fiber size and shape (porosity) due to their effect on jet velocity and transfer rate of polymer[18, 53]. Depending on the solvent type, a proper evaporation time should be provided by adjusting the flow rate or distance. For polystyrene (PS) fibers, it has been observed that, increase in the flow rate resulted in increase in the fiber diameter and the porosity[56, 57]. Also, morphological structure of fibers may change as a result of bead formation due to the limited evaporation time of solvent until polymer reaches to the collector[58–60].

1.1.4.3. Effect of Environmental Factors on Formation and Properties of Fiber

The environmental factors, especially temperature and humidity affect the electrospinnability and morphology of fibers. For instance, at higher temperatures the solution may behave less viscous and more polymer solution can be pumped in the same flow rate or the solvent evaporation might be faster at equal time period. The uniformity of fiber diameters may also differ with temperature. The effect of humidity on the morphology of fibers has not been generalized yet. The humidity may also influence pore diameter, and pore size distribution on the fibers[61].

1.1.5. Electrospun Biopolymers

Interest for synthesis, extraction and purification of biopolymers, also their utilization in the production of different type of materials, energy, or in any other fields has been increased enormously in the past decades. Not only the sustainable, ecological and renewable nature, but also many inherent properties of biopolymers including biocompatibility, biodegradability and antimicrobial activity raise their attractiveness. Electrospun nanofibers can be obtained from biopolymers similarly the as synthetic ones. So far in the literature, electrospun biopolymer nanofibers based on alginate[62–64],

chitosan[65–67] and chitin[68], cellulose derivatives[69–71], starch[49, 72], gelatin[73, 74], collagen[75], zein[39, 76], silk[77], pectin[78, 79] and pullulan[80] have been obtained. The electrospun biopolymers can be applied to biomedical, pharmacy and food applications. However, electrospinning of biobased polymers has been reported as to be more complicated than synthetic ones. The source of this problem is a consequent of the structural diversity of biopolymers and their own characteristic properties including ionic structure, poor chain flexibility, and partial solubility in the most of solvents[17]. In order to obtain biocompatible, low toxic, abundant and biodegradable bio-based nanofibers, to overcome these difficulties is very important. In Table 1.1, the studies that comprise the relation of rheological properties of different polymer solutions with the resultant electrospun nanofiber properties are given.

Table 1.1. Electrospinning studies using biopolymers in the rheological point of view.

Electrospinning solution			Solution properties			Rheological findings		Fiber properties	References
Main polymer, concentration	Process aid (carrier polymer, co-solvent, surfactant)	Solvent	Conductivity (mS/cm)	Surface tension (mN/m)	Viscosity (Pa.s)	Steady shear behavior	Dynamic behavior (G', G'', δ relaxation time)		
Agar, A-7002, 1% (w/v)	PVA (M_w=89-98 kDa), 10% (w/v) Agar:PVA=100:0-0:100	Water	Not measured	Not measured	0.03-0.4	Weak shear thinning behaviour	Above 50°C, G''>G', tanδ>1. In blends, PVA increased the elasticity	Best nanofibers obtained at higher PVA (30:70&20:80)	Sousa et al., 2014
Alginate (700–900 cps), 2% (w/v)	PVA (M_w=50 kDa), 7-9% (w/v); PEO (M_w=300 kDa), 8% (w/v)	Water	Not measured	Not measured	0.08-0.18 at 100 s^{-1}	Shear thinning PVA or PEO addition decreased viscosity	Not measured	Continuous fiber formation initiated at 7% PVA; the finest one is 8% PVA:Alginate (30:70) and 8% PEO:Alginate (50:50)	Safi et al., 2007
Alginate (3500 cps), 1.6-2% (w/v)	Glycerol, glycerol:water=0:1-2:1 (v/v)	Water	0.19-4.18	61.4-37.5	22-701 at 0.5 s^{-1}	Glycerol increased viscosity	G' and G'' increased with the glycerol amount	Non beaded fibers observed at 2% alginate and 2:1 glycerol:water.	Nie et al., 2008
Alginate (3500 cps), 2.8% (w/v)	PEO (M_w=1000 kDa), 0.175-0.7% (w/v); PEO (M_w=20 kDa), 4-35% (w/v)	Water	1.18-6.87	Not measured	8.74-61.79 at zero shear	M_w of PEO increased viscosity	Not measured	No fiber formation up to 60% PEO (M_w=20 kDa). Smooth fibers at 0.7% PEO (M_w=1000 kDa).	Nie et al., 2009
Alginate (1280 cps), 1.5% (w/v)	Ca^{2+}, Ca^{2+}:alginate=0:100-2:100 (w/w)	Water/ EtOH/ DMF	1.75-3.8	48-60.5	0.42-16.4 at 1 s^{-1}	Ca^{2+} increased viscosity	G' and G'' increased with the Ca^{2+} amount	Ca^{2+} enhanced intermolecular interactions of alginate, improved the electrospinnability.	Fang et al., 2011
Alginate (M_w=37 kDa), 13.5% (w/v);	PEO (M_w=600 kDa), 4% (w/v); PEG (M_w=35 kDa), 40% (w/v),	Water	3.53-7.15	29-63	14-22 at zero shear	Concentration and M_w of alginate increased	Alginate:PEO ratio did not change the relaxation time at same concentration	No fiber formation occurs without PEO. Surfactant prevents bead formation on	Bonino et al., 2011

(M_w=196 kDa), 4% (w/v)	Triton X-100, F127				viscosity			fiber.	
Alginate, (MV_L, MV_M, MV_G (M/G ratio < 0.67), 4% (w/v)	PEO (M_w=900 kDa), Alginate:PEO=70:30, Triton X-100	NaCl, 0.1 M	Not measured	Not measured	0.1-117.5 at zero shear	Shear thinning behavior	PEO and Triton amount decreased the thixotropic behaviour	Alginate with lower M/G ratio resulted stronger fiber mats compared to higher M/G	Dodero et al., 2019
Alginate (<250cps), 4% (w/v)	PEO (M_w=400 kDa), 4% (w/v)	Water	0.2-7.2	63-65	1-1.4 at zero shear	Shear thinning behavior. PEO decreased viscosity	Always G''>G'. Increasing PEO did not change G', decreased G''	At 80:20 ratio, (chitosan:PEO or alginate:PEO) bead free fibers were obtained	Rosic et al., 2012
Alginate (M_w=46 kDa & 100 kDa), 4% (w/v)	PEO (M_w=100, 2000 kDa), Alginate:PEO= 70:30-30:70, Triton X-100	Water	2.3-5.8	17.8-60.9	9.2-4.6	Not measured	Relaxation time increases with PEO	Only high M_w PEO blended with alginate yielded bead-free, alginate-rich fibers	Saquing et al., 2013
Hydroxypropyl-methylcellulose (M_w=86 kDa), 1-5% (w/v)	PEO (M_w=900 kDa), HPMC:PEO=4.5:1.5-1:1, Tween 20	Water	128-209	Not measured	1-44 Pa.s at 0.1 s^{-1}	Shear thinning behavior. HPMC increased k	G' and G'' increases with HPMC. Concentration increased the G' and G''	The increase in viscosity resulted in the increase at diameter.	Aydogdu et al., 2018
Chitosan (M_w=148, 400, 600 kDa), 1-8% (w/v)	PEO (M_w=900 kDa), 3% (w/v)	Acetic acid, 10-90% (v/v)	Not measured	Not measured	0.8-4 at zero shear	Shear thinning behavior. PEO decreased viscosity	Not measured	High M_w and high concentration of chitosan usage resulted in more uniform fibers.	Klossner et al., 2008
Chitosan (M_w=68, 148 kDa), 5% (w/v)	PEO (M_w=900 kDa), 4% (w/v), Tween 20	Acetic acid, 10, 50, 90% (v/v)	Not measured	40-60	0.85-1.77 at 100 s^{-1}	Shear thinning behavior	Not measured	Higher M_w of chitosan usage resulted in the formation of fibers with thicker diameter	Ziani et al., 2011
Chitosan (M_w=460, 1000 kDa), 2.5% (w/v)	PEO (M_w=6000 kDa), 2.5% (w/v), Chitosan:PEO=1:1 (v:v)	Acetic acid, 0.5 M	Not measured	Not measured	0.14-3.31 at zero shear	Shear thinning behavior	Not measured	At 2.5% of high M_w chitosan and 3.5% of low M_w chitosan smooth fibers obtained	Rieger et al., 2015

Chitosan (Mw=296 kDa), 2.5% (w/v)	PVA (Mw=85 kDa), 10% (w/v), Chitosan:PVA= 50:50-0:100	Acetic acid, 2% (v/v)	Not measured	Not measured	2.5-3.5 at 30 s^{-1} shear rate	Shear thinning behavior. PVA increased viscosity	Usually G''>G'. But, at 8.1% total concentration G'=G''	Fiber diameter was not affected by concentration or composition significantly.	Gonçalves et al., 2017
Galacturonic acid (Mw=25-50 kDa), 1-9% (w/v)	PVA (Mw=125 kDa). Galacturonic acid: PVA=10:90-90:10	SDS-water	Not measured	Not measured	0.78-1800 at 0.1 Pa.s shear rate	Newtonian up to 15% SDS, then shear thinning. PVA decreased viscosity	G' and G'' were decreased with PVA content	Non-beaded fibers were obtained at the ratio of 70:30	Gupta et al., 2019
Gelatin (Type B), 7, 20% (w/v)	-	Acetic acid, 20% (v/v)	2.78-4.77	36.2-34.9	0.04-1.49 at 0.29 s^{-1} shear rate	Shear thinning behavior	Not measured	Fiber formation was observed at 20% gelatin concentration.	Okutan et al., 2013
Gelatin (Type B), 20-40% (w/v)	-	Acetic acid, 25-100% (v/v)	Not measured	Not measured	0.08-9.7 at zero shear	Acid concentration affected thixotropy. If >50%, Newtonian behaviour.	Not measured	At low acetic acid and high gelatin concentration (≥30%) fibers were obtained.	Erencia et al., 2015
Gelatin (Type A), 2.5-60%; (Type B), 5-60% (w/v)	-	Formic acid	1.67-7.5	Not measured	0,01-27 at zero shear	Gelatin increased viscosity. Also, Type B>Type A	Not measured	Continuous fibers were obtained at 20-40% gelatin.	Ratanavaraporn et al., 2010
Pullulan, 8, 15% (w/v)		NaCl, 0.2-5 M; Na$_3$C$_6$H$_5$O$_7$,0.05-0.5 M	0-200 0-40	65-80	19-204; 27-333; 22-274	Pullulan increased viscosity	Not measured	Sodium salts eliminated bead formation on fibers	Li et al., 2017
Starch (amylose content=80, 70, 55, 25, 0-1%), 0.1-30% (w/v)	-	DMSO, 70-100%	Not measured	Not measured	0.01-8 at 1 s^{-1}	Newtonian up to 10% (w/v), then shear thinning	Not measured	The concentration of starch had to be 1.2−2.7 times the entanglement concentration.	Kong& Ziegler, 2012

Starch (amylose content=70%), 17% (w/v)	-	Formic acid, 60-100%	Not measured	Not measured	2-110 at zero shear	Thixotropic behavior. Acid decreased viscosity	G' decreased with acid content.	Uniform fibers were obtained only at 100 and 90% formic acid; at lower, beaded and bead-on-string type short fibers were seen.	Lancuški et al., 2015
Starch (amylose content=27.8, 50%), 0.6-2.4% (w/v).	Guar gum, starch:guar gum= 4:1-1:4 (w:w)	Water	Not possible to measure	Not possible to measure	6-1500 for 28%, and 1-2000 for 50% amylose at 0.1 s^{-1}	Strong shear thinning behavior. Decreased with guar gum concentration.	Decrease of guar gum, shifted crossover point (G'=G'') to a higher frequency.	Increasing the starch content resulted with the better fiber formation.	Yang et al., 2017

1.2. PECTIN AND PECTIN BASED MATERIALS

1.2.1. Properties of Pectin

Pectin is a heteropolysaccharide that is found in the middle lamella and primary cell walls of land plants, fruits and vegetables. Such as cellulose, pectin has an important role in their structure, providing the rigidity and integrity. Usually, pectin is obtained from citrus peel or apple pomace through extraction methods. Though pectin is preferred in different applications due to its abundancy, economic cost, biodegradability, biocompatibility and non-toxicity, it is applied in food industry to aid gelatinization, thickening and stabilizing frequently. Pectin is classified as GRAS by FDA.

Pectin has a quite complicated chemical structure that varies with the origin, the location in the plant and the extraction method. Its structure is composed of hairy and smooth regions (Figure 1.11). Smooth regions of the native pectin are made of homogalacturonan (HGA), the linear chains of α-(1–4) D-galacturonic acid units interrupted by α-(1–2)-bonds; whereas the hairy regions are composed of xylogalacturonan, rhamnogalacturonan I (RG-I), rhamnogalacturonan II (RG-II)[81, 82]. Pectin exhibits varying degree of side groups (methylated groups or amidated carboxyl groups), and also several neutral sugars (arabinose, galactose and rhamnose) are found in the structure (Figure 1.12).

Pectin contains approximately 60-65 percent of galacturonic acid groups[82]. Some of the galacturonic acid molecules are participated to esterification reactions with methyl groups in naturally. Commercially, pectin is divided into two main groups with respect to their esterification degree: high methyl esterified (>50 percent) and low methyl esterified (<50 percent). In addition to pectin that normally exist as high methyl esterified (HM), low methyl esterified (LM) pectin can be obtained by modification of extraction process or longer acid treatment. On the other hand, amidated groups also can be produced by the reaction of pectin with ammonia during manufacturing[83]. The degree of esterification (DE) and their distribution in the backbone are very important factors that designate pectin's properties, especially the gelling properties. Also, in some types of pectin, several galacturonic acid groups might be acetylated, and they cannot be utilized as gelling agent. The molecular weight of pectin varies depending on the amount and the size of side chains.
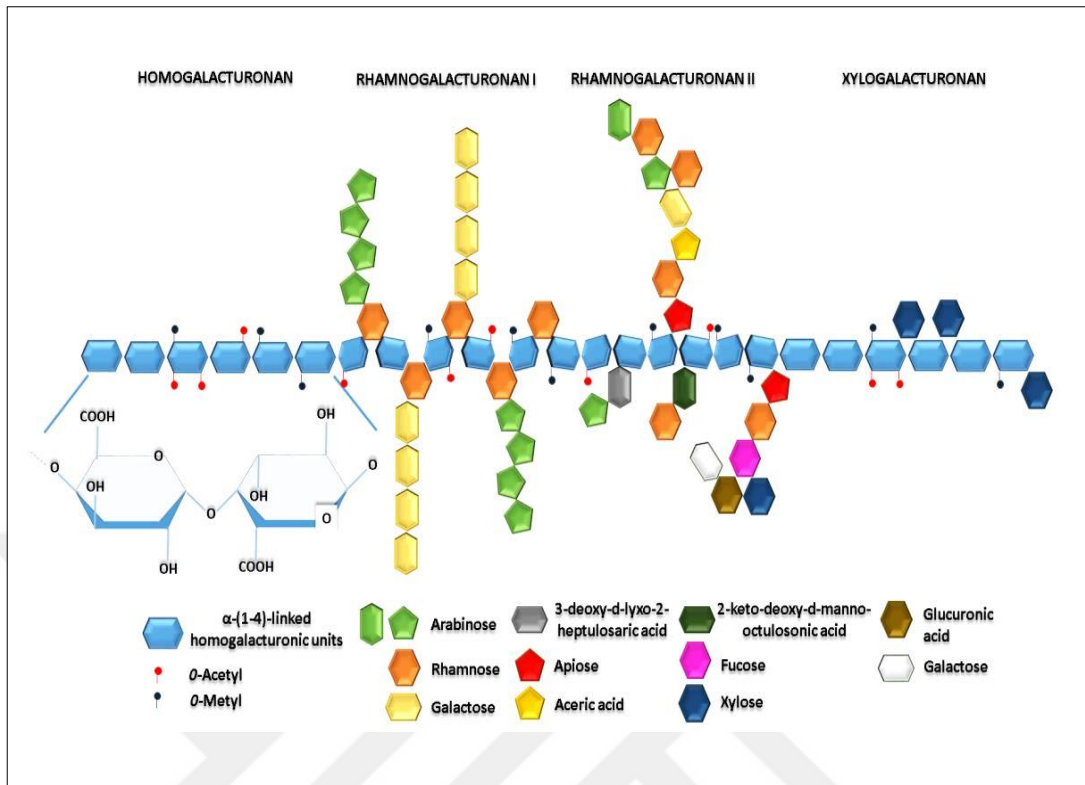
Figure 1.11. Illustration of pectin domains: HG and RG I are considered the major constituents, while XG and RG II are minor constituents[84].

Pectin is water soluble; however, it is insoluble in most of organic solvents. The solubility of pectin decreases with molecular weight; however increases with amount of esterified carboxyl groups. Also, the concentration, pH, temperature and the nature of solute have remarkable effects on the solubility of pectin. In aqueous environment, depending on concentration, pectin can create viscous solutions.

The viscosity of a pectin solution depends on different parameters, such as concentration and source of pectin, temperature, pH and the amount of salt that that might be found in solution. At very low concentrations, lower than 0.5 percent, pectin exhibits Newtonian behavior, but in higher concentrations pseudoplastic (shear thinning) behavior (decrease of the fluid viscosity with increasing shear rate) can be observed[82]. The zero shear viscosity expresses the viscosity of solution in the absence of shear rate. In Figure 1.12, zero shear viscosities depending on the concentration of LM amidated pectin was expressed. As seen in the Figure 1.12, zero shear viscosity of pectin is increased with the concentration.
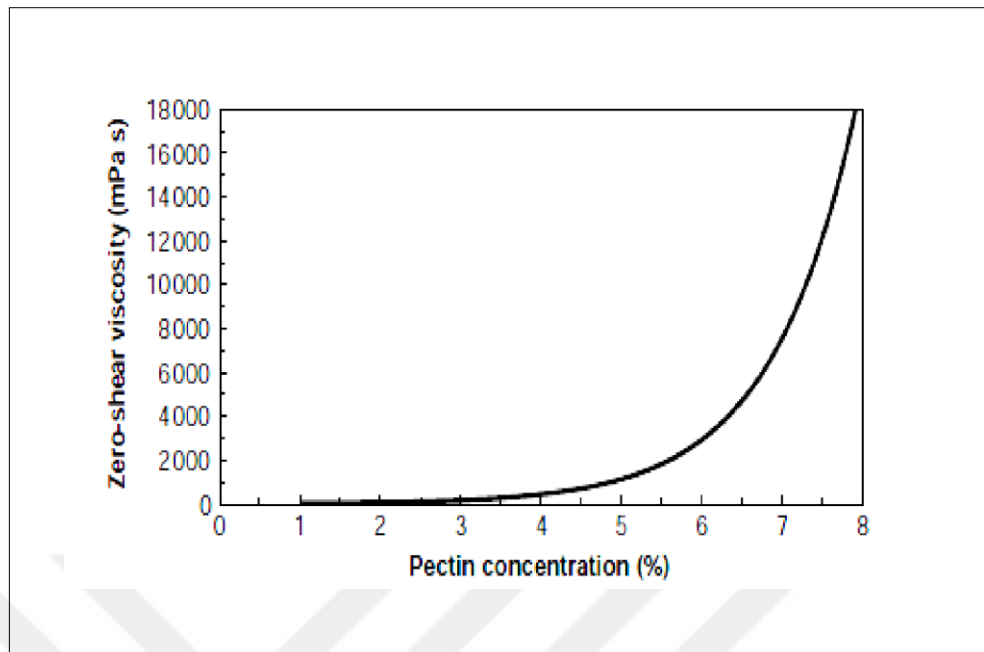
Figure 1.12. The viscosity values depending on the concentration of amidated LM pectin at zero shear (dissolved in water at pH=4 and 25°C)[82].

Pectins are negatively charged and have polyelectrolytic nature with a pKa of 3.55-4.10 varying with DE[85]. They behave differently as the pH of their environment changes. Pectin gelation differs with the amount of methoxyl groups. While LM pectins form gel in the existence of calcium ions, HM pectins require acidic environment. The electrostatic interaction between negatively charged cavities of LM pectin and cations leads to gelation which is known as egg box model as seen in Figure 1.13a. The chains are stabilized by the help of Van der Waals forces, electrostatic interactions and H-bonds[83]. The gelation of HM pectin occurs by the increase in chain-chain interaction as the electrostatic repulsions are decreased with the decrease in solution pH (Figure 1.13b).
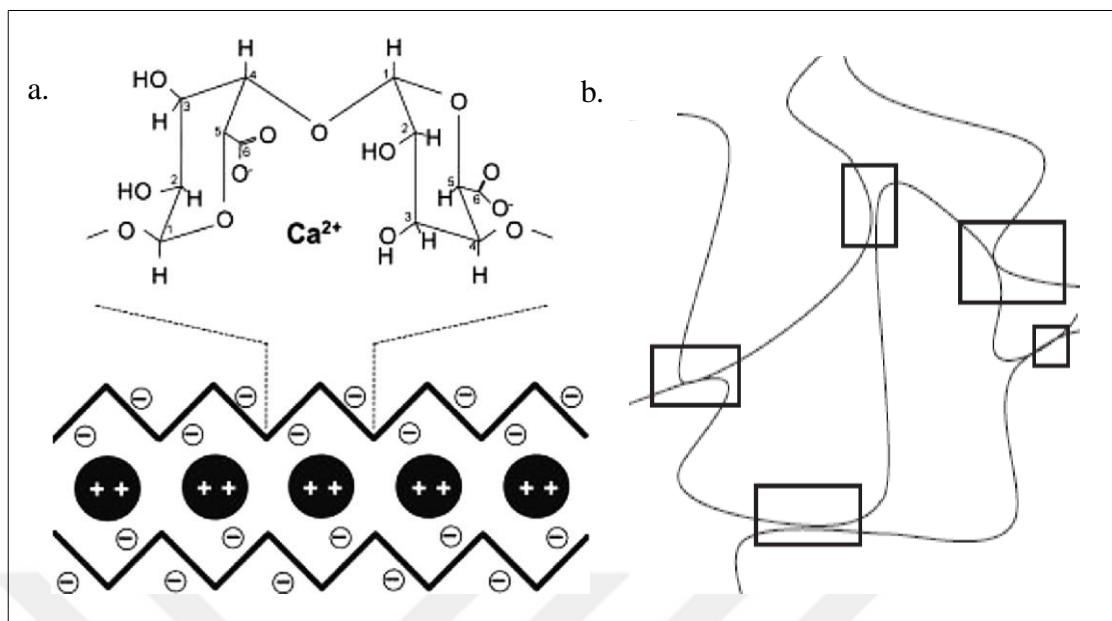
Figure 1.13. Gelation mechanism of (a) LM pectin[83]. (b) HM pectin[82].

1.2.2. Pectin Based Materials

Although pectin can be used as ingredient in food and pharmacy industry, polyelectrolyte nature, biodegradability, biocompatibility, and water solubility of pectin also opens up novel uses including coatings, edible film materials for food packaging applications. However, the intrinsically high hydrophilicity and low mechanical strength of pectin based films compared to ones produced from synthetic sources, currently limit utilization of pectin by itself[86–88]. In this context, to enhance the mechanical integrity and reduce brittleness, plasticizers can be added to pectin to form the films[89]. Plasticizers can ease processing while increasing the flexibility of the polymer chains by enhancing polymer chains motion and reducing their intra- and intermolecular forces[90]. Moreover, water dissolution of pectin can be decreased by in-situ crosslinking with divalent metal ions including Ca^{2+}, Zn^{2+} or Mg^{2+}[91, 92]. Also, the mechanical, thermal, and barrier properties of pectin-based films can be enhanced by blending with other biopolymer such as chitosan[93, 94], cellulose and derivatives[95, 96] or the addition of inorganic clays[87]. Furthermore, pectin films can show antioxidant and antimicrobial properties by the incorporation of essential oils (EOs)[97, 98] or metal nanoparticles (MNPs)[99].

In the polymer literature, pectin-based edible films and coatings have been already produced by casting, spraying and extrusion processes[100]. Pectin is also a favorable biobased raw material to be incorporated in fibers, because of its low cost and abundancy[78]. In order to obtain pectin fibers, electrospinning can be used as a simple and versatile method. Electrospun nanofibers may offer many functional advantages such as superior mechanical properties, large surface-to-mass ratio, tailored fiber morphology, and capability of encapsulation and release active and bioactive principles[9, 39, 101]. Pectin based fibers have been demonstrated to be used in different applications including engineered tissues[101–104], food encapsulation[105] and drug delivery[106, 107]. Nevertheless, few studies related to electrospun pectin nanofibers have arisen in the literature as seen in Table 1.2.

1.2.3. Electrospun Pectin Nanofibers

Due to its complex structure and poor solubility, electrospinning of pectin, such as other food grade polymers, has been very challenging[78]. Aqueous pectin solution cannot be electrospun alone based on the limited viscoelasticity of pectin solutions and insufficient chain entanglements[79, 102]. Stijnman et al.[51] focused on the relation between the rheology of different food grade polysaccharides and the ability of forming fiber via electrospinning. Among these polysaccharides, HM pectin can neither be electrospun nor form a jet. According to their observation, the shear thinning behaviour of pectin at low shear rates means that pectin exhibits low entanglement during spinning. So, the pectin chains might prevent jet and fiber formation, since the jet definitely breaks into pieces when drawn and stretched by the electrical forces.

Blending pectin with synthetic based polymers; including poly(vinyl alcohol) (PVOH) or polyethylene oxide (PEO), can enhance the chain flexibility and jet stability, which result in the production of uniform, continuous pectin nanofibers[79, 108]. Recently, electrospun pectin nanofibers have been obtained successfully when it was blended with a sufficient amount of PEO[78, 79, 102, 104, 108] and PVOH[107, 109, 110]. However, the addition of synthetic polymers into the formulations might bring toxicity issues in some applications such as the ones in biomedical area. Cui et al.[79] reduced the content of PEO up to 1.5 wt percent in pectin nanofibers by selective washing.

Table 1.2. Studies related to electrospinning of pectin in the literature.

Polymers			Solution Properties			Rheological Tests		Fiber Properties	Author, Year
Pectin, type, source, % (w/v)	Other Biopolymer, % (w/v)	Carrier Polymer/ Surfactant	Conductivity (mS/cm)	Surface Tension (mN/m)	Viscosity (Pa.s)	Steady shear	Oscillation: G', G'', δ, Relaxation Time		
Apple, 0.9-1.5%	Alginate, 2.1-3.5%, (Pec:Alg)= (30:70)	PEO, (Tot.:PEO)= (20:80)-(50:50) (w:w)	2.2-7	56.5-63.5	5-25 at 5000 s^{-1}	Shear thinning behavior (n<1) for all concentrations	-	Bead free fiber (at 5% total con.)	Alborzi et al., 2010
HM, 3.4%	-	-	0.4	-	5.14 at low shear	Shear thinning	-	No fiber or jet formation	Stijnman, et al., 2011
HM, apple 0.25-2%	-	PEO, 1.5%, (Pec:PEO)= (0.2:1.0)- (2:1) (w:w)	-	-	-	-	-	Higher diameter variation when pectin is increased	Furlan et al., 2012
Pectin,30–100kDa, 2%	Chitosan, 6%, (Pec:Chi)= (1:3)	PVA, 5%, (Pec+Chi:PVA)= (4:5)	-	-	-	-	-	Beaded fiber. Pectin-chitosan-PVA fibers were stronger than chitosan-PVA	Lin et al., 2013
Apple, LM citrus, SBP, HM, 3%	-	PEO, 3%, (Pec:PEO)= (50:50) (v/v)	-	-	-	-	-	Fiber diameter increases with DM of pectin	Rockwell et al., 2014
Citrus, apple, HM; sunflower, apple, LM, 5-8%	-	PEO, 5%, (Pec:PEO)=(60:40)-(80:20) (w/w), Triton X100, 1%; DMSO, 5%	-	-	-	-	-	Bead free fiber at 1.5% PEO when both surfactant and cosolvent added	Cui et al., 2016
Citrus, 2%	-	Glycerol, 1: 22.2 (w/w), Tween 20, 0.2%	-	-	0.123	-	-	Electrosprayed Film formation	Gaona-Sanchez et al., 2016
Citrus, HM, DE=68%, 3-15% (w/v)	Pullulan, 3-15% (w/v) Pectin:PUL= (1:1) (v/v)	-	0.5-2.2	76-86	Specific vis was calculated	Shear thinning behavior at high con.	η' (dynamic vis.) of PEC solutions was increased by addition of PUL	Bead-free fibers at 15 wt%. and Pectin:PUL= (1:1) (v:v). Increase at PUL increased diameter	Liu et al., 2016
Citrus, 4% (w/v)	Rectorite (REC)	PVA, 8% (w/v) Pectin:PVA= (0:100)-(100:0)	-	-	-	-	-	Bead free fibers at Pectin:PVA= (20:80).	Ye et al., 2016

LM, 4% (w/v)	-	PEO, (Mw=600 kDa), 4%, (w/v). Pectin:PEO=(70:30) -(40:60) (v:v) F-127, 2-10% (w/v))	-	-	-	-	-	Non beaded fibers at pectin:PEO= 65:35 (v/v), 5% (w/v) Pluronic® F-127	McCune et al., 2018
Apple, DE=70%, 10−15% (w/w)	-	PEO, (M_w= 5000kDa), Pectin:PEO=(80:20) Triton X-100.	-	-	-	-	-	Fibers are crosslinked	Chen et al., 2018

Although electrospun pectin nanofibers have been proposed to be used in different areas, its utilization for the purpose of food packaging has never been explored. The reason for this is related to the discontinuity and porous structure of the electrospun nanofiber mats. To this end, the electrospun mats can be subjected to a thermal post-treatment above the glass transition (T_g) and below the melting temperature (T_m), also named annealing, in order to remove or minimize their porosity and produce continuous and homogenous films[111]. Until now, this technology has been successfully applied to different polyester-type biopolymers with different potential applications in the food packaging field. For instance, electrospun poly(3-hydroxybutyrate) (PHB) films exhibited equal permeability, better optical properties, and higher mechanical properties in comparison with equivalent films obtained by a different method, which was compression molding[112]. Electrospun films of PHB, PVOH, and polylactide (PLA) were also developed by electrospinning and originally applied as coating materials to a paper based packaging material to develop multilayers with improved barrier properties to water and limonene vapors[148]. In another study carried out by Cherpinski et al., (2018), a similar strategy was followed to coat nanopapers by means of electrospun PHB and poly(3-hydroxybutyrate-*co*-3-hydroxyvalerate) (PHBV) layers[153]. Similarly, electrospun ultrathin fibers of biowaste derived PHBV were subjected to annealing by Melendez-Rodriguez et al. (2018) to successfully produce continuous biopolymer films with similar barrier performance than petroleum-based polyethylene terephthalate (PET) films[113]. Other recent studies have been investigated the effect of antimicrobial or antioxidant ingredients in the electrospun fibers, which can be thereafter incorporated as active coating layer in packaging applications[114, 154]. For instance, Figueroa-Lopez et al. (2019) prepared electrospun active films of PHBV with antimicrobial and antioxidant properties by the incorporation into the fibers of essential oils and natural extracts[154]. Also, Quiles-Carrillo et al. (2019) developed multilayer bioactive films with controlled release capacity of natural antioxidants by the incorporation of electrospun PLA interlayers into cast-extruded PLA films[115]. Lastly, Radusin et al. (2019) prepared antimicrobial PLA films containing *Allium ursinum L.* extract by electrospinning[155].

1.3. OBJECTIVE

Rheological properties of the solutions are known to be very important to determine whether a polymer solution can be electrospun or not. Different research groups presented different theories on which of the rheological finding are the most effective factors for smooth fiber production; yet, the results have not been adequate to clarify the relation between rheology of biopolymers and their electrospinnability. The objective of the study is at first, to examine the effect of solution properties, especially in the rheological view, on smooth fiber production from pectin only and pectin blend solutions, as well as on the morphological properties of the obtained pectin nanofibers.

As the second part of this study, the obtained pectin nanofibers will be used as potential candidates for food packaging applications. To do this, first, pectin fibers were obtained by electrospinning adding different amounts of PEO and in combination with two different types of plasticizers to select the best system to produce a film. Thereafter, the resultant electrospun mats were subjected to annealing to produce films. The morphology, chemical, and thermal properties of the fibers were characterized. The optimal film was, finally, applied as an interlayer in a multilayer structure based on poly (3-hydroxybutyrate-co-3-hydroxyvalerate) (PHBV). The morphological and barrier properties against to water and limonene of the multilayers were analyzed. Also, the results were compared to those of multilayer containing a cast-film pectin interlayer and PHBV-PHBV bilayer films.

2. MATERIALS AND METHODS

2.1. MATERIALS

Low methyl esterified amidated pectin was kindly received from AROMSA Inc (Gebze, Turkey). The product (GENU pectin, LM-104 AS-FS, degree of esterification 27 percent, degree of amidation 20 percent) was produced and delivered in powder form by CP Kelco (Copenhagen, Denmark).

Poly(ethylene oxide) (PEO) at three different molecular weights (M_w=600, 1000 and 2000 kDa) were delivered in powder form from chemical companies. PEO_{600} with a M_w of 600 kDa was purchased from Acros Organics, Fisher Scientific. PEO_{1000} was obtained by Sigma-Aldrich chemical company (MO, U.S.A.). PEO_{2000}, with a commercial name of SENTRYTM POLYOXTM WSR N80-LEO NF grade was obtained by The Dow Chemical Company (Midland, MI USA). Poly(ethylene glycol) (PEG) with M_w of 900 kDa (PEG_{900}) was provided by Honeywell Fluka Chemicals Company (Bucharest, Romania). Bacterial aliphatic copolyester poly(3-hydroxybutyrate-co-3-hydroxyvalerate) (PHBV) was purchased by NaturePlast (Ifs, France). It was reported to be manufactured by Tianan Biologic Materials (Ningbo, China). The PHBV had a 1.23 g/cm³ true, and a 0.74 g/cm³ bulk density as determined by ISO 1183 and ISO 60 standard methods.

Span® 20, calcium chloride, dichloromethane, 2,2,2-trifluoroethanol (TFE), ≥99 percent purity, and glycerol, ≥99.5 percent purity were obtained from Sigma-Aldrich S. A. (Madrid, Spain).

2.2. METHODS

2.2.1. Preparation of Polymer Solutions

Pectin solutions, at concentrations of 6-12 wt. percent were dissolved in distilled water at 70°C and left for overnight stirring at room temperature. PEO solutions were prepared at 2 wt. percent by dissolving at 25°C. Pectin-PEO blends were prepared by stirring them

during overnight at equal volume. In Table 2.1, the compositions of blend mixtures were given.

Table 2.1. The prepared solution compositions of pectin-PEO$_{600}$, pectin-PEO$_{1000}$ and pectin-PEO$_{2000}$ in distilled water for the rheological studies.

Pectin (wt%)	PEO$_{600}$ (wt%)	PEO$_{1000}$ (wt%)	PEO$_{2000}$ (wt%)	Water (wt%)
3	1	-	-	96
4	1	-	-	95
5	1	-	-	94
6	1	-	-	93
3	-	1	-	96
4	-	1	-	95
5	-	1	-	94
6	-	1	-	93
3	-	-	1	96
4	-	-	1	95
5	-	-	1	94
6	-	-	1	93

In order to obtain electrospun pectin based films, the total concentration of solids in distilled water to prepare the fiber-forming solution for electrospinning was set at 10 wt. percent and pectin-PEO ratio was been changed. While PEO$_{2000}$ with or without a plasticizer (glycerol or PEG$_{900}$) was used as process aid, Span 20 was added as a surfactant to the solutions at 2 wt. percent with respect to the total solid weight content.

Table 2.2 summarizes the compositions of the solutions prepared to produce electrospun films. For the electrospinning of PHBV, the copolyester was dissolved at 10 wt. percent in TFE at room conditions during 24 h.

Table 2.2 Different solutions prepared for pectin based film production according to the weight content of pectin, PEO_{2000}, glycerol, and PEG_{900} in distilled water.

Solution	Pectin (wt%)	PEO_{2000} (wt%)	Glycerol (wt%)	PEG_{900} (wt%)	Water (wt%)
S1	9.9	0.1	-	-	90
S2	9.75	0.25	-	-	90
S3	9.5	0.5	-	-	90
S4	9.0	1.0	-	-	90
S5	7.5	0.5	2.0	-	90
S6	7.0	0.5	2.5	-	90
S7	6.5	0.5	3.0	-	90
S8	7.5	0.5	-	2.0	90
S9	7.0	0.5	-	2.5	90
S10	6.5	0.5	-	3.0	90

2.2.2. Characterization of Polymer Solutions

2.2.2.1. Surface Tension, Conductivity and pH of Solutions

The pH of polymer solutions was measured by using a pH meter (PHM210, Radiometer Analytical SAS, France). Electrical conductivity was measured by using two different conductivity meters (CDM210, Radiometer Analytical SAS, France) and (HI 98192, Hanna Instruments, Inc., Romania). Surface tension of solutions was determined through Wilhelmy plate method by using two different models of tensiometer (Easy Dyne K20 and DCAT 11EC, Krüss GmbH Data Physics Instruments, Hamburg, Germany). All measurements were performed in triplicate.

2.2.2.2. Rheological Analysis of Solutions

The viscosity of solutions was measured by a viscometer (VISCO BASIC Plus L, Fungilab, Spain). The detailed viscosity measurements, creep tests and dynamic measurements were conducted by using a Kinexus Rheometer (Malvern Instruments Ltd, UK) as given in Figure 2.1. Also, the rheological data were obtained from the instrument's software (rSpace for Kinexus). Rheometer is connected to a compressor (Jun Air).

The cone and plate (angle=4°, D=40 mm) was utilized for shear rate ramp test and parallel plate geometry (D=40 mm) was utilizes for dynamic measurements. The measurements were carried out at room temperature and were replicated three times.
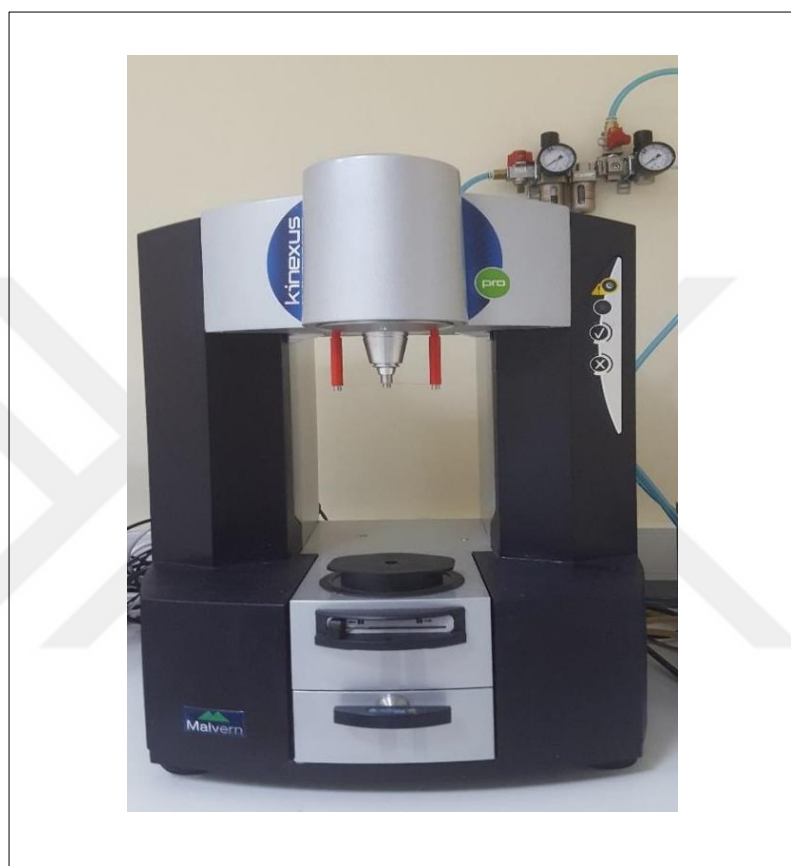
Figure 2.1. Rotational rheometer (Kinexus, Malvern Instruments Ltd, UK).

The zero shear viscosity values of the solutions were measured by using creep test. A 0.1 Pa stress was applied to polymer solutions during 5 minutes. Flow behavior and viscosity of solutions were obtained from shear rate ramp tests performed between a shear rate range of 0.1-1000 s^{-1}. The flow behaviour index 'n' calculated using the power law model. For the Newtonian fluids, the viscosity of the sample is independent of applied shear force which means the linear increase in stress is observed with increasing the shear rates continuously (n=1). But, in Non-Newtonian fluids, the viscosity changes with the difference in applied stress or strain. If the viscosity of fluid is decreased, it is called as shear thinning fluid (n<1); otherwise it is dilatant (n>1).

The tip viscosity was taken as the viscosity at the maximum shear rate value, which was calculated from Equation 1[116]. Where "R" is the inside radius of the syringe tip, "Q" is the volumetric flow rate (ml/h), and "n" is the flow behavior index obtained by the power law model equation. Average of the replicates were reported for zero shear and tip viscosity values.

$$\dot{\gamma}_{max} = \left(\frac{3n+1}{4n}\right) \times \frac{4Q}{\pi R^3}$$ (2. 1)

Viscoelastic measurements were conducted to by dynamic analysis. A strain value was selected in linear viscoelastic regions (LVR) of the solutions. In order to do that, strain sweep test was carried out at a frequency of 2 Hz and at 25°C and shear strain was increased from 0.1 to 1000 percent. The polymer solutions are strained by different forces, especially the electrical ones during spinning. In this reason, dissimilar with the literature, the elastic modulus (G'), and phase angle (δ) results were obtained by response of the solutions to percent strain. The averages of the G' and δ values in a common LVR for all samples, which corresponded to 1-10 percent strain, were reported. In order to determine the strength of internal structure, the cohesive energy (C.E.) values of the polymer solutions were calculated by using the critical strain "γ_{cr}" (above which the linear response changes to a nonlinear response) and the elastic modulus within the LVR, "G'" where it is independent on the applied strain[117].

$$C.E. = \frac{1}{2} \times G' \times \gamma_{cr}^2$$ (2.2)

2.2.3. Electrospinning of Polymer Solutions

In order to obtain electrospun fibers, two different systems were utilized (NE300 Inovenso, Turkey and Fluidnatek® LE500, Bioinicia S.L., Spain). The visuals of electrospinning machines are given in Figure 2.2a and 2.2b. In the first system, the high voltage power supply is connected to a syringe pump (New Era NE1000, USA) where the flow rate of polymer solutions can be adjusted. The solutions were put into a syringe (V=10 ml) with a capillary diameter of 0.8 mm that is attached to a pump.

Figure 2.2. The (a) first and (b) second electrospinning systems.

Different conditions were tested for electrospinning pectin and the electrical voltage was determined as 18-22 kV. While the distance from syringe tip to the collector was fixed at 20 cm, the flow rate of solution was set at 0.2 ml/h. The spinning was conducted for 3 hours. In the second system, the electrospinning machine (Fluidnatek® LE500, Bioinicia S.L., Valencia, Spain) exists in a closed chamber and is connected to an environmental control unit.

Fibers were collected in vertical mode on a rectangular plate collector covered with aluminum foil in both of electrospinning. While the applied electrical voltage ranged from 16 to 20 kV, the distance between the syringe tip and collector was set at 25 cm. The solution was fed at 3 ml/h where the injector ran in scanning mode.

For the electrospinning of PHBV, the electrical voltage was set at 10 kV, 15 cm was the tip to collector distance, and 6 ml/h was the flow rate. All experiments were conducted at $25^{o}C$ and 30 percent relative humidity (RH).

2.2.4. Production of Pectin Based Films

2.2.4.1. Electrospun Pectin Based Films

In order to achieve film formation, the resultant electrospun pectin-based fibers were washed by soaking the mats into dichloromethane for 60 s. The washed mats were then placed in vacuum oven (Vaciotem-TV, P. Selecta, Spain) connected to a vacuum pump (Vacuubrand, P. Selecta, Spain) working at $27^{o}C$ and 100 mmHg pressure for 18 h to remove the remaining solvent. The washed fibers were subjected to annealing in a bench top manual heated press (12-12H, Carver, Inc Wabash, USA). A set of experiments were conducted to optimize temperature, time, and load to produce homogenous and transparent films.

2.2.4.2. Solvent Casted Pectin Based Films

Solvent casted pectin films were also prepared by casting as a control material. To this end, 2 g of pectin powder was first dissolved in 100 ml of distilled water and then 0.92 g of glycerol was added. After 24 h of mixing, 10 ml of solution was poured into polystyrene petri dishes (D=9 cm). The, the solutions were left at room conditions, that is $25^{o}C$ and 40 percent, for 3 days to produce the cast films.

2.2.5. Production of Multilayer Films

The multilayer films were prepared by placing the solvent-casted or electrospun pectin-based films as an interlayer between two layers of PHBV. This was accomplished by electrospinning PHBV fibers on the previously prepared pectin films. The resultant coated films were turned down and coated on the other side. The two side coated films were then placed in the press and annealed at 160º C for 10 s based on our previous research[112]. Control films made of two layers of PHBV were prepared in the same conditions.

2.2.6. Characterization of Electrospun Fibers and Films

2.2.6.1. Thickness of Mats and Films

Prior to testing, the thickness of the electrospun mats and films was measured by using a digital micrometer (Mitutoyo Corporation, Kawasaki, Japan) with ±0.001 mm accuracy. The thickness of films and mats were measured at least from ten different positions and the average values were calculated. The samples were kept in a glass made desiccator at 25°C and 0 percent relative humidity for 24 h.

2.2.6.2. Morphology

Two different Scanning Electron Microscopes (SEMs) (EVO 40 series, Carl Zeiss AG, Germany and S-4800, Hitachi, Japan) were utilized to carry out structural analysis of nanofibers. All samples were covered with gold and gold/palladium alloy by using two different coaters (SCD 005, Bal-Tec AG, Germany and Polaron sputter coater, Quarum Technologies, UK, respectively) prior to analysis. A 5 kV voltage was applied during SEM analysis. For the multilayers, the samples were cryo-fractures using nitrogen liquid and their fracture surfaces were observed. The fiber diameters were determined by the software ImageJ, version of 1.52a (Java, USA) from the measurement of at least 50 fibers.

2.2.6.3. Thermal Analysis

The thermal transitions of samples were investigated by a differential scanning calorimetry (DSC) (PerkinElmer, Inc, Waltham, USA), connected to a cooling system (Intracooler 2, PerkinElmer, Inc, Waltham, USA). Approximately 3 mg of sample was placed into the aluminum pan; also a reference aluminum pan was used as unfilled. The calibration of instrument was conducted with indium. The pectin, PEO powders and fibers were heated from (-70) ˚C to 160 ˚C at first, then cooled back to (-70) ˚C, and secondly heated to 300 ˚C. 10 ˚C/min heating and cooling rates were utilized and the experiments were under nitrogen atmosphere. All tests were performed in triplicate.

Thermogravimetric analysis (TGA) of the pectin powder, PEO_{2000}, and the electrospun fibers and films was conducted under nitrogen atmosphere in a thermogravimetric analyzer (TGA/STDA851e/LF/1600 Thermobalance TG-STDA, Mettler Toledo, Switzerland). The samples were conditioned for 5 min at 30°C before test. The test was conducted by heating the samples from 25 °C to 700 °C at a rate of 10 °C/min. All tests were carried out in triplicate.

2.2.6.4. Fourier Transform Infrared Spectroscopy

Fourier transform infrared spectroscopy (FT IR) spectra were obtained from average of 20 scans by a Bruker Tensor 37 (Rheinstetten, Germany) spectrometer that was connected with a Golden Gate of Specac, Ltd (Orpington, U.K.) attenuated total reflection (ATR) accessory. The scans were collected in the wavelength values between 4000 and 600 cm^{-1} at a resolution of 4 cm^{-1}.

2.2.6.5. Barrier Measurements

Water Vapor Permeance

The water vapor permeance of multilayer films was decided by ASTM 2011 gravimetric method. A Payne cup (Inside diameter = 3.5 cm) was filled with 5 ml of water. The films were located on the cups so that one side of film was sustained to 100 percent humidity

without touching water. Then, the cups were locked with silicon rings and kept in a conditioned desiccator (25 °C and 0 percent RH). In order to calculate the water sealing during the analysis, aluminum contained cups were placed in desiccator too. The cups were weighed regularly by an analytical balance having an accuracy of ±0.0001 g, until the values stay constant. Water vapor permeation rate corresponded to the slope value of the obtained by the steady state line of time versus weight loss (loss of sample – loss of control) per unit area. When water vapor permeation rate was corrected for permeant partial pressure, water permeance was found. Tests were conducted in triplicate.

Limonene Vapor Permeance

Limonene vapor permeance was determined as similar with water vapor. To achieve this aim, 5 mL of D-limonene was put into the Payne cups instead of water. The film having metal cups were located at controlled conditions during analysis (25 °C and 40 percent RH). Again, aluminum contained cups were placed in desiccator as control. Limonene permeance was calculated from the same method explained above. Tests were conducted in triplicate.

2.2.6.6. Statistical Analysis

All data were analyzed statistically by SPSS version 17.0 (IBM, USA). Tukey's HSD test was used to determine the significant differences among samples ($p < 0.05$).

3. RESULTS AND DISCUSSION

3.1. EFFECT OF POLYMER RHEOLOGY ON FIBER FORMATION

3.1.1. Conductivity, Surface Tension and pH of Polymer Solutions

The conductivity, surface tension (SFT), and pH of the polymer solutions were measured prior to electrospinning (Table 3.1). The conductivity of LM pectin solutions was found to increase (from 2.68 to 4.79 mS/cm) with increasing pectin concentration (from 3 to 6 percent). The conductivity of pectin solutions can be attributed to the ionized (carboxyl) groups of the pectin molecules in the solution. Thus, as the concentration of pectin increases, one would expect an increase in the conductivity due to the increase in the number of ionizable carboxyl groups. PEO addition decreased the conductivity of pectin solutions significantly except for the solutions with 3 wt. percent pectin. This finding is in line with Alborzi et al.[118] and the reduction observed might be resulted from the decrease of the total ion concentration per unit polymeric volume. The effect of the molecular weight of PEO on the conductivity of the polymer solutions was found to be insignificant.

With the addition of PEO, the surface tension of pectin solutions increased significantly at lower pectin concentrations (3 percent and 4 percent) and was not affected significantly at higher pectin concentrations (5 percent and 6 percent). Alborzi et al.[118] reported that as the PEO (M_w=900 kDa) content was increased up to 50 percent, the surface tension of alginate-pectin blends was reduced; however, after that ratio the value stayed constant or increased. In our case, PEO addition to pectin solutions did not lower the surface tension; on the contrary increased SFT at lower pectin concentrations and did not affect at higher concentrations. This result suggests that the total amount of polymer concentration, and pectin: PEO ratio, are influential on how PEO addition affects the surface tension of pectin/PEO blends. The difference between our findings and that of Alborzi et al.[118] can be explained by the differences in the nature of the blends that were used. According to Fleer et al.[119], the polymers in multicomponent structure and the chain length and surface activity distribution of the different components are important for their surface

activity. It has been reported in the earlier studies that, even when used alone, PEO has a very complex solution and phase behavior where surface activity at the air/water interface increases with the molecular weight and concentration[120–123]. Thus, each polymeric system has its own dynamic properties, which are affected by the polymer type, molecular weight, concentration, the polymer ratios in the blends etc. The results of Alborzi et al.[118] along with ours suggest that it is not possible to generalize the effect of PEO addition on the surface tension of other biopolymer solutions, since it depends on many factors. Although there is no general correlation between the viscosity of polymeric solutions and the surface tension, the fact that we observed no change in SFT at pectin concentrations of 5 percent and 6 percent, suggested possible hindrance in the movement of PEO to the air/water interface due to increased entanglement and viscosity. Similar to our results Alborzi et al.[118] also reported that at the same PEO: polymer blend ratios (> 50 percent) and the same concentration (4 percent), medium viscosity polymer blend behaved differently (SFT stayed constant) from low viscosity blend (SFT increased).

The pH values of PEO only and pectin only solutions were around 8.0 and 4.0, respectively. However, the pH values were found to be similar for all solutions containing pectin, which indicated that blending pectin with PEO did not change the pH value of pectin solutions.

Table 3.1. Conductivity, surface tension and pH of polymer solutions prepared for rheological studies.

Polymer concentration (wt%)			Conductivity‡ (mS/cm)	pH	Surface Tension (mN.m)
Pectin	PEO*	Total			
0	PEO_{600}	1	0.12±0.07	8.49±0.47	59.78±2.22
	PEO_{1000}	1	0.07±0.04	8.30±0.72	62.08±0.36
	PEO_{2000}	1	0.09±0.01	8.12±0.09	62.54±0.53
3	-	3	$2.68±0.06^a$	$4.27±0.04^a$	$52.15±0.58^a$
	PEO_{600}	4	$2.54±0.02^a$	$4.36±0.05^a$	$61.76±0.24^b$
	PEO_{1000}	4	$2.48±0.18^a$	$4.28±0.01^a$	$60.13±0.41^b$

	PEO$_{2000}$	4	2.63±0.07^a	4.31±0.03^a	61.33±0.46^b
4	-	4	3.36±0.14^A	4.20±0.03^A	53.29±0.75^A
	PEO$_{600}$	5	2.91±0.17^B	4.29±0.08^A	59.28±2.86^{A,B}
	PEO$_{1000}$	5	3.02±0.00^B	4.21±0.03^A	61.72±0.04^B
	PEO$_{2000}$	5	3.04±0.09^B	4.20±0.05^A	62.70±0.20^B
5	-	5	4.19±0.04$^\alpha$	4.15±0.03$^\alpha$	55.27±0.43$^\alpha$
	PEO$_{600}$	6	3.68±0.17$^\beta$	4.19±0.02$^\alpha$	57.01±1.01$^\alpha$
	PEO$_{1000}$	6	3.86±0.19$^\beta$	4.17±0.04$^\alpha$	59.98±2.25$^\alpha$
	PEO$_{2000}$	6	3.47±0.12$^\beta$	4.17±0.06$^\alpha$	58.53±0.20$^\alpha$
6	-	6	4.79±0.05$^\Phi$	4.13±0.03$^\Phi$	57.08±2.61$^\Phi$
	PEO$_{600}$	7	3.65±0.16$^{''}$	4.21±0.03$^\Phi$	54.16±1.87$^\Phi$
	PEO$_{1000}$	7	4.04±0.38$^{''}$	4.16±0.06$^\Phi$	57.38±1.25$^\Phi$
	PEO$_{2000}$	7	4.43±0.10$^{''}$	4.16±0.05$^\Phi$	57.48±0.70$^\Phi$

* PEO was constant at 1 (wt%)..‡ Each pectin concentration was statistically analyzed by groups.

3.1.2. Rheology of Polymer Solutions

LM pectin blends showed Newtonian behaviour at low shear rates then behaved shear-thinning (pseudoplastic) at high shear rates (Figure 3.1-3.4). The increase in the molecular weight of PEO has resulted to raise in the zero shear viscosity values of blends. The greater values for the viscosity of blends compared to the pure pectin and pure PEO can be explained by a possible proliferation in the entanglement number. In only pectin solutions, the methyl groups and amine groups found in the structure of low methylester amidated pectin involved in non-covalent chain associations including hydrophobic interactions and existence of new H-bonding, respectively. Moreover, H-bonds could have been formed between free, non-dissociated carboxyl groups of pectin chains[124]. Once the PEO was introduced to the pectin solutions, the nonionic and flexible PEO chains might have interacted with the rigid backbone of the pectin and disrupted the self-association of the pectin chains. Similar to our results, Rosic et al.[31] also reported that PEO addition reduces the inter- and intra- interactions between the molecules of chitosan and alginate. The mechanisms of interaction between PEO and pectin were also based on physical means such as hydrophobic interactions (CH_2CH_2 component of PEO is sufficiently

hydrophobic and can interact with methyl groups of pectin), H-bonding (between oxygen of ether groups on PEO and OH groups on pectin), and van der Waals interactions[78]. The reduction of self-association of pectin chains through the interactions between pectin and PEO might have resulted in an increase in the hydrodynamic volume and promoted chain entanglement, which in turn increased the viscosity.

The blends demonstrated more pseudoplasticity than pure solutions of components. The onset of shear thinning was earlier in the blends having PEO with larger molecular weights. The flow behavior of the solutions including PEO_{600} and PEO_{1000} were quite comparable as seen in Figure 3.5. However, the blends including PEO at a molecular weight of 2000 kDa had a significant higher viscosity as well as showing stronger pseudoplasticity. The earlier onset of pseudoplasticity might be contributed to the higher crystallinity PEO_{2000}. Pectin is reported as amorphous and PEO is semi-crystalline polymers[78]. So, more crystalline regions of PEO than pectin may influence to the alignment of the polymer chains in the direction of flow, which as a result might enhance the pseudoplasticity of the blends.

The zero shear viscosities increased with the increase in pectin amount (Table 3.2). The zero shear viscosity values of solutions containing PEO_{2000} were significantly higher at all pectin concentration investigated (Table 3.2). A similar trend was observed in tip viscosity values as well. When the viscosity values are compared based on the total polymer concentration, it can be concluded that there are synergistic effects between pectin and PEO polymers. For example, at a total polymer concentration of 4 wt. percent, the zero shear viscosity of pectin-PEO_{2000} blend was 2.14 Pa.s, which was ten times higher than the sum of the zero shear viscosities of 3 percent pectin-only and 1 percent PEO_{2000}-only solutions, which were 0.09 Pa.s and 0.11 Pa.s, respectively (Table 3.2).

Figure 3.1. The flow curves of polymer solutions composed of 1 wt% PEO and 3 wt% pectin. (Representative graphs from the three replicates are given, statistics are presented in Table 3.2).
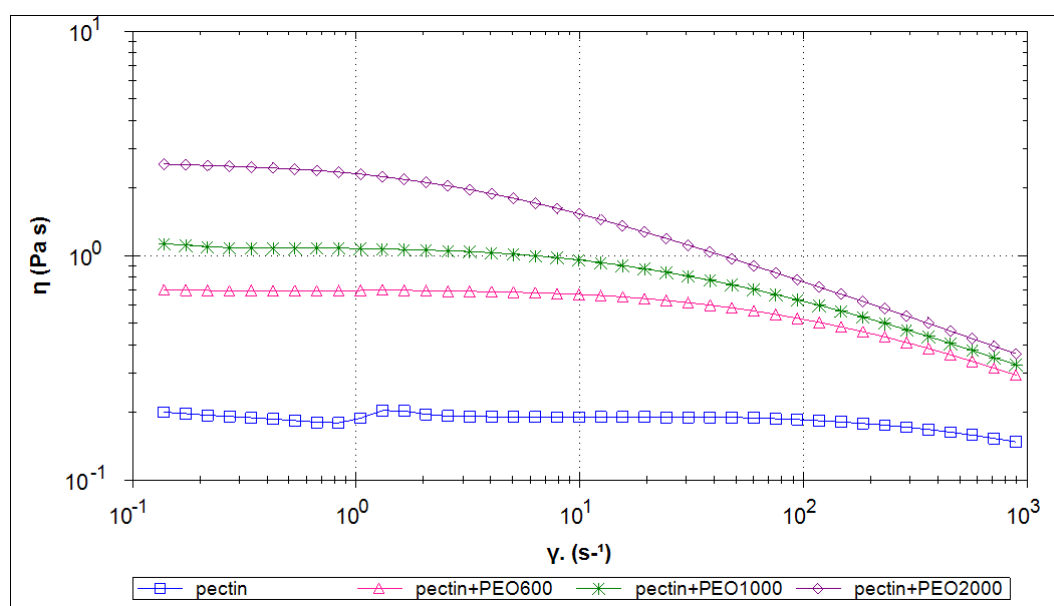
Figure 3.2. The flow curves of polymer solutions composed of 1 wt% PEO and 4 wt% pectin. (Representative graphs from the three replicates are given, statistics are presented in Table 3.2).
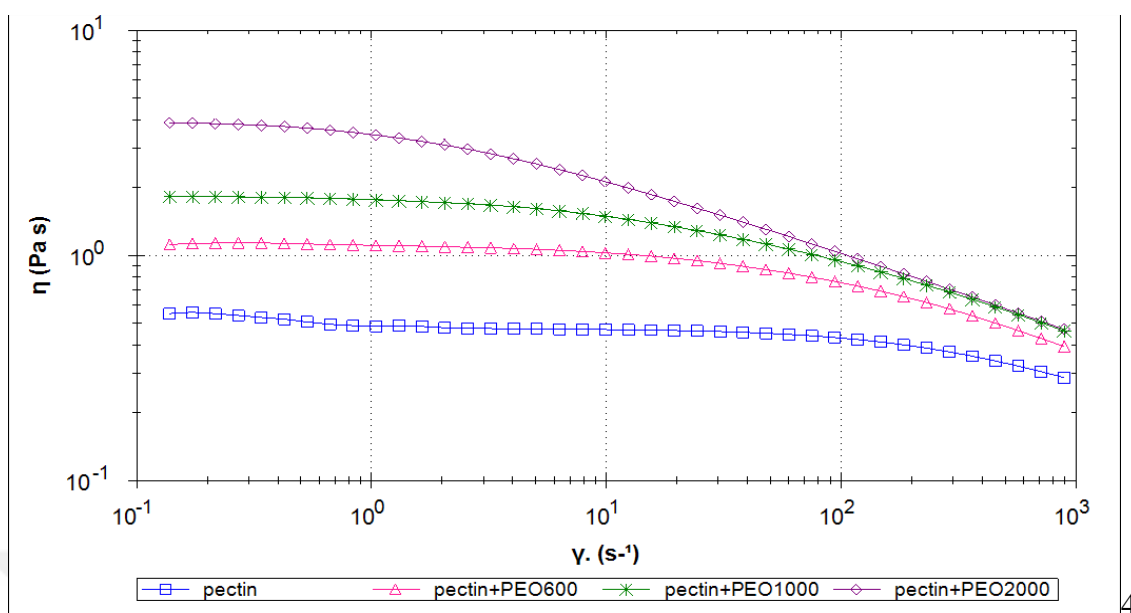
Figure 3.3. The flow curves of polymer solutions composed of 1 wt% PEO and 5 wt% pectin. (Representative graphs from the three replicates are given, statistics are presented in Table 3.2).

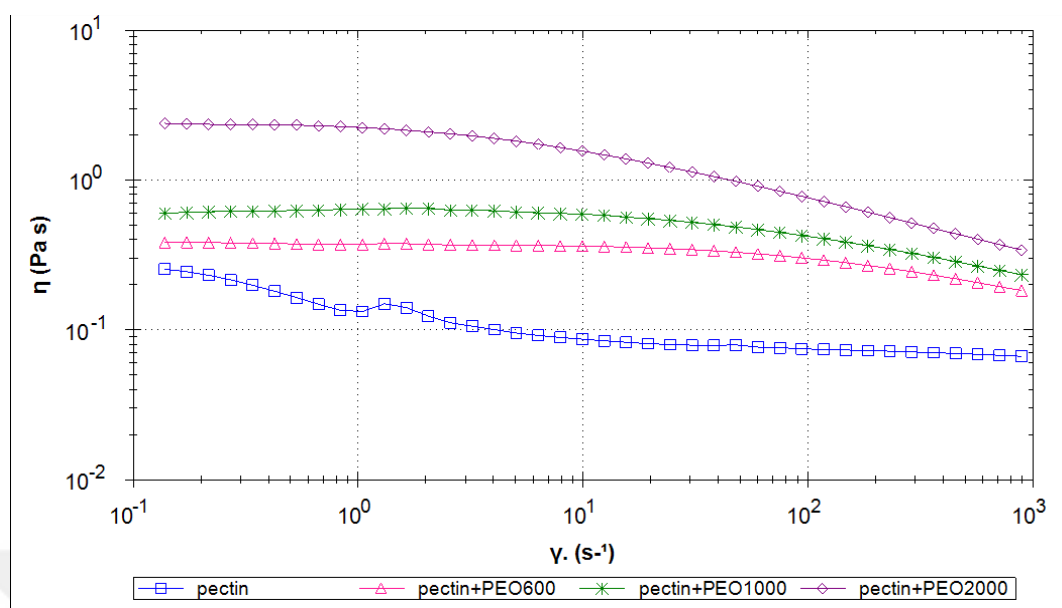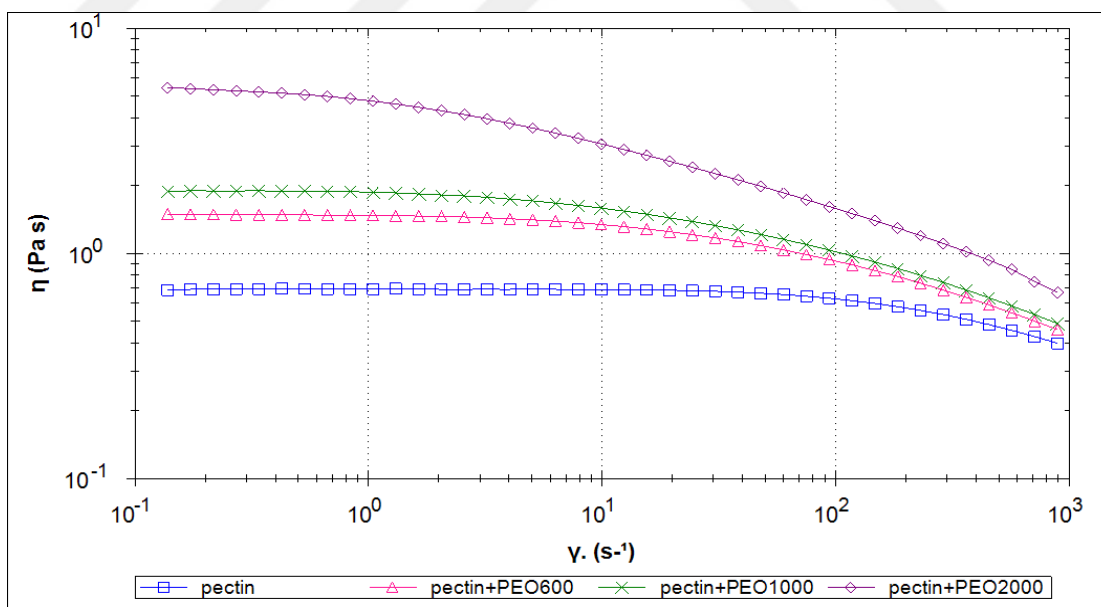Figure 3.4. The flow curves of polymer solutions composed of 1 wt% PEO and 6 wt% pectin. (Representative graphs from the three replicates are given, statistics are presented in Table 3.2).
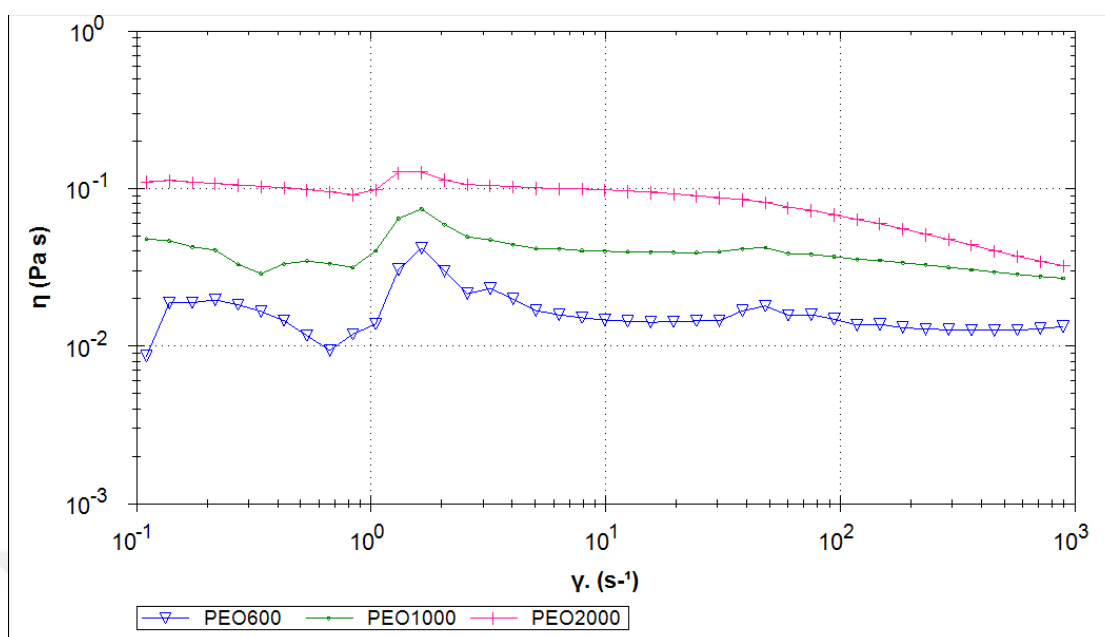
Figure 3.5. The flow curves of polymer solutions composed of 1 wt% PEO. (Representative graphs from the three replicates are given, statistics are presented in Table 3.2).

Figure 3.6-3.9 shows the elastic modulus (G') values of the polymer solutions. Since blends are extended by the electrical field during the electrospinning process, for a comparison under the conditions similar to the process itself, elastic modulus (G') and phase angle (δ) values were determined from the response of fiber forming solutions to percent strain and the average of G' values under 1-10 percent strain are given in Table 3.2. As can be seen in Table 3.2, when PEO_{2000} was blended with pectin solutions, the elastic modulus values increased significantly at all pectin concentrations. This could be attributed to the more stable structure of PEO_{2000}, as evidenced by a longer range of percent strain where the G' value stays constant (Figure 3.10). Moreover, since higher molecular weight means longer chain length, the number of weak interactions between pectin and PEO chains (hydrophobic interactions, van der Waals interactions and hydrogen bonds) would increase. As a result of more interactions, a more stable system, thus higher G' values were attained when PEO_{2000} was used.

The phase angle (δ) of all pure pectin, pure PEO, and pectin-PEO blends were higher than 45° for all pectin concentrations (Table 3.2). Thus, the liquid-like character was dominant for all solutions[116]. However, increasing the molecular weight of PEO in the blends

mostly increased the elastic behavior, which was evidenced by a decrease in the δ. The δ values of blends containing PEO_{2000} were significantly lower than other blends at all pectin concentrations.

Our results also showed that the cohesive energy of the solutions was increased as pectin concentration increased. Moreover, with the rise in the M_w of PEO, the cohesive energy increased significantly at all pectin concentrations. It can be once again attributed to the increase in the number of weak physical bonds (van der Waals and hydrophobic interactions, also hydrogen bonds) between PEO and pectin chains as the chain length of PEO increased with M_w. Moreover, the higher crystallinity of PEO[78] might be another underlying reason for the increased cohesive energy. Presence of more physical bonds and increased crystallinity means that more energy is required to destabilize the system. Since the cohesive energy is a measure of the internal structure (the bonding strength), higher cohesive energy values can be indicative of a more stable system.

Table 3.2. Rheological properties of polymer solutions

Polymer concentration (wt %)			Zero Shear Viscosity‡ (Pa.s)	Tip Viscosity**‡ (Pa.s)	Elastic Modulus‡ G'(Pa)	Phase Angle‡ (δ)	Cohesive Energy***,‡ (Pa)	Fiber	Fiber Diameter‡ (nm)
Pectin	PEO*	Total							
0	PEO_{600}	1	0.02±0.00	0.03±0.01	0.29±0.16	44.42±3.37	1244.9±127.1	Mostly Bead	-
	PEO_{1000}	1	0.03±0.00	0.04±0.00	0.27±0.04	63.45±4.63	1293.0±15.68	Mostly Bead	-
	PEO_{2000}	1	0.11±0.01	0.12±0.01	0.30±0.1	72.44±2.00	1898.4±7.87	Mostly Bead	-
3	-	3	0.09±0.01[a]	0.16±0.02[a]	0.13±0.01[a]	80.21±0.02[a]	311.6±65.78[a]	No jet	-
	PEO_{600}	4	0.45±0.09[a]	0.57±0.19[a]	0.49±0.02[a]	82.03±0.07[b]	2250.9±8.1[b]	Beaded	155±20.2[a]
	PEO_{1000}	4	0.64±0.01[a]	0.62±0.02[a]	1.10±0.11[a]	77.41±0.82[b]	2307.3±63.3[b]	Beaded	202±24.5[b]
	PEO_{2000}	4	2.14±0.20[b]	1.92±0.30[b]	4.74±0.71[b]	63.69±1.00[c]	4708.2±58.5[c]	Smooth	240±21.3[b]
4	-	4	0.20± 0.03[A]	0.20±0.01[A]	0.16±0.03[A]	85.22±0.76[A]	489.1±56.1[A]	No jet	-
	PEO_{600}	5	0.69±0.07[A]	0.66±0.04[A]	0.84±0.07[A]	81.01±0.2[B]	2460.5±130.8[B]	Beaded	160±21.0[A]
	PEO_{1000}	5	1.13±0.09[A]	1.06±0.02[A]	1.93±0.08[A]	75.88±0.77[C]	3533.9±132.0[C]	Beaded	208±25.3[B]
	PEO_{2000}	5	3.87±0.86[B]	2.77±0.50[B]	7.04±1.04[B]	61.76±0.11[D]	5594.4±267.4[D]	Smooth	254±32.6[C]
5	-	5	0.52±0.06[α]	0.40±0.04[α]	0.41±0.02[α]	84.56±0.95[α]	1273.7±89.08[α]	No jet	-

	PEO$_{600}$	6	1.44±0.13$^{\alpha,\beta}$	1.27±0.17$^{\alpha,\beta}$	1.84±0.29$^{\alpha}$	78.95±0.77$^{\alpha,\beta}$	3206.6±91.3$^{\beta}$	Beaded	165±22.5$^{\alpha}$
	PEO$_{1000}$	6	2.00±0.14$^{\beta}$,	1.67±0.09$^{\beta}$	3.12±0.25$^{\alpha,\beta}$	75.08±0.53$^{\beta}$	5719.2±180.5$^{\gamma}$	Beaded	212±32.0$^{\beta}$
	PEO$_{2000}$	6	4.98±0.34$^{\theta}$	3.66±0.30$^{\theta}$	6.04±1.34$^{\beta}$	65.37±1.56$^{\gamma}$	8539.4±62.4$^{\theta}$	Smooth	260±30.2$^{\beta}$
6	-	6	1.00±0.05$^{\Phi}$	0.66±0.03$^{\Phi}$	0.60±0.16$^{\Phi}$	85.23±0.89$^{\Phi}$	1649.3±241.2$^{\Phi}$	No jet	-
	PEO$_{600}$	7	1.36±0.06$^{\Phi}$	1.33±0.14$^{\Phi,\upsilon}$	2.04±0.34$^{\Phi}$	79.02±1.09$^{\Phi,\upsilon}$	3337.2±71.7$^{\upsilon}$	Beaded	165±19.5$^{\Phi}$
	PEO$_{1000}$	7	2.49±0.68$^{\Phi}$	1.97±0.11$^{\upsilon}$	4.64±1.35$^{\Phi}$	74.68±1.10$^{\upsilon}$	8916.8±57.7$^{\int}$	Beaded	224±25.6$^{\upsilon}$
	PEO$_{2000}$	7	5.41±0.56$^{\upsilon}$	4.28±0.09$^{\int}$	11.13±1.84$^{\upsilon}$	64.60±1.22$^{\int}$	10310.5±895.9$_{\S}$	Smooth	265±20.8.$^{\int}$

* PEO was constant at 1 (wt%). ** The tip viscosity was found by using Equation 1. ***The cohesive energy was calculated by using Equation 2. ‡ Each pectin concentration was statistically analyzed by groups.

Figure 3.6. The response of the polymer solutions to % strain. The solutions are composed of 1 wt% PEO and 3 wt% pectin. (Representative graphs from the three replicates are given, statistics are presented in Table 3.2).

Figure 3.7. The response of the polymer solutions to % strain. The solutions are composed of 1 wt% PEO and 4 wt% pectin. (Representative graphs from the three replicates are given, statistics are presented in Table 3.2).
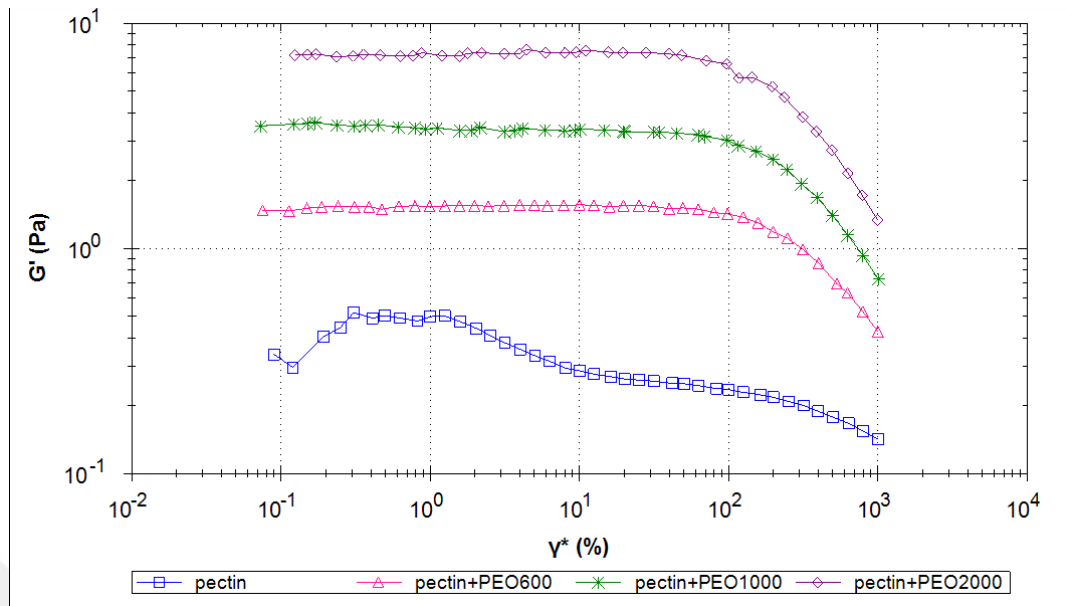
Figure 3.8. The response of the polymer solutions to % strain. The solutions are composed of 1 wt% PEO and 5 wt% pectin. (Representative graphs from the three replicates are given, statistics are presented in Table 3.2).
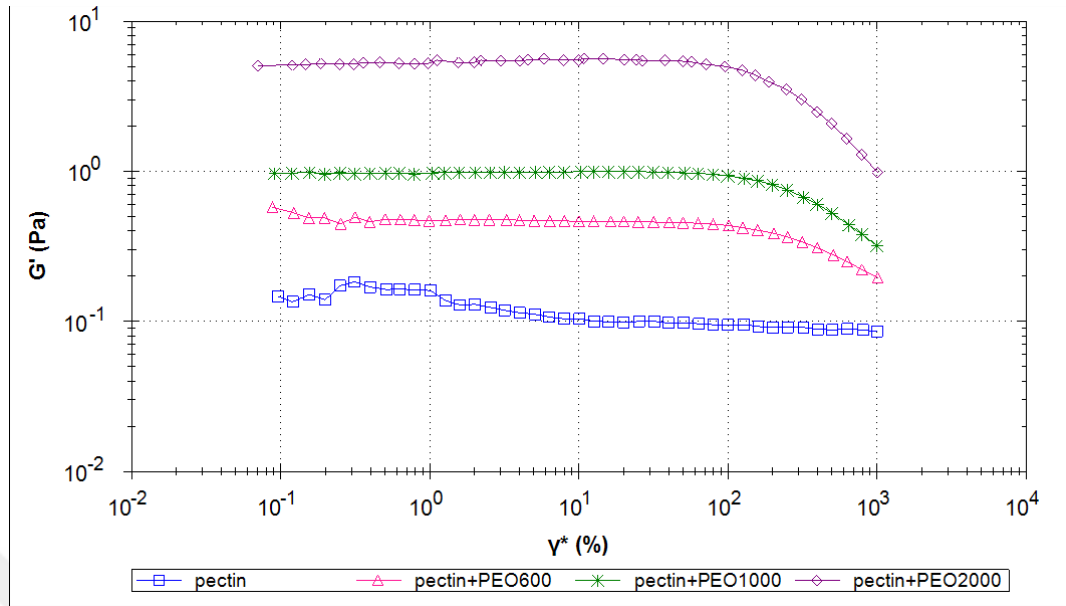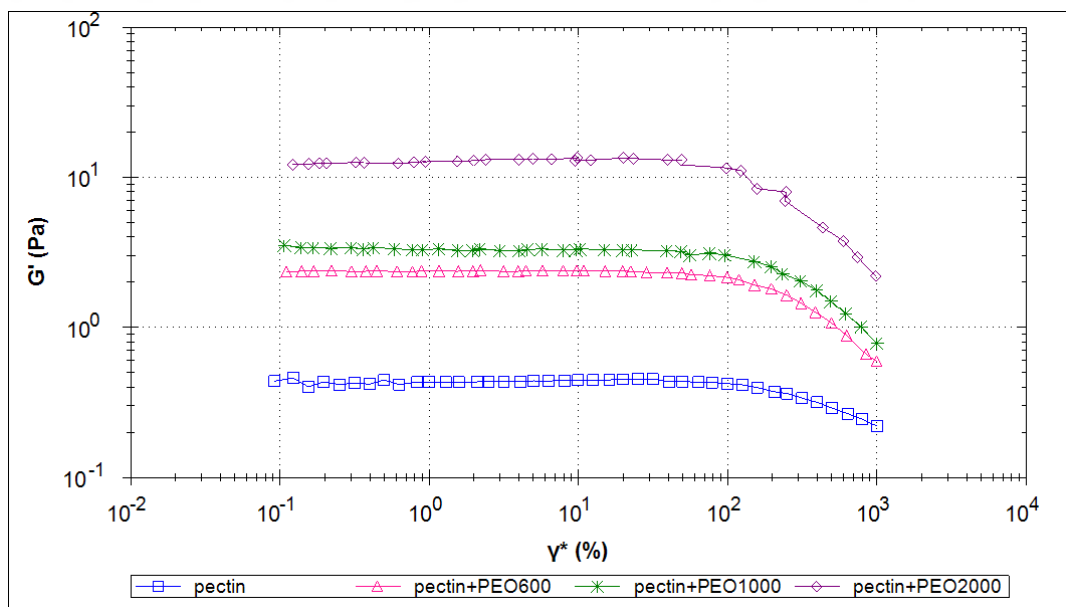

Figure 3.9. The response of the polymer solutions to % strain. The solutions are composed of 1 wt% PEO and 6 wt% pectin. (Representative graphs from the three replicates are given, statistics are presented in Table 3.2).
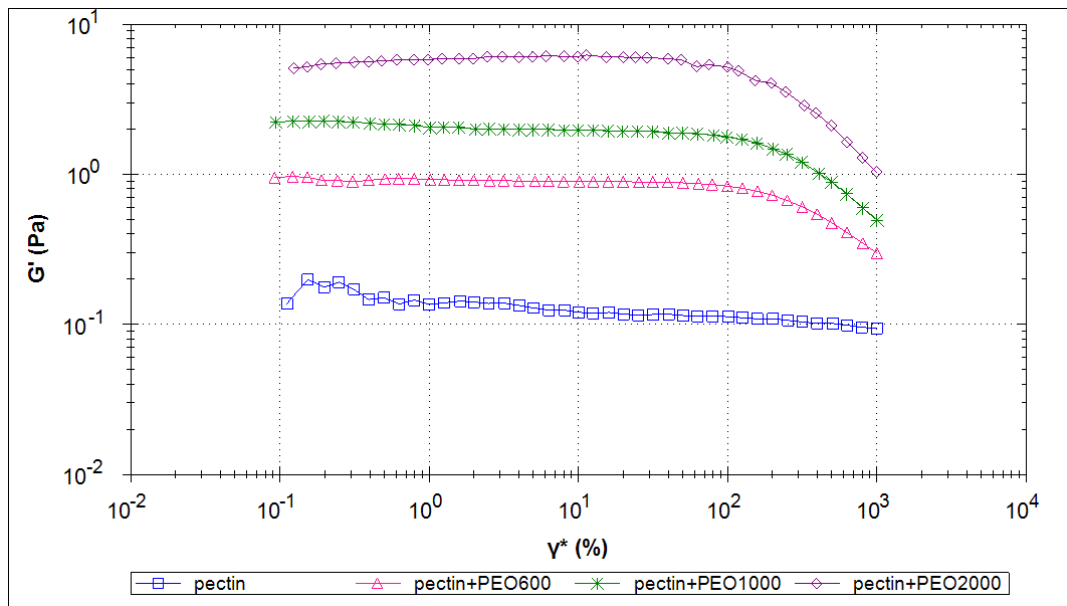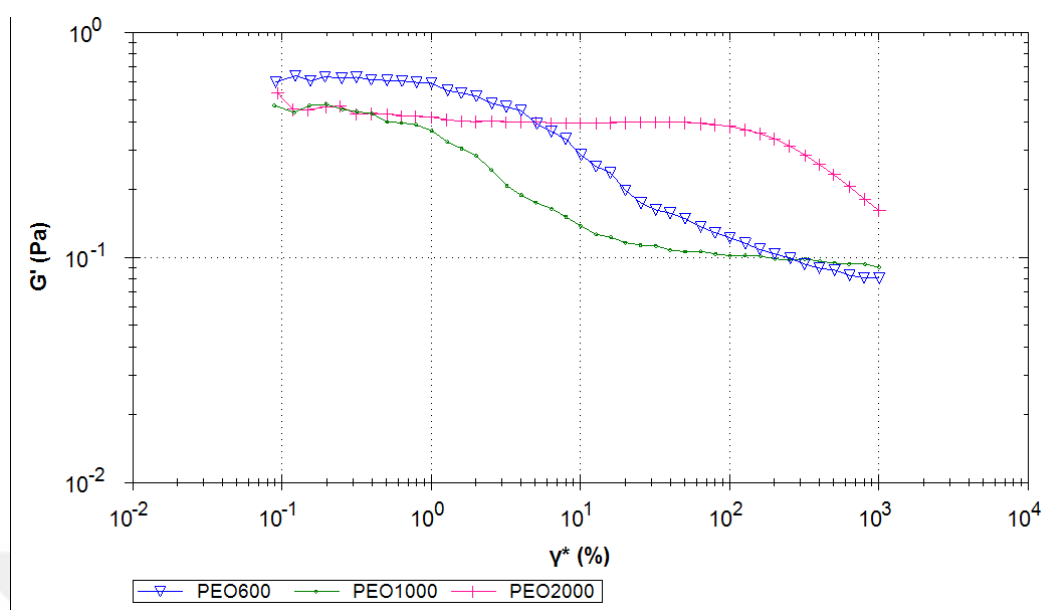
Figure 3.10. The response of the polymer solutions to % strain. The solutions are composed of 1 wt% PEO. (Representative graphs from the three replicates are given, statistics are presented in Table 3.2).

3.1.3. Effect of Solution Properties on Fiber Formation and the Morphology of Pectin-PEO Nanofibers

LM pectin solutions at concentrations between 2-12 wt. percent were initially tested but they resulted with only discontinuous drops instead of stable and continuous jets under applied voltage, indicating the non-existence of any sufficient chain entanglement[79, 102, 125]. On the contrary, from the electrospinning of 1 wt. percent PEO, the jet was obtained, however the fibers were obtained in mostly beaded morphology as seen in Table 3.3. This result suggests that viscosity of the solution is not an indication of jet formation, since PEO solutions formed jets despite of their very low viscosities while pectin-only solutions could not even at higher viscosities (Table 3.2).
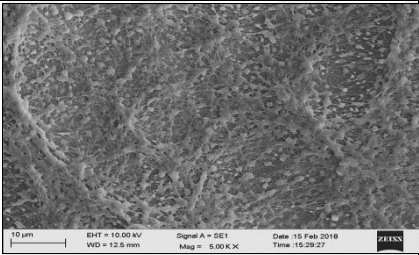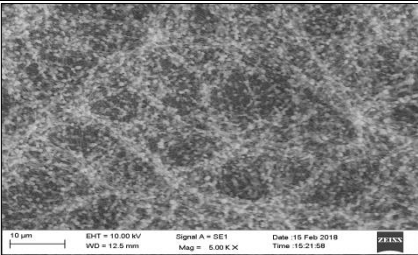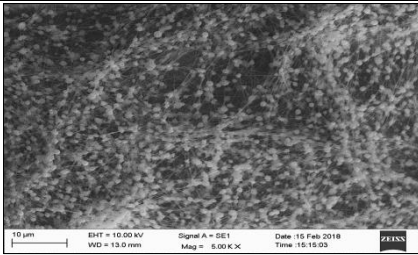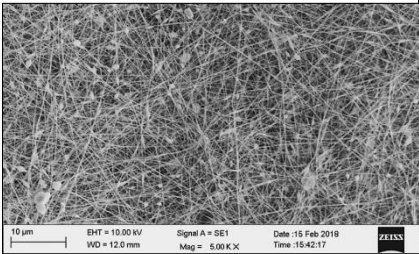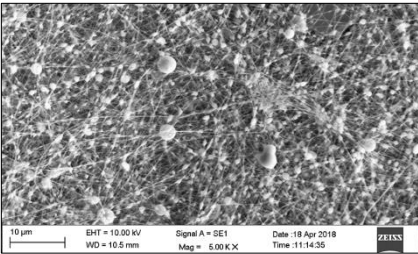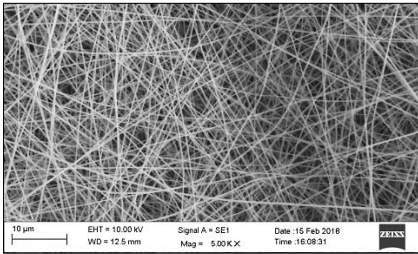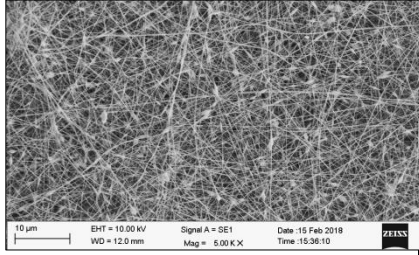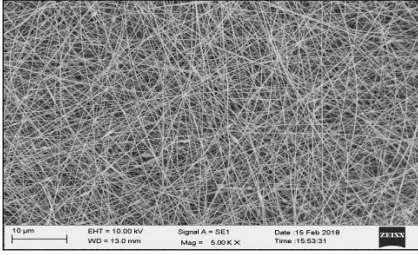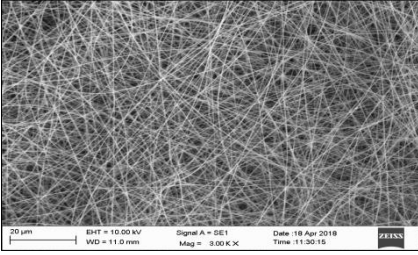
From the electrospinning of pectin and PEO blend solutions, stable jet was attained, and the fibers were collected as a mesh on the collector plate. Rigidity and low elasticity are the main limiting factors for biopolymers that prevent fiber formation[79]. Addition of PEO might have helped reducing the repulsive forces among negatively charged pectin chains, which in turn promoted chain entanglement and fiber formation as in the case of

other charged biopolymers[78, 103, 118]. The blends of pectin- PEO_{600} and pectin-PEO_{1000} were resulted with the formation of beaded nanofibers. Nevertheless, non-beaded and continuous nanofiber formation was observed at any pectin concentrations of pectin-PEO_{2000} blends (Table 3.3). In order to further elucidate this finding, the effect of each solution property on fiber formation and fiber morphology is discussed below.

The conductivity of PEO-pectin blends used in this study varied from 2.48 to 4.43 mS/cm (Table 3.1). In the literature, conductivity values were found to be associated with the fiber formation and fiber diameter[50, 126]. Spinning solutions (especially from synthetic polymers) are expected to have low enough conductivity values to achieve non-beaded nanofibers[127]. However, our results showed that in the case of PEO-pectin blends, conductivity could not be directly related to smooth fiber formation (Table 3.1 and Table 3.2). As an example, while the blend composed of 3 percent pectin and PEO_{600} formed beaded fibers, the blend composed of 3 percent pectin and PEO_{2000} formed non-beaded fibers despite the fact that their conductivity values were not significantly different. A similar trend was observed at other pectin concentrations as well. Moreover, since pH values of all solutions were similar to each other, it can be assumed that there was no change in the rigidity of pectin that would affect fiber formation and morphology.

Previous work in the literature indicated that polymer solutions need to have a surface tension that is low enough to maintain jet initiation during electrospinning process. In our study, PEO addition to pectin solutions did not lower the surface tension; on the contrary increased SFT at lower pectin concentrations. Despite the fact that pectin-PEO blends were able to form nanofibers while pectin only solutions could not. Our results showed that, pH, conductivity, and surface tension of the blends with PEO_{2000} did not significantly differ from other blends at the same pectin concentration. For this reason, these parameters cannot explain why smooth and non-beaded fibers can only be achieved when PEO_{2000} was used.

Table 3.3. Morphological results of nanofibers produced from polymer solutions composed of pectin (0, 3, 4, 5 and 6 wt%) and 1 wt% PEO with different molecular weights (600, 1000 and 2000 kDa).

Pectin (wt/v)	PEO* Molecular Weight		
	600 kDa	1000 kDa	2000 kDa
0			
3			
4			

5			
6			
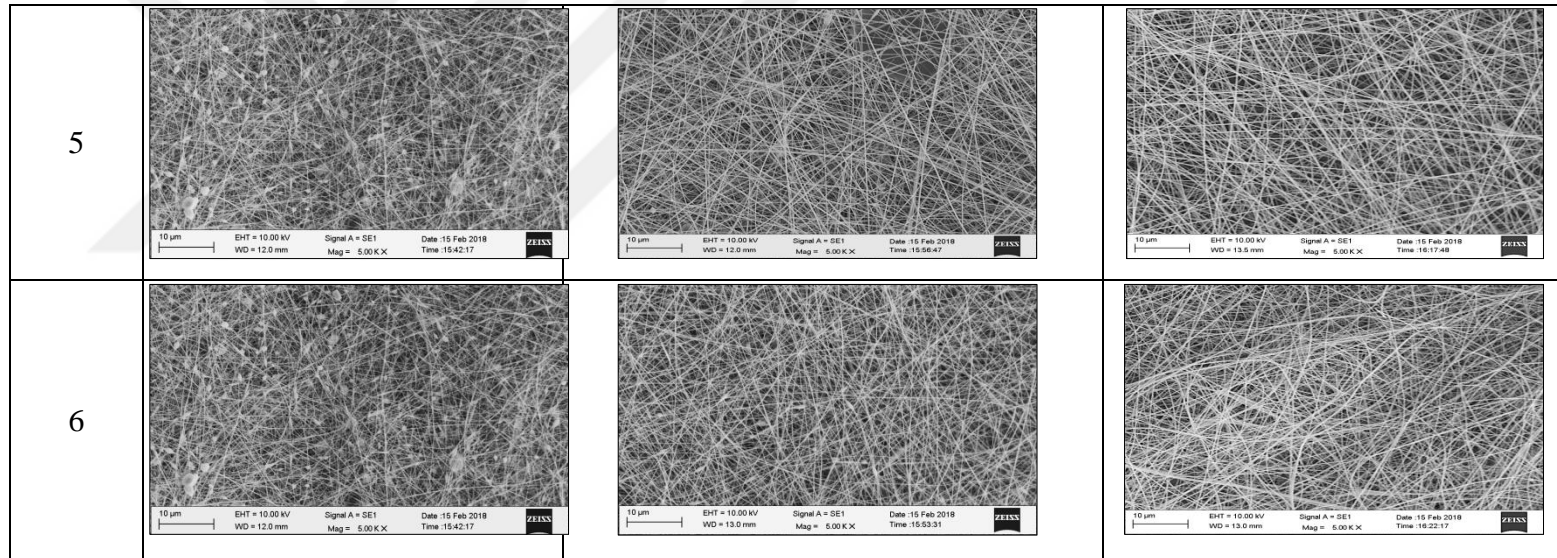
*PEO concentration was the same for each blends (1 wt%).

Among the blends, those with PEO_{2000} exhibited the most zero shear and tip viscosities as given in Table 3.2, which indicated more entanglement favoring the electrospinning process. Studies in the literature support the effect of high molecular weight on fiber formation and diameter[35, 128, 129]. It has been announced that the solution viscosity has a very influencing effect on the formation of smooth nanofibers. When the viscosity is high the Rayleigh and varicose instability are inadequate. Consequently, when the whipping instability is dominant, it inhibits the bead formation[130]. Among the three types of jet instability that cause the bead formation, the Rayleigh instability is occurred by the surface tension, whereas the varicose and whipping instability are produced by the self-features of electricity (i.e. the charge density on the jet which is associated to the conductivity of the polymer solution)[28, 45, 48, 131]. Since SFT and conductivity values of smooth and beaded fibers have not been changed significantly, and the applied voltage was constant, it is postulated that all jets encountered similar Rayleigh and varicose instabilities. This suggests that one of the reasons for formation of smooth nanofibers from blends containing PEO_{2000} was the dominant whipping instability resulted from chain entanglements evidenced by significant elevation of zero and tip viscosities. Moreover, the onset of shear thinning was found to be early for these blends (Figure 3.1-3.4), which might have enhanced the jet stability during electrospinning process. In addition to this, our results indicated, when pectin concentration was the same, elastic modulus raised by increasing the chain length of PEO (Figure 3.6-3.9 & Table 3.2).

Previous studies also support that high elasticity is needed for a polymer to be electrospun[31, 32, 45]. However, when we examined our data more closely, we concluded that the definition of 'elasticity' is critical for a successful electrospinning process. Although, at all pectin concentrations, the including PEO_{2000} to pectin solution increased the elasticity as the most significantly, but only G' values would not be enough for making a conclusion about non-beaded and continuous fiber formation. As can be seen in Table 3.2, G' values of beaded fibers (e.g. 6 percent pectin-PEO_{1000}) might be similar to G' values of smooth fibers (e.g. 3 percent pectin-PEO_{2000}). We believe that, in addition to G', another parameter, the phase angle, is important for smooth fiber formation. PEO_{2000} having blend solutions showed the lowest phase angles (61.76-65.37) among other blends and the pure pectin solutions, which might be the underlying reason for non-beaded fiber formation. On the other hand, only low phase angle values did not indicate a successful

electrospinning process as in the case of PEO-only solutions. PEO-only solutions had low phase angles but, since they also had very low G' values, beaded structure was obtained. For this reason, we concluded that high elastic modulus values are required together with low phase angle values for a solution to be electrospun into non-beaded continuous fibers.

The diameter of pectin nanofibers, which increased with the rise in the PEO M_w, varied between average values of 155 to 265 nm (Table 3.2). Our results indicated that the increase in pectin concentration in blends did not have an effect on fiber diameter (Table 3.2). However, enhancing the PEO chain length from 600 kDa to 1000 kDa resulted in a significant rise on the fiber diameter at all pectin concentrations.

Although smooth and uniform nanofiber formation is mostly desired in many applications[132], bead-on-string nanofibers also have potential in different applications such as drug deliver and air or water filtration[54, 133]. Regardless of the final fiber morphology desired (beaded or smooth)[77, 130, 134, 135], a thorough understanding of the effects of SFT, conductivity and rheological properties of the spinning solutions would make it possible to develop prescribed nanofibers tailored for specific needs.

3.2. THE DEVELOPMENT OF PECTIN NANOFIBERS FOR FOOD PACKAGING APPLICATIONS

3.2.1. Preparation of Electrospun Pectin-Based Fibers

The morphology of the resultant electrospun fibers, which were prepared in the compositions of according to Table 2.2, is shown in Figure 3.11. A solution of pure pectin was initially also tested but, instead of continuous jets, it formed large droplets when subjected to high voltages during electrospinning due to the limited viscoelasticity and insufficient chain entanglements of the carbohydrate as explained before. Therefore, in order to increase the viscoelasticity of pectin, different quantities of PEO_{2000} from 0.1 wt. percent to 1 wt. percent were added to the pectin solutions for electrospinning, the here so-called S1 to S4. The primary intention was to keep the PEO_{2000} content at a minimum value in order to produce electrospun fibers with the highest content of pectin. In Figure 3.11a it can be seen that the electrospinning of the pectin solution having 0.1 wt. percent

PEO_{2000}, that is, S1, resulted in fibers with a discontinuous and beaded morphology. The fibers produced from S2, shown in Figure 3.11b, which is based on 0.25 wt. percent PEO_{2000}, were continuous and non-beaded but the resultant electrospun mat showed poor integrity. In the case of S3, made of a pectin solution with 0.5 wt. percent PEO_{2000}, neat fibers free of beads and with a uniform diameter were produced as it can be observed in Figure 3.11c. Branched and thick pectin fibers were obtained for the electrospinning of S4, which contained 1 wt. percent of PEO_{2000} and are shown in Figure 3.11d. This results confirms that the use of a carrier polymer in an appropriate amount is a key parameter in order to achieve continuous and non-defected fibers during electrospinning. Based on these results, S3 was selected due to it contained the optimal amount of PEO_{2000} that yielded the fibers with the highest uniformity and a relatively low diameter, whereas S1, S2, and S4 were discarded from the study. In order to improve the film-forming capacity of the electrospun pectin mats, different types and amount of plasticizers were also tested. Therefore, glycerol or PEG_{900} were added to the pectin solution based on the S3 composition in which the PEO_{2000} content was kept constant at 0.5 wt. percent. One can observe in Figures 3.11e-j that similar morphologies, based on smooth and continuous fibers but slightly thinner in the case of PEG_{900}-containing fibers, were generated when the plasticizers were added. The average diameters of the electrospun pectin-based fibers are summarized in Table 3.4.

The solution properties were determined to better understand the morphologies of the attained electrospun mats of the ultrathin pectin-based fibers. The values of viscosity, surface tension, and conductivity of the fiber-forming solutions are also given in Table 3.4. For the non-plasticized solutions, that is, S1–S4, viscosity of the pectin-based solutions increased significantly when the amount of PEO_{2000} was increased. One can observe that the addition of plasticizers did not create any significant difference in the solution viscosity. Even when the content of glycerol or PEG_{900} was increased to 3 wt. percent, the solution viscosity did not change considerably, showing a value around 6000–6400 cP. The surface tension slightly increased from approximately 29 mN/m to values in the range of 31–33 mN/m when the PEO_{2000} content was increased above 0.5 wt. percent. It can be also observed that, due to the inherent polyelectrolyte nature of pectin [136], its aqueous solutions were highly conductive, showing values in the 6-7 $\mu S^{\cdot}cm$ range. However, the conductivity values decreased up to values close to 4 $\mu S^{\cdot}cm$ when the PEO_{2000} content was

increased and, particularly, when the plasticizers were added since the amount of pectin in the solution was reduced. Therefore, the present results suggest that the fiber formation was attained due to a combined effect of viscosity increase and conductivity decrease. The optimal values were particularly attained in the range of ~5500–6500 cP and ~5-6 µS·cm of viscosity and conductivity, respectively. Therefore, moderate-to-high viscosities in combination with relatively low conductivities tended to produce the most optimal fibers morphology, while the effect of surface tension was negligible[137].

In relation to the plasticizers, one can observe that the diameters of the fibers varied from 156±33 nm to 329±42 nm, which could be related to differences in the solution properties described above. Significantly thicker fibers were obtained with the increase in the PEO content for the non-plasticized samples due to the change in solution properties. This finding was explained by Alborzi et al.[118] by the fact that the incorporation of plasticizers, especially of glycerol, can lead to thicker fibers due to it favors molecular entanglements. A similar phenomenon was also reported by Cui et al.[138]. Also, glycerol-plasticized solutions resulted in fibers with higher diameters than those obtained from PEG_{900}-plasticized solutions. For example, if one compares the solutions containing 2.5 wt. percent of plasticizer, which were termed as S5 and S8, the glycerol-containing ones yielded fibers with an average diameter of 272±43 nm, while the solutions with PEG_{900} produced fibers in the range of 189±40 nm. As mentioned earlier, electrospinning of the 1 wt. percent PEO containing solution, that is, S1, resulted in pectin-based fibers with a discontinuous and beaded morphology, which is a consequence of the formation of solution with low viscosity and high conductivity.
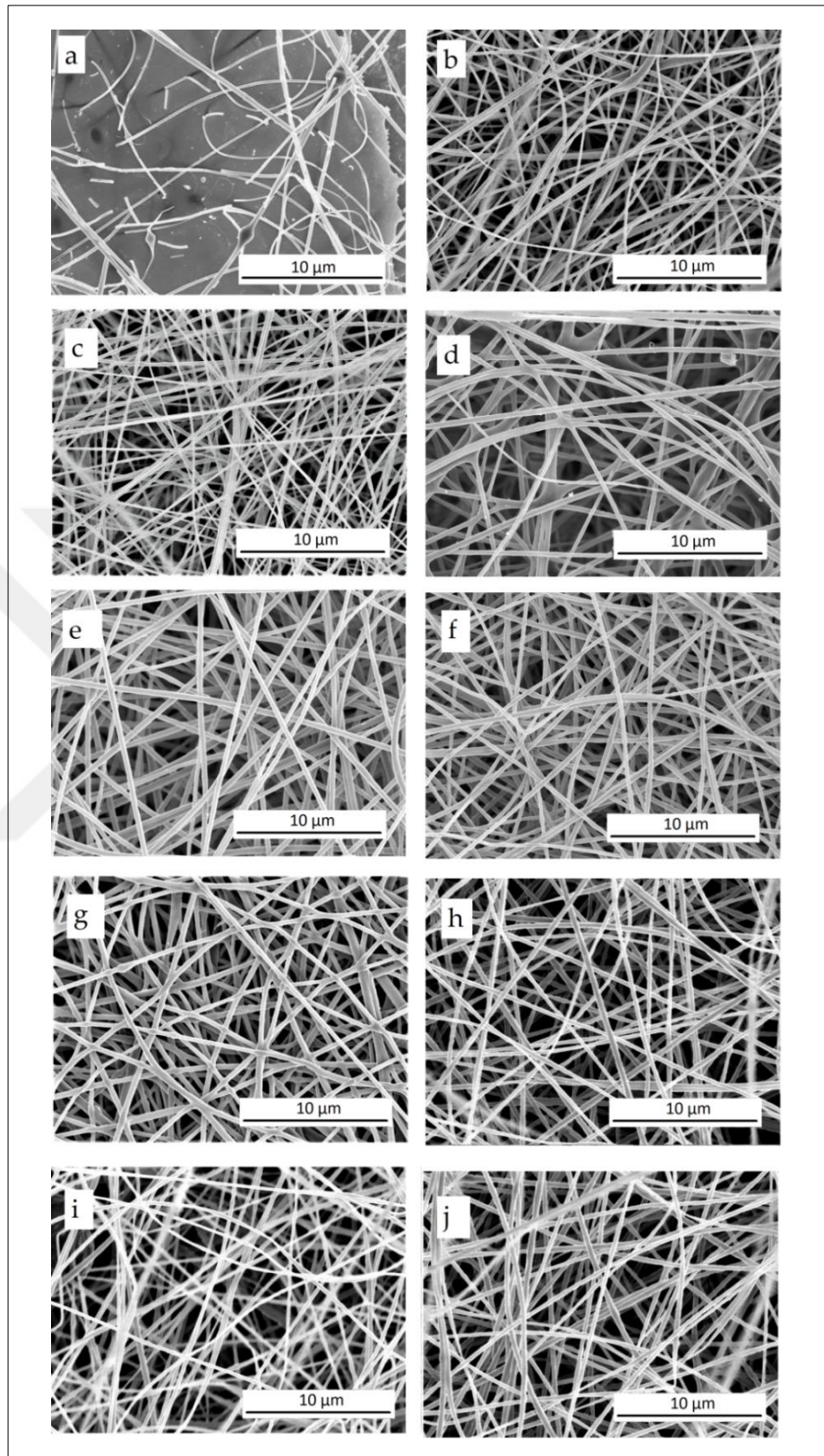
Figure 3.11. Scanning electron microscopy (SEM) images of the electrospun mats obtained from the pectin-based solutions of: (a) S1, (b) S2, (c) S3, (d) S4, (e) S5, (f) S6, (g) S7, (h) S8, (i) S9, (j) S10.

Table 3.4. Solution properties and diameters of pectin based electrospun fibers.

Solution ‡	Viscosity (cP)	Surface tension (mN/m)	Conductivity (µS·cm)	Fiber diameter (nm)
S1	1892 ± 78^a	28.8 ± 0.2^a	7.25 ± 0.12^a	-
S2	3066 ± 48^b	28.4 ± 0.3^a	$6.37 \pm 0.15^{a,b}$	156 ± 33^a
S3	$5950 \pm 219^{c,e}$	$30.3 \pm 0.2^{b,d}$	6.10 ± 0.10^c	186 ± 32^b
S4	12155 ± 1660^d	32.9 ± 0.2^c	$5.99 \pm 0.25^{b,c}$	299 ± 41^c
S5	5511 ± 299^c	$31.6 \pm 0.2^{b,e,f}$	$5.64 \pm 0.37^{c,d}$	272 ± 43^d
S6	5751 ± 401^c	$30.9 \pm 0.3^{d,e}$	$5.30 \pm 0.13^{c,d}$	$304 \pm 56^{c,d}$
S7	$6440 \pm 327^{c,e}$	$32.1 \pm 0.2^{g,f}$	$4.98 \pm 0.09^{c,d}$	$329 \pm 42^{c,d}$
S8	6047 ± 219^e	31.2 ± 0.3^e	$5.11 \pm 0.20^{c,e}$	189 ± 40^b
S9	6106 ± 124^e	31.1 ± 0.3^e	4.82 ± 0.21^e	197 ± 44^b
S10	6317 ± 364^e	$32.5 \pm 0.2^{g,c}$	4.72 ± 0.22^e	223 ± 33^b

‡ Statistical analysis was performed within each column.

3.2.2. Thermal Properties of Electrospun Pectin-Based Fibers

The DSC curves corresponding to the cooling and second heating steps of the as-received PEO_{2000} and pectin powders and the electrospun pectin fibers obtained from S3 to S10 are gathered in Figure 3.12. During the cooling process, shown in Figure 3.12a, it was observed that PEO_{2000} crystallized from the melt showing a crystallization temperature (T_c) of approximately 40 ˚C[150]. Alternatively, the pectin powder showed no crystallization during cooling in the whole tested thermal range. The crystallization peak attributed to PEO_{2000} was not observed in the electrospun PEO_{2000}-containing pectin fibers due to its relative low content. However, a small exothermic peak was observed at approximately 23 ˚C for the electrospun pectin fibers obtained from S10, which can be attributed to the crystallization of the PEG_{900} confined in the carbohydrate[150, 151]. In Figure 3.12b one can observe the melting temperature (T_m) of PEO_{2000} at approximately 68 ˚C and also two low-intense melting peak corresponding to the melting of the PEG_{900} fraction in the pectin fibers obtained from S10 at approximately 24 ˚C and 40 ˚C[151].

Figure 3.12. The diagram of (a) cooling, (b) 2nd heating DSC results of pectin powders, PEO powders and fibers.

Pectin did not exhibit any thermal transition of first order, that is, crystallization or melting, thus confirming the carbohydrate is fully amorphous[89, 149]. Moreover, no glas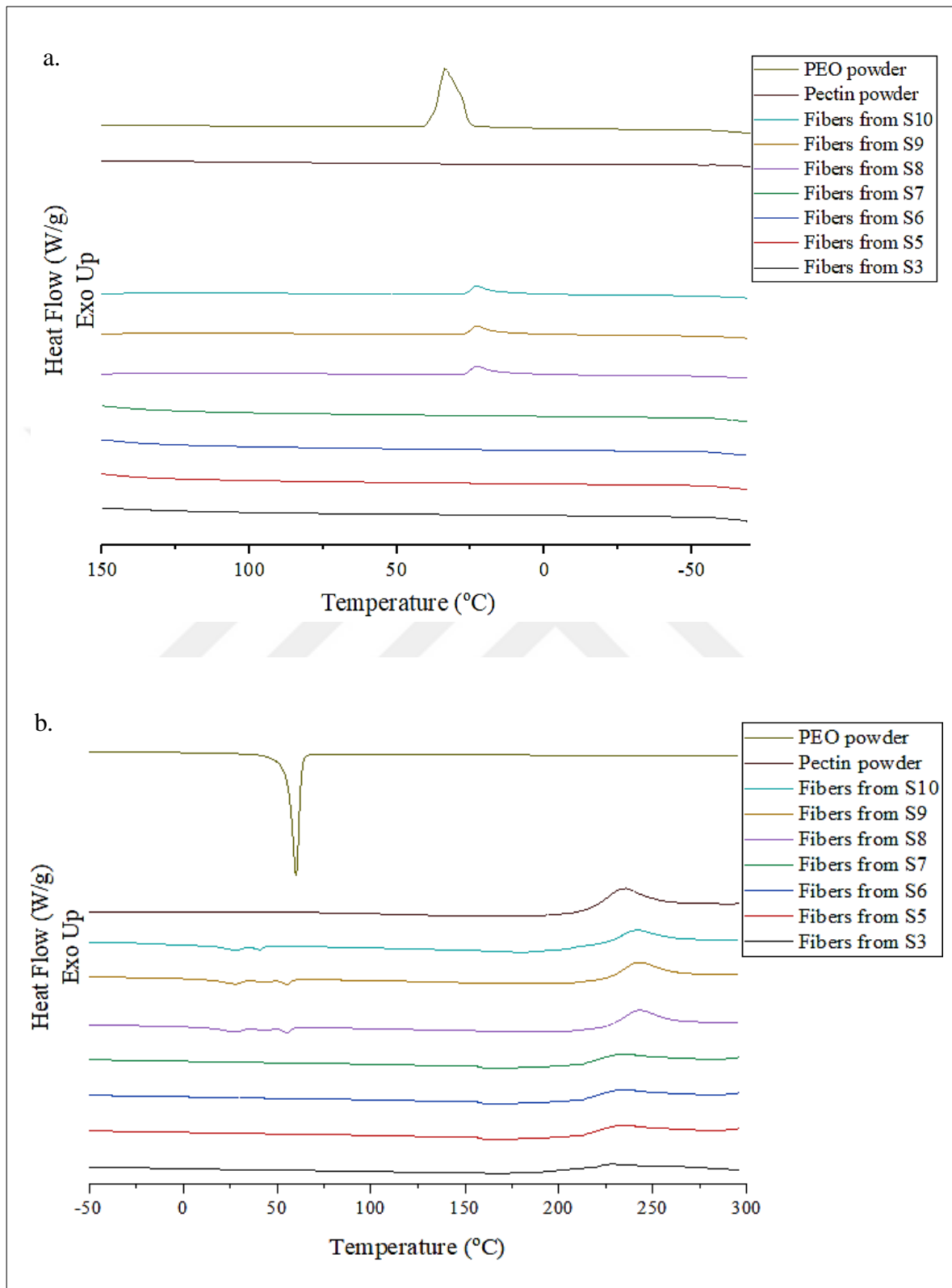s transition was observed up to nearly 230 ˚C, temperature from which the carbohydrate started thermal degradation. Previous studies on the thermal properties of pectin reported that thermal degradation of this carbohydrate is an exothermic process[149, 152]. It is worthy to note that the degradation temperature (T_{deg}) of pectin shifted from 232 ˚C, for the neat powder, to 236 ˚C, for the electrospun fibers obtained from S10, which suggests that the thermal stability of the carbohydrate was slightly enhanced by the addition of PEG_{900}.

The TGA curves of the neat pectin and PEO_{2000} powders as well as the electrospun pectin-based fibers are shown in Figure 3.13. The most relevant thermal parameters obtained from the TGA curves are given in Table 3.5. One can notice that pectin exhibited three significant main weight losses, occurring at approximately 100 ^{o}C, 217 ^{o}C, and 240 ^{o}C. The first mass loss, which occurred in the 75–110 °C range, can be ascribed to the removal of bound water from the carbohydrate due to it is highly hydrophilic. In this regard, Gloyna et al. (1998) indicated that water evaporation observed between 50 °C and 150 °C, with a maximum at 100 °C, is identical to the dehydration process of other polysaccharides[139]. Kastner et al. (2012)[140] and Nisar et al. (2018)[141] also observed a second weight loss between 195−350 °C. According to their studies, pectin shows a two-step degradation process in this range. The pectin has lost approximately 60 percent of its weight till 350°C whereas, in the range of 350−697 °C, it loses 15 percent of its original weight and the maximum amount of weight loss was obtained around 235 °C. During thermal degradation the carbohydrate faces with different depolymerization reactions, including demethoxylation, depolymerization by backbone hydrolysis and hydrolytic cleavage of neutral sugar side chains[156, 157, 158]. Depending on pectin properties, that is, pH, source, degree and pattern of methyl esterification, acid hydrolysis or β-elimination reactions take place[159]. In particular, the here-used LM pectin results in acid hydrolysis reactions with the temperature increase[160, 161]. Above 250 °C, a secondary degradation of pectin occurs, including release of functional side groups and chains break. Finally, gasification of char residues arises at temperatures around 600 °C[162].
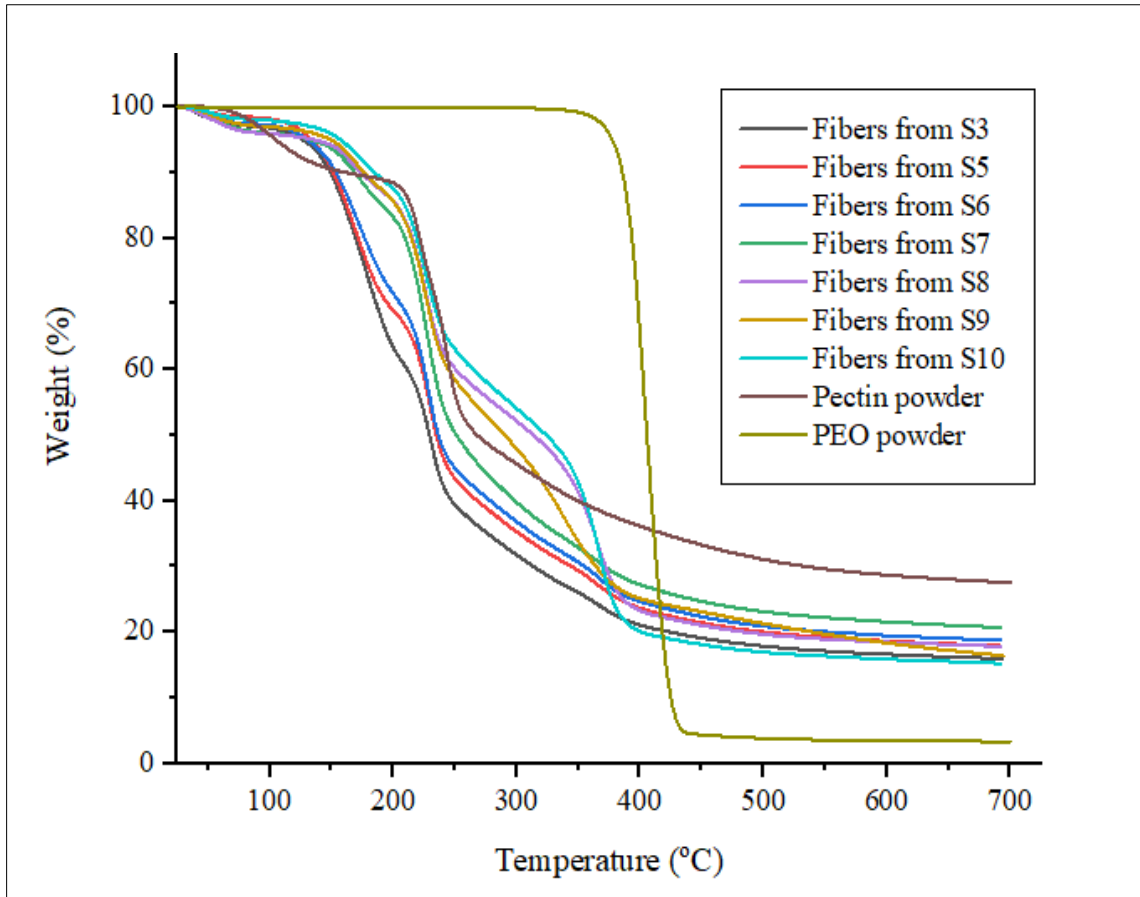
Figure 3.13. Thermogravimetric analysis (TGA) curves of the neat pectin powder, PEO$_{2000}$ powder, and the electrospun pectin-based fibers from the different solutions.

Table 3.5. Main thermal parameters of the neat pectin powder, PEO$_{2000}$ powder, and the electrospun pectin-based fibers from the different solutions in terms of onset temperature of degradation (T$_{onset}$), degradation temperature (T$_{deg}$).

Sample	T$_{onset}$ (^{o}C)	T$_{deg1}$ (^{o}C)	T$_{deg2}$ (^{o}C)	T$_{deg3}$ (^{o}C)	Residual mass (%)
Pectin powder	98.0 ± 5.2	217.4 ± 3.2	240.2 ± 2.1	-	27.4 ± 3.2
PEO$_{2000}$ powder	375.3 ± 2.4	-	-	400.0 ± 2.1	23.7 ± 1.2
Fibers from S3	175.4 ± 2.5	230.5 ± 3.2	-	367.5 ± 3.2	19.2 ± 1.1

Fibers from S5	169.3 ± 3.7	230.3 ± 3.1	297.3 ± 1.1	367.3 ± 2.1	20.2 ± 1.9
Fibers from S6	169.5 ± 2.1	229.8 ± 2.0	297.5 ± 1.2	367.1 ± 2.0	21.2 ± 2.0
Fibers from S7	170.3 ± 4.1	227.5 ± 2.1	297.4 ± 1.1	367.3 ± 3.2	23.4 ± 1.5
Fibers from S8	165.5 ± 5.2	226.4 ± 2.2	-	366.4 ± 2.6	21.2 ± 1.3
Fibers from S9	168.2 ± 4.4	226.2 ± 2.1	-	367.4 ± 3.1	20.0 ± 1.6
Fibers from S10	173.6 ± 5.0	227.2 ± 3.0	-	369.5 ± 2.0	17.3 ± 1.2

Alternatively, it can be observed that PEO_{2000} was highly thermally stable, showing values of onset degradation temperature (T_{onset}) and maximum degradation temperature (T_{deg}) of approximately 375 ^{o}C and 400 ^{o}C, respectively. One can also observe that the incorporation of PEO_{2000} successfully delayed the thermal degradation of pectin up to nearly 175 ^{o}C. The pectin-based fiber obtained from the electrospinning of S3, S5, and S6 showed a similar thermal degradation profile than the neat pectin powder but with even lower values of T_{deg}. This result suggests that, even though PEO_{2000} delays the onset of degradation of pectin, it also catalyzes its thermal degradation. Interestingly, the presence of both plasticizers contributed to increasing the thermal degradation of the PEO_{2000}-containing pectin fibers.

The pectin-based fibers obtained from the electrospinning of S5–S10, which included glycerol or PEG_{900}, showed a similar thermal degradation profile in comparison with the PEO_{2000}-containing pectin fibers but with slightly lower values of T_{onset}. Additionally, the new weight loss obtained nearly 290 ^{o}C can be attributed to glycerol degradation. One can then consider that the plasticizers played a significant role in the pectin chains motion that favored chain scission during thermal degradation. Similar results were found for chia mucilage-glycerol films in the study performed by Dick et al.[142], showing that the glycerol addition lowered the heat resistance of the carbohydrate. Moreover, lower residual

masses were observed for the plasticizer-containing fibers compared with the non-plasticized fibers. This effect was particularly intense for the electrospun pectin fibers obtained from S10, that is, the solution containing 3 wt. percent PEG_{900}, which showed a residual mass of 17 wt. percent.

3.2.3. Film-Forming Process of Electrospun Pectin-Based Fibers

A thermal post-treatment, also called annealing was applied to the electrospun pectin mats due to eliminating or minimizing the porosity and then to obtain homogenous and continuous films. Based on the DSC results shown above, pure pectin is fully amorphous. Therefore, a heat treatment in a wide range of temperatures, that is, 50-220 ºC, was applied for different processing times, that is, from 5 s to 60 s, to find out the best conditions. In order to investigate film formation, the cryo-fracture morphology of the mats afterward post-treatment at varying parameters was analyzed. Figure 3.14 shows the visual aspect of the different electrospun films obtained after annealing where Figure 3.15 includes the SEM micrographs of their surface fracture. However, it was observed that, at any of these conditions, the annealing failed to provide films from the fibers obtained from non-plasticized pectin solution, that is, from S3. Moreover, because of the low degradation temperature of pectin, the color of films became darker when they were subjected to temperatures above 160 ºC.

As seen in Figures 3.14a and 3.14b, by increasing the temperature or time, not only the color of the pectin materials developed a dark color but also the fiber mats lost their integrity. Therefore, based on these results, one can consider that the non-plasticized pectin-based fibers were too rigid to gain flexibility by the only application of heat. Therefore, pressure was also applied during annealing to promote fibers rearrangement and the removal of porosity. In Figure 3.14c it can be observed that some transparent regions on the pectin-based materials were successfully attained when the mats were subjected to temperatures above 165 ºC with an applied pressure of 12-24 kN for 1 min. Nevertheless, the resultant materials also exhibited an intense brownish color, partially lost their integrity and also became too brittle to be applied as packaging materials. This morphological change was further confirmed by comparison of the SEM images of the cross-sections of the electrospun pectin-based mats from S3 prior to annealing, shown in Figure 3.15a, and

post-processed at 220 ^{o}C for 20 s, shown in Figure 3.15b. Nevertheless, interestingly, it can be observed that a compact packing reorientation of the nanofibrous structures was observed by a process of fibers coalescence. The continuous film could be obtained as a result of this process. However, some voids were also formed that could result from the evaporation of gases during thermal decomposition.
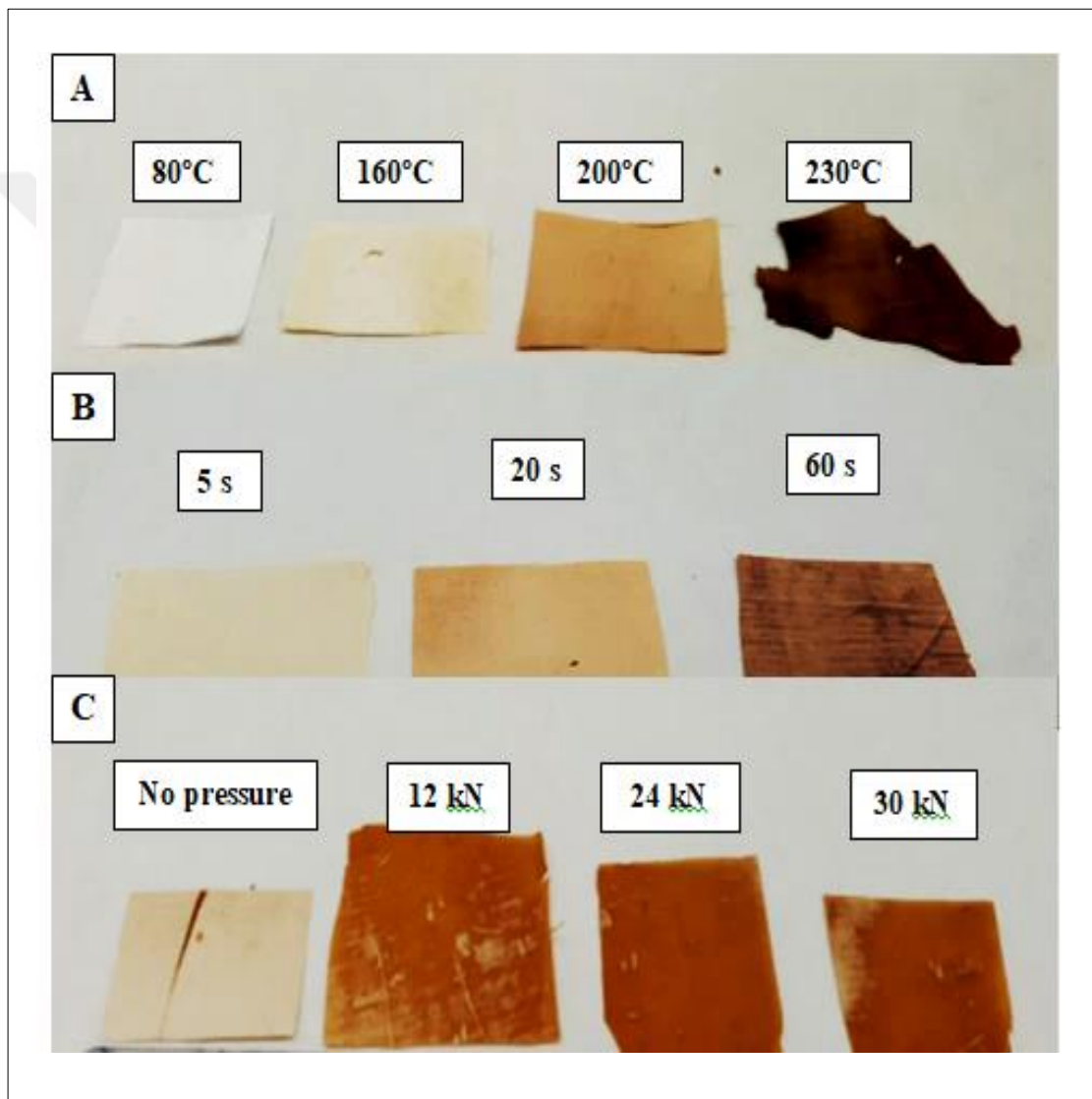

Figure 3.14. The effect of post-treatment (a) temperature, (b) time, (c) pressure on the pectin-based materials obtained from S3. (a) Different temperatures were applied for 1 min without pressure. (b) Different times were applied at 190 ˚C without pressure. (c) Different pressures were applied at 175 ˚C for 60 s.
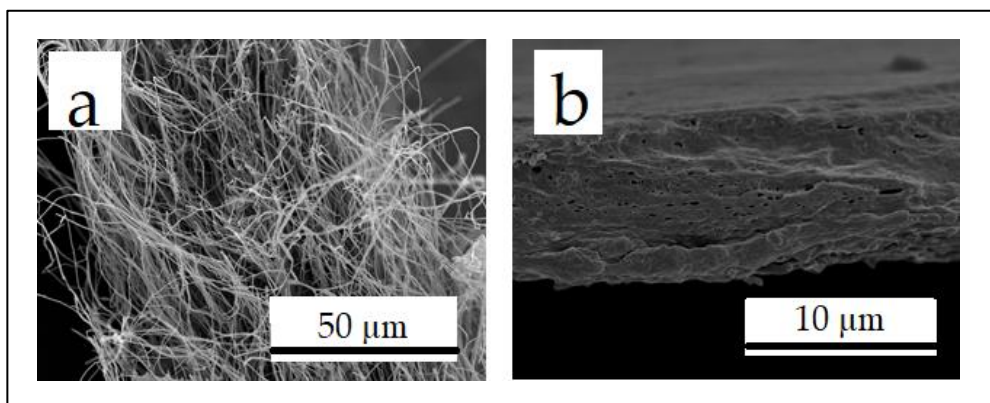
Figure 3.15. Scanning electron microscopy (SEM) images of the fracture surface of the electrospun pectin-based fibers from S3: (a) Without any post-treatment and (b) Treatment at 220 $^{\circ}$C temperature for 20 s with a pressure 24 kN.

Based on the results shown above, the effect on the film-forming process of the two plasticizers, that is, glycerol and PEG$_{900}$, was analyzed. The SEM images of the pectin films obtained from the fibers produced with the solutions containing the plasticizers are gathered in Figure 3.8. The electrospinning of the PEO$_{2000}$-containing pectin solutions with 20-30 wt. percent glycerol, that is, S5, S6, and S7, resulted in electrospun mats that, after annealing at 150 $^{\circ}$C, produced softer and more flexible films. A similar improvement was attained for the electrospun PEO$_{2000}$-containing pectin mats with 20-30 wt. percent PEG$_{900}$, those are S8, S9, and S10, after annealing at 155 $^{\circ}$C, though the films were less homogenous. As mentioned earlier, the role of plasticizers in pectin is based on increasing the chain mobility and free volume by creating H-bond interactions between the polymer chains[90]. The use of plasticizers thus opens up the processing of the electrospun mats by annealing. However, temperatures around 160 $^{\circ}$C were still needed, which is very close to T$_{deg}$ previously measured for pectin and responsible for darkening the film sample. Also, for all the formulations, the annealed materials still comprised some porosity, as one can observe in the SEM images gathered in the left column of Table 3.6.

To increase the homogeneity of the resultant pectin materials, the pectin-based nanofibers were washed with dichloromethane prior to annealing. As seen in the SEM images shown in the middle column of Table 3.6, the washed fibers partially coalesced, which could potentially enable to reduce the energy requirement for annealing. Dichloromethane is a

solvent that does not dissolve pectin, but it dissolves glycerol whereas PEG_{900} and PEO_{2000} are slightly soluble.

When pectin fiber mats containing glycerol were immersed in dichloromethane, they did not lose their integrity but, due to the removal of glycerol, fibers partially coalesced. Thereafter, annealing of the washed fibers was successful when applied at 150 ^{o}C and 140 ^{o}C for the fibers obtained from the solutions containing glycerol (S5, S6, and S7) and PEG_{900} (S8, S9, and S10), respectively. As it can be observed in the right SEM images of Table 3.6, the most homogenous film structures were obtained for the pectin fibers mats with 25 wt. percent and 30 wt. percent glycerol and 5 wt. percent PEO_{2000} were annealed. These results can also be seen in the optical images of the film samples gathered in Figure 3.16. Due to the low porosity and completely homogenous film structure, the pectin-based film obtained from S7, that is the pectin formulation with 30 wt. percent glycerol and 5 wt. percent PEO_{2000}, was selected as the most appropriate candidate for multilayer films.
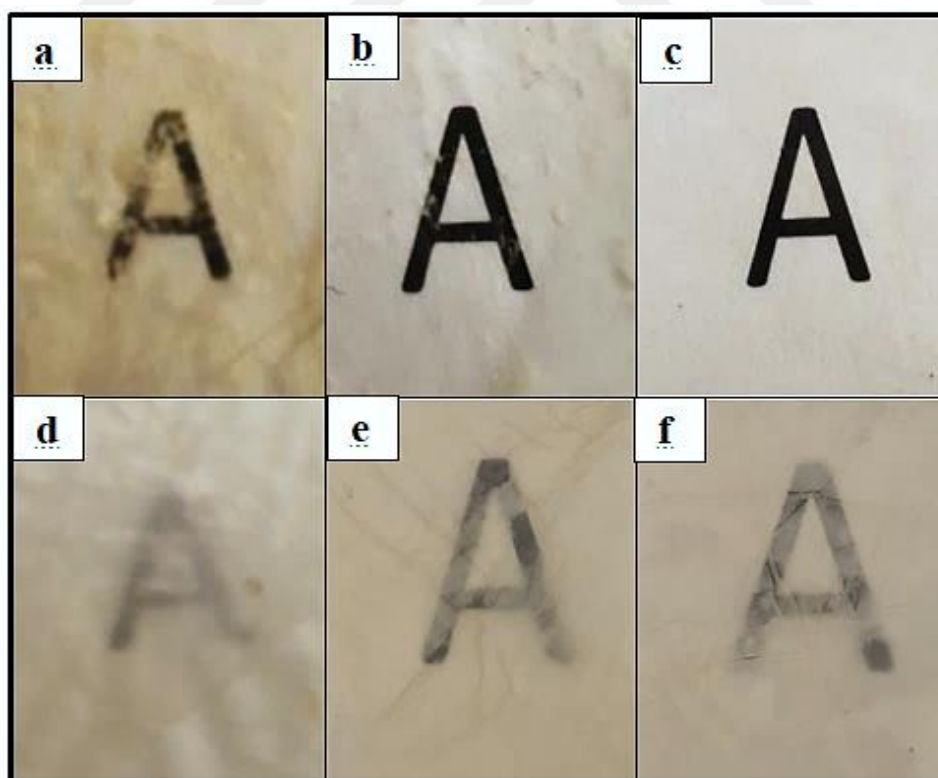
Figure 3.16. Optical images of films obtained from the washed fibers of (a) S5, (b) S6, (c) S7, (d) S8, (e) S9, (f) S10.

Table 3.16. Scanning electron microscopy (SEM) images of the electrospun mats before washing, after washing and after annealing.

Annealed non-washed fibers	Washed fibers	Washed and annealed fibers
S5		
S6		
S7		
S8		
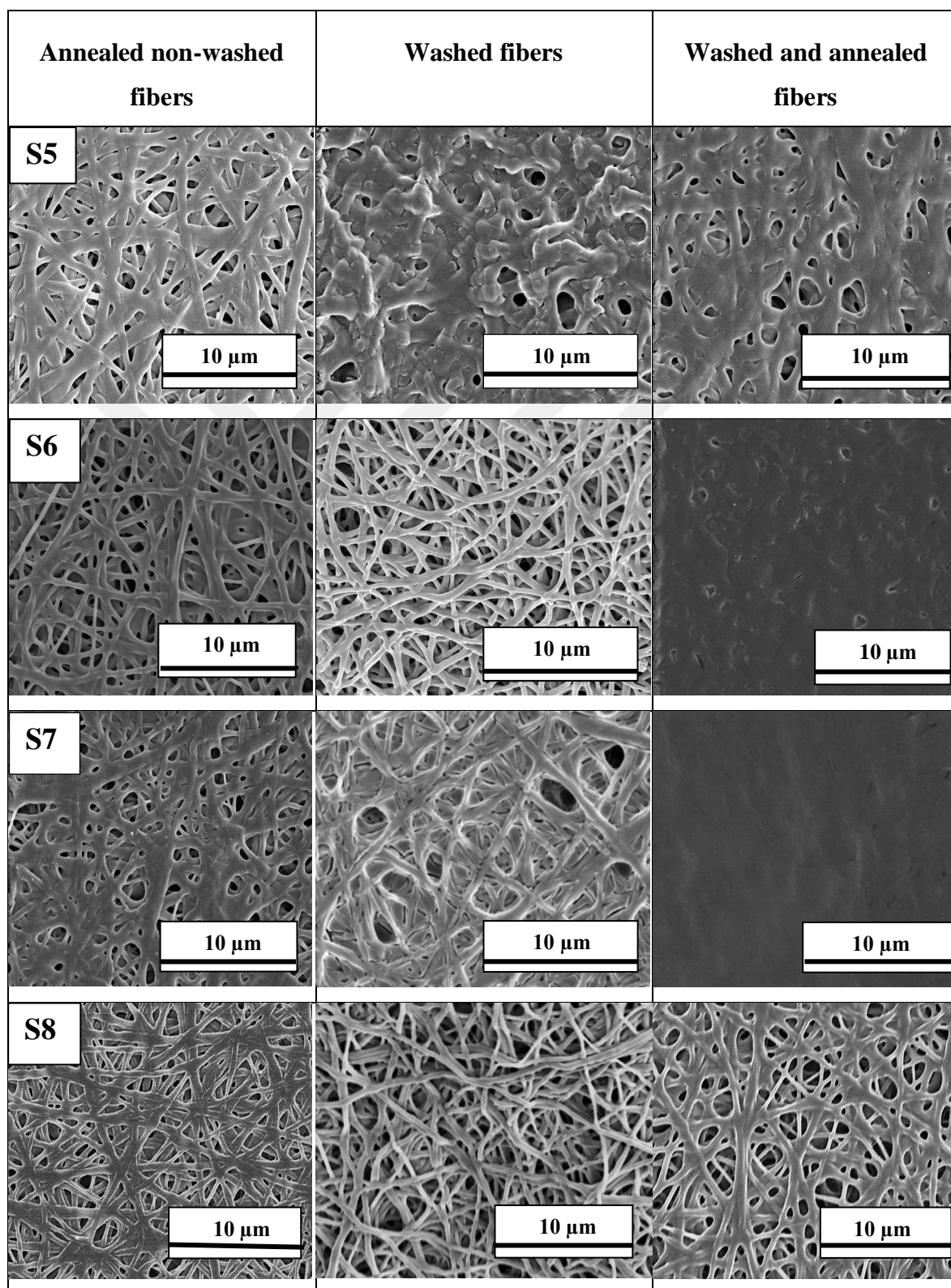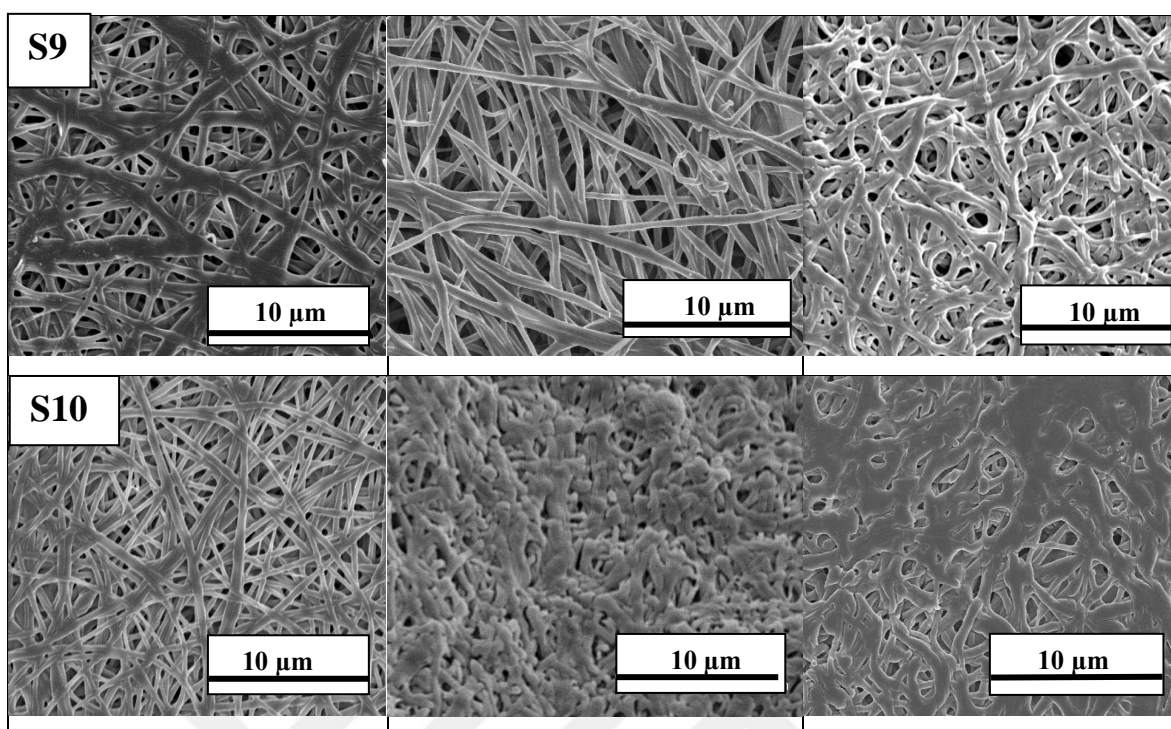
3.2.4. Chemical Characterization of Pectin Based Electrospun Films

FTIR was carried out on the selected film to ascertain the effect of PEO_{2000} and glycerol on pectin and the thermal post-treatment. The FTIR spectra of pure components, that is, the pectin powder, glycerol, and PEO_{2000}, were also collected. Figure 3.17 gathers the spectra of these components and of the pectin-based fibers and film. One of the characteristic peaks of pectin was seen at 1741 cm^{-1}, which refers to the C≡H stretching of carboxyl groups (COOH). Also, the two characteristic bands at 1672 cm^{-1} (amide I) and 1595 cm^{-1} (amide II) relate to the presence of amide groups[81, 43]. The peaks centered at 1132 cm^{-1} and 1070 cm^{-1} may be ascribed to the contribution of the C—C and C—O bonds in secondary alcohol groups of —CH—OH. For glycerol, five characteristic bands at the wavenumbers in the 1150-850 cm^{-1} range arise from the vibrations of C—C and C—O linkages.[144] The FTIR spectrum of PEO_{2000} exhibited CH_2 scissoring at 1465 cm^{-1}, CH_2 wagging at 1357 cm^{-1} and 1340 cm^{-1}, CH_2 bending at 1280 cm^{-1} and 1240 cm^{-1}, C—O—C stretching at 1093 cm^{-1} and 1145 cm^{-1}, and CH_2 rocking at 962 cm^{-1} and 847 cm^{-1}[145].

The shift in the wavenumber values related to the —CH bending from 1423 cm^{-1}, for the pectin powder, to 1411 cm^{-1}, for the pectin fibers and film, could be contributed to

decrease in the interaction between pectin molecules, can be defines as the plasticizing feature of glycerol. No differences were seen in the FTIR spectrum of the pectin-based material from fibers to film after the annealing, which proves the absence of chemical reactions and degradation during the thermal post-treatment.
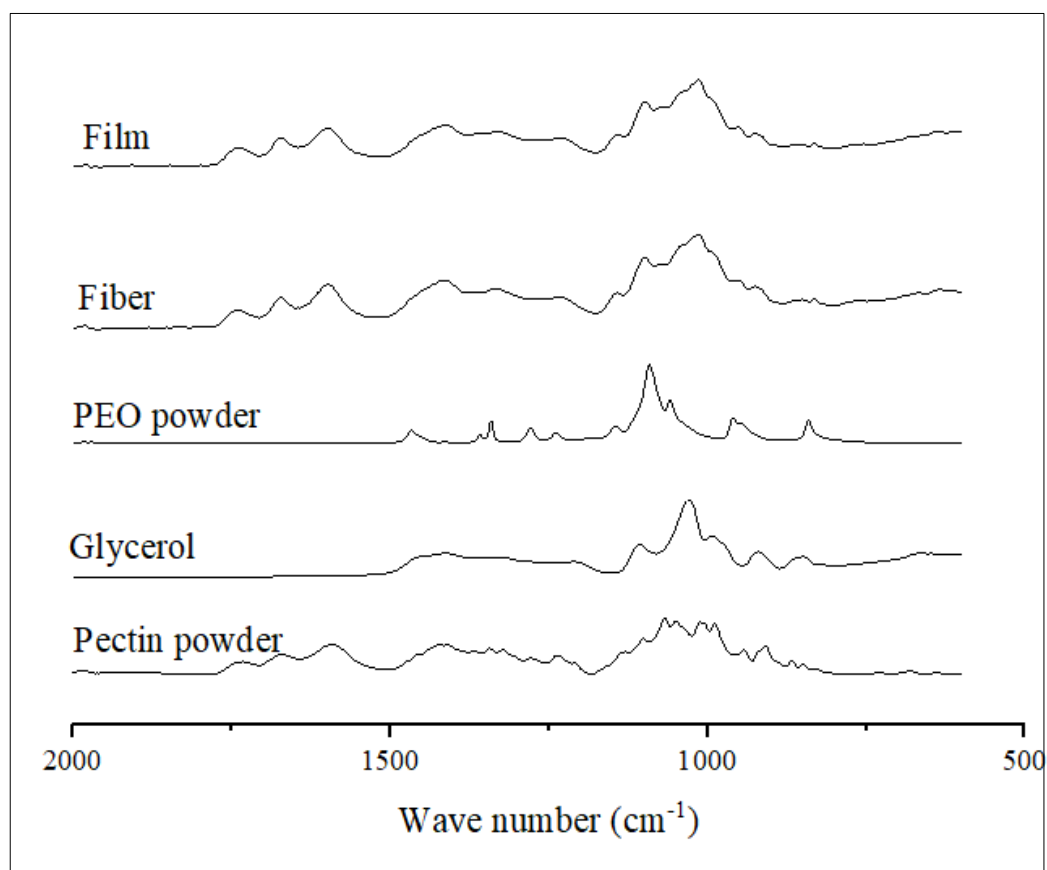
Figure 3.17. Fourier transform infrared spectroscopy (FTIR) spectra, from bottom to top, of pectin powder, glycerol, and polyethylene oxide 2000 (PEO_{2000}), and electrospun fibers and film obtained from S7.

3.2.5. Multilayer Electrospun Films

3.2.5.1. Application of Pectin-Based Electrospun Film in Multilayers

The electrospun pectin film was integrated as an inner layer into two electrospun PHBV films prepared as described by Cherpinski et al.[112]. The objective of this multilayer was to apply the here-prepared pectin film as a barrier layer that was protected from humidity by two external electrospun layers of PHBV, a bio-based and biodegradable hydrophobic polyester. The whole multilayer structure was formed by electrospinning and annealing in order to achieve a high adhesion between the layers. A cast film of pectin was also applied in the same conditions for comparison purposes. The cross-sectional SEM images of obtained multilayer structures are displayed in Figure 3.18. As seems in 3.18a that the bilayer control of PHBV/PHBV formed a continuous structure in which both layers could not be discerned. In relation to the PHBV/pectin/PHBV multilayers, it can be seen that the structure obtained from the electrospun-based pectin film, shown in Figure 3.18b, presented higher adhesion between layers. However, the multilayer structure seen in Figure 3.18c based on the cast film of pectin easily delaminated during the preparation and analysis by SEM. Therefore, multilayer assemblies with a high interlayer adhesion can be successfully improved by combining electrospinning and annealing treatments[149].
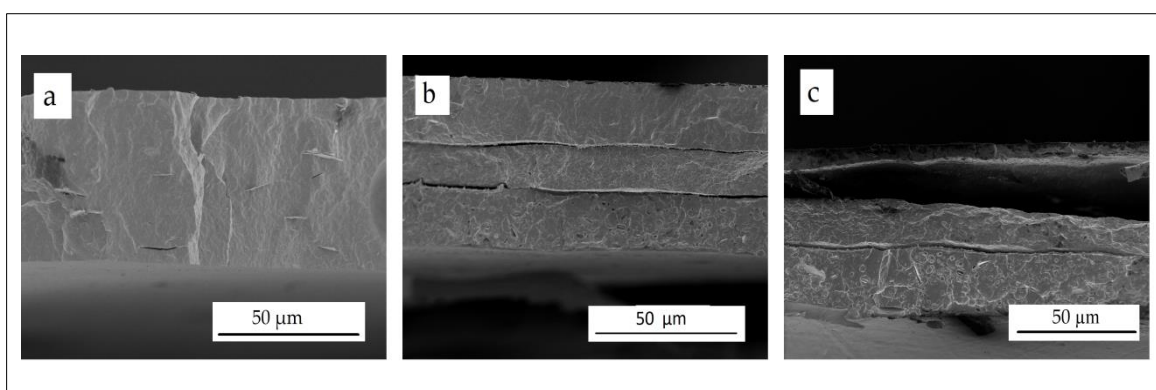
Figure 3.18. Scanning electron microscopy (SEM) images of cross-sections of the multilayer films based on pectin and poly(3-hydroxybutyrate-*co*-3-hydroxyvalerate) (PHBV): (a) PHBV/PHBV; (b) PHBV/electrospun pectin/PHBV; (c) PHBV/solution-casted pectin/PHBV. Scale markers of 50 μm.

3.2.5.2. Barrier Properties of Multilayer Films

Finally, the permeance of the multilayer films to water and limonene was measured. Permeance is the permeability expression with eliminating thickness factor used to ascertain the barrier of multilayer structures under conditions where the inside gas concentration is reached to equilibrium with environment[147]. On account of comparing the permeance values of multilayer films, thicknesses of the inner and outer layers remained in the same range. Table 3.7 shows the water and limonene permeance values and the thickness of each layer and the whole structure. In terms of water vapor, the PHBV/PHBV and PHBV/solution-casted pectin/PHBV multilayer films exhibited higher permeance values, that is, $5.0 \pm 0.83 \times 10^{-10}$ kg.m^{-2}.Pa^{-1}.s^{-1} and $3.94 \pm 0.56 \times 10^{-10}$ kg.m^{-2}.Pa^{-1}.s^{-1}, respectively, than the PHBV/electrospun pectin/PHBV multilayers, that is, $1.75 \pm 0.14 \times 10^{-10}$ kg.m^{-2}.Pa^{-1}.s^{-1}. The value of water permeance is similar but slightly higher to that reported by Cherpinski et al. (2018a) for electrospun PHB films of approximately 26 μm, that is, 2.7×10^{-10} kg.m^{-2}.Pa^{-1}.s^{-1}[148]. Therefore, the incorporation of the electrospun pectin interlayer into PHBV enhanced the barrier properties against water vapor, even though pectin has intrinsically a hydrophilic character. However, the pectin interlayer that was produced by solvent casting did not provided a significant reduction of water vapor permeance in the multilayer. This result can be more likely ascribed to the higher plasticizer content of the solution-casted pectin interlayer since water permeation mostly depends on water solubilization of the polymer matrix of the films. Moreover, since the solution-casted film was obtained from the evaporation of water, some water could remain entrapped, whereas in the electrospun pectin-based films water evaporated effectively during both electrospinning and subsequent annealing. Also, layers delamination can facilitate the permeation of the water molecules through the multilayer structure.

Limonene permeance analysis was also carried out since its validation allows predicting the aroma barrier performance of films. One can observe that the multilayers containing the pectin-based interlayers significantly reduced the limonene permeance, having both the electrospun and solution-casted pectin films the same performance. Limonene permeability, similar to water, is also based on solubility rather than diffusivity. Indeed, solubility of limonene in PHBV is relatively high and 100-μm PHBV films can uptake up to 12.7 wt. percent of limonene[148]. Therefore, it can be considered that the presence of

the pectin interlayer blocked the passage of the aroma molecules due to its low solubility of limonene. The presented multilayers containing the pectin-based interlayers showed a lower permeance than monolayer polylactide (PLA) electrospun film, that is, $2.62 \pm 1.54 \times 10^{-10}$ kg·m^{-2}·Pa^{-1}·s^{-1}, and PET electrospun film, that is, $0.64 \pm 0.11 \times 10^{-10}$ kg·m^{-2}·Pa^{-1}·s^{1} [146].

Table 3.7. Water vapor and limonene permeance of the multilayer films based on pectin and poly(3-hydroxybutyrate-*co*-3-hydroxyvalerate) (PHBV).

Multilayer Structure	Water vapor permeance $\times 10^{10}$ (kg·m^{-2}·Pa^{-1}·s^{-1})	Limonene permeance $\times 10^{10}$ (kg·m^{-2}·Pa^{-1}·s^{-1})	Thickness (µm)		
			PHBV Layers	Pectin Layer	Total
PHBV/PHBV	5.0 ± 0.83	3.81 ± 0.47	72 ± 9	-	72 ± 9
PHBV/electrospun pectin/PHBV	1.75 ± 0.14	0.22 ± 0.11	73 ± 7	25 ± 5	98 ± 8
PHBV/solvent-casted pectin/PHBV	3.94 ± 0.56	0.22 ± 0.08	70 ± 5	24 ± 5	95 ± 5

4. CONCLUSION

Pectin-only solutions resulted with discontinuous droplets instead of continuous jets during electrospinning, while PEO-only solutions formed jets but fibers were mostly beaded. This result suggests that viscosity of the solution is not an indication of jet formation, since PEO solutions formed jets despite of their very low viscosities while pectin solutions could not even at higher viscosities. When pectin was blended with PEO, stable jet formation was achieved. On the other hand, smooth and continuous nanofibers were achieved only when PEO_{2000} was used in the blends. This finding suggests that the molecular weight of the PEO is important to form smooth nanofibers. Since the pH, conductivity, and surface tension of the blends with PEO_{2000} did not differ from other blends at the same pectin concentration, these parameters cannot explain why non-beaded fibers can only be achieved when PEO_{2000} was used. Among the blends, those with PEO_{2000} exhibited the highest zero shear and tip viscosities, which indicated more entanglement favoring jet stability. Moreover, the onset of shear thinning was seen to be early for the blends with PEO_{2000}, which might have enhanced the stability during electrospinning. When viscoelastic properties of fiber forming solutions were compared, we concluded that, G' values should be considered together with the phase angle values to predict the spinnability of pectin blends. In conclusion, high zero shear and tip viscosities, as well as high elastic modulus values are required together with low phase angle values for pectin solutions to be electrospun into non-beaded continuous fibers. In this study, this was achieved by blending pectin with high molecular weight PEO.

Pectin based electrospun films were produced by electrospinning, followed by annealing process. Among different compositions of blend mixtures, the most homogenous and transparent film formation was obtained by selecting the polymer blend solutions of 6.5 percent pectin, 3.0 percent glycerol and 0.5 percent PEO_{2000} based on their weight percentages. Washing fibers with dichloromethane had also a positive effect on the pectin fibers coalescence. The annealing conditions were found optimal at 140 ^{o}C and 12 kN for 1 min. The resultant electrospun pectin-based films were finally incorporated as interlayers between two external layers of electrospun PHBV to produce multilayer structures with high barrier properties. The electrospun pectin interlayer successfully decreased the water

and limonene barrier values of PHBV and it also showed higher barrier performance when compared with an equivalent multilayer based on a solution-casted pectin interlayer. In this context, the produced electrospun pectin-based films can be considered as promising materials to be used for packaging applications to enlarge shelf life of food products.

REFERENCES

1. MacDiarmid AG, Jones WE, Norris ID, Gao J, Johnson AT, Pinto NJ, Hone J, Han B, Ko FK, Okuzaki H, Llaguno M. Electrostatically-generated nanofibers of electronic polymers. *SyntheticMetals*. 2001;119(27):1–3.

2. He JH, Liu Y, Mo LF, Wan YQ, Xu L. *Electrospun nanofibres and their applications*. Shawbury, UK: ISmithers; 2009.

3. Hartgerink J, Beniash E, Stupp S. Self-assembly and mineralization of peptide-amphiphile nanofibers. *Science*. 2001;294(5547):1684–8.

4. Ma P, Zhang R. Synthetic nano-scale fibrous extracellular matrix. *Journal of Biomedical Materials Research: An Official Journal of the Society for Biomaterials, the Japanese Society for Biomaterials, and the Australian Society for Biomaterials*. 1999;46(1):66–72.

5. Ward GF. Meltblown nanofibres for nonwoven filtration applications. *Filtration & Seperation*. 2001;38(9):42–3.

6. Feng L, Li S, Li H, Zhai J, Song Y, Jiang L, Zhu D. Super-hydrophobic surface of aligned polyacrylonitrile nanofibers. *Angewandte Chemie International Edition*. 2002;41(7):1221–1223.

7. Zhang S. Fabrication of novel biomaterials through molecular self-assembly. *Nature Biotechnolgy*. 2003;21(10):1171-1174.

8. Moore EM, Papavassiliou DV, Shambaugh RL. Air velocity, air temperature, fiber vibration and fiber diameter measurements on a practical melt blowing die. *International Nonwovens Journal*. 2018;13(3):13-16.

9. Frenot A, Chronakis IS. Polymer nanofibers assembled by electrospinning. *Current Opinion in Colloid and Interface Science*. 2003;8(1):64–75.

10. Ramakrishna S, Fujihara K, Teo WE, Yong T, Ma Z, Ramaseshan R. Electrospun nanofibers: solving global issues. *Materials Today*. 2006;9(3):40–50.

11. Zhang Y, Chwee TL, Ramakrishna S, Huang ZM. Recent development of polymer nanofibers for biomedical and biotechnological applications. *Journal of Material Science: Materials in Medicine.* 2005;16(10):933–946.

12. Zeleny J. The electrical discharge from liquid points, and a hydrostatic method of measuring the electric intensity at their surfaces. *Physical Review.* 1914;3(2):69-73.

13. Burger C, Hsiao BS, Chu B. Nanofibrous materials and their applications. *Annual Review of Materials Research.* 2006;36(1):333–368.

14. Formhals A. US Patent No. 1,975. 1934. p. 504.

15. Formhals A. U.S. Patent No. 2,077. 1937. p. 373.

16. Formhals A. U.S. Patent No. 2,187. 1940. p. 306.

17. Kriegel C, Arrechi A, Kit K, Mcclements DJ. Fabrication, functionalization, and application of electrospun biopolymer nanofibers and application of electrospun biopolymer nanofibers. *Critical Reviews in Food Science and Nutrition.* 2015;48(8):8398-8402.

18. Bhardwaj N, Kundu SC. Electrospinning: A fascinating fiber fabrication technique. *Biotechnology Advances.* 2010;28(3):325–347.

19. Zhan N, Li Y, Zhang C, Song Y, Wang H, Sun L, Hong X. A novel multinozzle electrospinning process for preparing superhydrophobic PS films with controllable bead-on-string/microfiber morphology. *Jounal of Colloid and Interface Science.* 2010;345(2):491–495.

20. Kim J, Noh J, Jo S, Park KE, Park WH, Lee TS. Simple technique for spatially separated nanofibers/nanobeads by multinozzle electrospinning toward white-light emission. *ACS Applied Material Interfaces.* 2013;5(13):6038–6044.

21. Ramakrishnan R, Gimbun J, Samsuri F, Narayanamurthy V. Needleless electrospinning technology – An entrepreneurial perspective. *Indian Journal of Science and Technology.* 2016;9(15):1-11.

22. Zhang JF, Yang DZ, Xu F, Zhang ZP, Yin RX, Nie J. Electrospun core-shell structure nanofibers from homogeneous solution of poly(ethylene oxide)/chitosan.

Macromolecules. 2009;42(14):5278–5284.

23. Zhang Y, Huang Z, Xu X, Lim CT, Ramakrishna S. Preparation of core-shell structured PCL-r-gelatin bicomponent nanofibers by coaxial electrospinning. *Chemistry of Materials.* 2004;12(22):3406–3409.

24. Li J, Feng H, He J, Li C, Mao X, Xie D, Ao N, Chu B. Coaxial electrospun zein nanofibrous membrane for sustained release. *Journal of Biomaterials Science, Polymer Edition.* 2013;24(17):1923–1934.

25. Sun Z, Zussman E, Yarin AL, Wendorff JH, Greiner A. Compound core–shell polymer nanofibers by co-electrospinning. *Advanced Materials.* 2003;15(22):1929–1932.

26. Ghorani B, Tucker N. Fundamentals of electrospinning as a novel delivery vehicle for bioactive compounds in food nanotechnology. *Food Hydrocolloids.* 2015;51:227–240.

27. Taylor G. Electrically driven jets. *Proceedings of the Royal Society of London. A. Mathematical and Physical Sciences.* 1969;313(1515):453–475.

28. Reneker DH, Yarin AL. Electrospinning jets and polymer nanofibers. *Polymer.* 2008;49(10):2387–2425.

29. Huang ZM, Zhang YZ, Kotaki M, Ramakrishna S. A review on polymer nanofibers by electrospinning and their applications in nanocomposites. *Composites Science and Technolgy.* 2003;63(15):2223–2253.

30. Deitzel JM, Kleinmeyer J, Harris D, Beck Tan NC. The effect of processing variables on the morphology of electrospun nanofibers and textiles. *Polymer.* 2001;42(1):261–272.

31. Rošic R, Pelipenko J, Kocbek P, Baumgartner S, Bešter-Rogač M, Kristl J. The role of rheology of polymer solutions in predicting nanofiber formation by electrospinning. *European Polymer Journal.* 2012;48(8):1374–1384.

32. Shenoy SL, Bates WD, Frisch HL, Wnek GE. Role of chain entanglements on fiber formation during electrospinning of polymer solutions: Good solvent, non-specific

polymer-polymer interaction limit. *Polymer.* 2005;46(10):3372–3384.

33. McKee MG, Wilkes GL, Colby RH, Long TE. Correlations of solution rheology with electrospun fiber formation of linear and branched polyesters. *Macromolecules.* 2004;37(5):1760–1767.

34. McKee MG, Hunley MT, Layman JM, Long TE. Solution rheological behavior and electrospinning of cationic polyelectrolytes. *Macromolecules.* 2006;39(2):575–583.

35. Bonino CA, Krebs MD, Saquing CD, Jeong SI, Shearer KL, Alsberg E,Khan SA. Electrospinning alginate-based nanofibers: From blends to crosslinked low molecular weight alginate-only systems. *Carbohydrate Polymers.* 2011;85(1):111–119.

36. Aydogdu A, Sumnu G, Sahin S. A novel electrospun hydroxypropyl methylcellulose/polyethylene oxide blend nanofibers: Morphology and physicochemical properties. *Carbohydrate Polymers.* 2018;181:234–246.

37. He JH, Mo LF, Wan YK, Xu L. *Electrospun nanofibers and their applications.* Shopshire, UK: Smithers; 2008.

38. Alehosseini A, Ghorani B, Sarabi-Jamab M, Tucker N. Principles of electrospraying: A new approach in protection of bioactive compounds in foods. *Critical Reviews in Food Science and Nutrition.* 2018;58(14):2346–2363.

39. Torres-Giner S, Martinez-Abad A, Ocio MJ, Lagaron JM. Stabilization of a nutraceutical omega-3 fatty acid by encapsulation in ultrathin electrosprayed zein prolamine. *Journal of Food Science.* 2010;75(6):69-76.

40. Sreekumar S, Lemke P, Moerschbacher BM, Torres-Giner S, Lagaron JM. Preparation and optimization of submicron chitosan capsules by water-based electrospraying for food and bioactive packaging applications. *Food Additive and Contaminants: Part A.* 2017;34(10):1795–1806.

41. Likhtman AE, Ponmurugan M. Microscopic definition of polymer entanglements. *Macromolecules.* 2014;47(4):1470–1481.

42. Wool RP. Polymer entanglements. *Macromolecules.* 1993;26(7):1564–1569.

43. Munir MM, Suryamas AB, Iskandar F, Okuyama K. Scaling law on particle-to-fiber formation during electrospinning. *Polymer.* 2009;50(20):4935–4943.

44. Yu JH, Fridrikh SV, Rutledge GC. The role of elasticity in the formation of electrospun fibers. *Polymer.* 2006;47(13):4789–4797.

45. Yu JH, Fridrikh SV, Rutledge GC. The role of elasticity in the formation of electrospun fibers. *Polymer.* 2006;47(13):4789–4797.

46. Regev O, Vandebril S, Zussman E, Clasen C. The role of interfacial viscoelasticity in the stabilization of an electrospun jet. *Polymer.* 2010;51(12):2611–2620.

47. Pelipenko J, Kristl J, Rošic R, Baumgartner S, Kocbek P. Interfacial rheology: An overview of measuring techniques and its role in dispersions and electrospinning. *Acta Pharm.* 2012;62(2):123–140.

48. Hohman MM, Shin M, Rutledge G, Brenner MP. Electrospinning and electrically forced jets. I. Stability theory. *Physical Fluids.* 2001;13(8):2201–2220.

49. Perez-Masia R, Lagaron JM, Lopez-Rubio A. Surfactant-aided electrospraying of low molecular weight carbohydrate polymers from aqueous solutions. *Carbohydrate Polymers.* 2014;101(1):249–255.

50. Hayati I, Bailey AI, Tadros TF. Investigations into the mechanisms of electrohydrodynamic spraying of liquids: I. Effect of electric field and the environment on pendant drops and factors affecting the formation of stable jets and atomization. *Journal of Colloid and Interface Science.* 1987;117(1):205–221.

51. Stijnman AC, Bodnar I, Hans Tromp R. Electrospinning of food-grade polysaccharides. *Food Hydrocolloids.* 2011;25(5):1393–1398.

52. Zhang C, Yuan X, Wu L, Han Y, Sheng J. Study on morphology of electrospun poly(vinyl alcohol) mats. *European Polymer Journal.* 2005;41(3):423–432.

53. Sill TJ, von Recum HA. Electrospinning: Applications in drug delivery and tissue engineering. *Biomaterials.* 2008;29(13):1989–2006.

54. Zhao S, Wu X, Wang L, Huang Y. Electrospinning of ethyl–cyanoethyl cellulose/tetrahydrofuran solutions. *Journal of Applied Polymer Science.*

2004;91(1):242–246.

55.   Ki CS, Baek DH, Gang KD, Lee KH, Um IC, Park YH. Characterization of gelatin nanofiber prepared from gelatin-formic acid solution. *Polymer.* 2005;46(14):5094-5100.

56.   Megelski S, Stephens JS, Chase DB, Rabolt JF. Micro-and nanostructured surface morphology on electrospun polymer fibers. *Macromolecules.* 2002;35(22):8456–8466.

57.   Zong X, Kim K, Fang D, Ran S, Hsiao BS, Chu B. Structure and process relationship of electrospun bioabsorbable nanofiber membranes. *Polymer.* 2002;43(12):4403–4412.

58.   Wannatong L, Sirivat A, Supaphol P. Effects of solvents on electrospun polymeric fibers: preliminary study on polystyrene. *Polymer International.* 2004;53(11):1851–1859.

59.   Yuan X, Zhang Y, Dong C, Sheng J. Morphology of ultrafine polysulfone fibers prepared by electrospinning. *Polymer International.* 2004;53(11):1704–1710.

60.   Kim KH, Jeong L, Park HN, Shin SY, Park WH, Lee SC, Ku Y. Biological efficacy of silk fibroin nanofiber membranes for guided bone regeneration. *Journal of Biotechnology.* 2005;120(3):327–339.

61.   Pelipenko J, Kristl J, Janković B, Baumgartner S, Kocbek P. The impact of relative humidity during electrospinning on the morphology and mechanical properties of nanofibers. *International Journal of Pharmaceutics.* 2013;456(1):125–134.

62.   Saquing CD, Tang C, Monian B, Bonino CA, Manasco JL, Alsberg E, Khan SA. Alginate-polyethylene oxide blend nanofibers and the role of the carrier polymer in electrospinning. *Industrial & Engineering Chemistry Research.* 2013;52(26):8692–8704.

63.   Ghani M, Rezaei B, Ghare Aghaji A, Arami M. Novel cross-linked superfine alginate-based nanofibers: Fabrication, characterization, and their use in the adsorption of cationic and anionic dyes. *Advanced in Polymer Technolgy.* 2016;35(4):428–438.

64. Bhattarai N, Li Z, Edmondson D, Zhang M. Alginate-based nanofibrous scaffolds: Structural, mechanical, and biological properties. *Advanced Materials.* 2006;18(11):1463–1467.

65. Torres-Giner S, Ocio MJ, Lagaron JM. Development of active antimicrobial fiber based chitosan polysaccharide nanostructures using electrospinning. *Engineering in Life Sciences.* 2008;8(3):303–314.

66. Rieger KA, Birch NP, Schiffman JD. Electrospinning chitosan/poly(ethylene oxide) solutions with essential oils: Correlating solution rheology to nanofiber formation. *Carbohydrate Polymers.* 2016;139:131–138.

67. Klossner RR, Queen HA, Coughlin AJ, Krause WE. Correlation of Chitosan's rheological properties and its ability to electrospin. *Biomacromolecules.* 2008;9(10):2947–2953.

68. Schiffman JD, Schauer CL. A review: Electrospinning of biopolymer nanofibers and their applications. *Polymer Reviews.* 2008;48(2):317–352.

69. Wu X, Wang L, Yu H, Huang Y. Effect of solvent on morphology of electrospinning ethyl cellulose fibers. *Journal of Applied Polymer Science.* 2005;97(3):1292–1297.

70. Rezaei A, Nasirpour A, Fathi M. Application of cellulosic nanofibers in food science using electrospinning and its potential risk. *Comprehensive Reviews in Food Science and Food Safety.* 2015;14(3):269–284.

71. Ohkawa K. Nanofibers of cellulose and its derivatives fabricated using direct electrospinning. *Molecules.* 2015;20(5):9139–9154.

72. Kong L, Ziegler GR. Role of molecular entanglements in starch fiber formation by electrospinning. *Biomacromolecules.* 2012;13(8):2247–2253.

73. Okutan N, Terzi P, Altay F. Affecting parameters on electrospinning process and characterization of electrospun gelatin nanofibers. *Food Hydrocolloids.* 2014;39:19–26.

74. Lin L, Zhu Y, Cui H. Electrospun thyme essential oil/gelatin nanofibers for active

packaging against *Campylobacter jejuni* in chicken. *LWT.* 2018;97:711–718.

75. Zhang X, Tang K, Zheng X. Electrospinning and rheological behavior of poly (vinyl alcohol)/collagen blended solutions. *Journal of Wuhan University Technology-Mater. Sci. Ed.* 2015;30(4):840–846.

76. da Silva FT, da Cunha KF, Fonseca LM, Antunes MD, El Halal SLM, Fiorentini ÂM, da Rosa Zavareze E, Guerra Dias AR. Action of ginger essential oil (Zingiber officinale) encapsulated in proteins ultrafine fibers on the antimicrobial control in situ. *International Journal of Biological Macromolecules.* 2018;118:107–115.

77. Jin HJ, Fridrikh SV, Rutledge GC, Kaplan DL. Electrospinning Bombyx mori silk with poly(ethylene oxide). *Biomacromolecules.* 2002;3(6):1233–1239.

78. Rockwell PL, Kiechel MA, Atchison JS, Toth LJ, Schauer CL. Various-sourced pectin and polyethylene oxide electrospun fibers. *Carbohydrate Polymers.* 2014;107(1):110–118.

79. Cui S, Yao B, Sun X, Hu J, Zhou Y, Liu Y. Reducing the content of carrier polymer in pectin nanofibers by electrospinning at low loading followed with selective washing. *Materials Science and Engineering: C.* 2016;59:885–893.

80. Li R, Tomasula P, de Sousa AMM, Liu SC, Tunick M, Liu K, Liu L. Electrospinning pullulan fibers from salt solutions. *Polymers.* 2017;9(1):1–13.

81. Mishra RK, Anis A, Mondal S, Dutt M, Banthia AK. Reparation and Characterization of Amidated Pectin Based Polymer Electrolyte Membranes. *Chinese Journal of Polymer Science.* 2009;27(05):639-643.

82. Brejnholt SM. Pectin. *Food Stabilizers, thickeners and gelling agents.* 2010: 237–263.

83. Fraeye I, Duvetter T, Doungla E, Van Loey A, Hendrickx M. Fine-tuning the properties of pectin-calcium gels by control of pectin fine structure, gel composition and environmental conditions. *Trends in Food Science and Technology.* 2010;21(5):219–228.

84. Albuquerque P, Coelho LC, Teixeira JA, Carneiro-da-Cunha MG. Approaches in

biotechnological applications of natural polymers. *AIMS Molecular Science.* 2016;3(3):386–425.

85. Sriamornsak P. Chemistry of pectin and its pharmaceutical uses: A review. *Silpakorn University International Journal.* 2003;3(1):206–228.

86. Bernhardt DC, Pérez CD, Fissore EN, De'Nobili MD, Rojas AM. Pectin-based composite film: Effect of corn husk fiber concentration on their properties. *Carbohydrate Polymers.* 2017;164:13–22.

87. Yu WX, Wang ZW, Hu CY, Wang L. Properties of low methoxyl pectin-carboxymethyl cellulose based on montmorillonite nanocomposite films. *International Journal of Food Science & Technology.* 2014;49(12):2592–2601.

88. Da Silva MA, Bierhalz ACK, Kieckbusch TG. Alginate and pectin composite films crosslinked with Ca^{2+} ions: Effect of the plasticizer concentration. *Carbohydrate Polymers.* 2009;77(4):736–742.

89. Jantrawut P, Chaiwarit T, Jantanasakulwong K, Brachais CH, Chambin O. Effect of plasticizer type on tensile property and in vitro indomethacin release of thin films based on low-methoxyl pectin. *Polymers.* 2017;9(7):289-295.

90. Vieira MGA, Da Silva MA, Dos Santos LO, Beppu MM. Natural-based plasticizers and biopolymer films: A review. *European Polymer Journal.* 2011;47(3):254–263.

91. Pavlath AE, Voisin A, Robertson GH. Pectin-based biodegradable water insoluble films. *Macromolecular Symposia.* 1998;39(1):692-695.

92. Penhasi A, Meidan VM. Preparation and characterization of in situ ionic cross-linked pectin films: Unique biodegradable polymers. *Carbohydrate Polymers.* 2014;102(1):254–260.

93. Lorevice MV, Otoni CG, de Moura MR, Mattoso LHC. Chitosan nanoparticles on the improvement of thermal, barrier, and mechanical properties of high- and low-methyl pectin films. *Food Hydrocolloids.* 2016;52:732–740.

94. Martelli MR, Barros TT, de Moura MR, Mattoso LH, Assis OB. Effect of chitosan nanoparticles and pectin content on mechanical properties and water vapor

permeability of banana puree films. *Journal of Food Sciences.* 2013;78(1):98–104.

95. Chaichi M, Hashemi M, Badii F, Mohammadi A. Preparation and characterization of a novel bionanocomposite edible film based on pectin and crystalline nanocellulose. *Carbohydrate Polymers.* 2017;157:167–175.

96. Šešlija S, Nešić A, Škorić ML, Krušić MK, Santagata G, Malinconico M. Pectin/carboxymethylcellulose films as a potential food packaging material. *Macromolecular Symposium.* 2018;378(1):160–163.

97. Chaiwarit T, Ruksiriwanich W, Jantanasakulwong K, Jantrawut P. Use of orange oil loaded pectin films as antibacterial material for food packaging. *Polymers.* 2018;10(10):1144-1150.

98. Sasaki RS, Mattoso LH, De Moura MR. New edible bionanocomposite prepared by pectin and clove essential oil nanoemulsions. *Journal of Nanoscience and Nanotechnology.* 2016;16(6):6540–6544.

99. Shankar S, Tanomrod N, Rawdkuen S, Rhim JW. Preparation of pectin/silver nanoparticles composite films with UV-light barrier and properties. *International Journal of Biological Macromolecules.* 2016;92:842–849.

100. Espitia PJP, Du WX, Avena-Bustillos R de J, Soares N de FF, McHugh TH. Edible films from pectin: Physical-mechanical and antimicrobial properties - A review. *Food Hydrocolloids.* 2014;35:287–296.

101. Torres-Giner S, Martinez-Abad A, Lagaron JM. Zein-based ultrathin fibers containing ceramic nanofillers obtained by electrospinning. II. Mechanical properties, gas barrier, and sustained release capacity of biocide thymol in multilayer polylactide films. *Journal of Applied Polymer Science.* 2014;131(18):9270–9276.

102. Furlan R, Rosado JAM, Rodriguez GG, Fachini ER, da Silva ANR, da Silva MLP. Formation and characterization of oriented micro- and nanofibers containing poly (ethylene oxide) and pectin. *Journal of Electrochemical Society.* 2012;159(3):K66–71.

103. Lin HY, Chen HH, Chang SH, Ni TS. Pectin-chitosan-PVA nanofibrous scaffold

made by electrospinning and its potential use as a skin tissue scaffold. *Journal of Biomaterials Science, Polymer Edition.* 2013;24(4):470–484.

104. Chen S, Cui S, Zhang H, Pei X, Hu J, Zhou Y, Liu Y. cross-linked pectin nanofibers with enhanced cell adhesion. *Biomacromolecules.* 2018;19(2):490–498.

105. Alborzi S, Lim LT, Kakuda Y. Encapsulation of folic acid and its stability in sodium alginate-pectin-poly(ethylene oxide) electrospun fibres. *Journal of Microencapsulation.* 2013;30(1):64–71.

106. Akhgari A, Hossein Rotubati M. Preparation and evaluation of electrospun nanofibers containing pectin and time-dependent polymers aimed for colonic drug delivery of celecoxib. *Nanomedicine Journal.* 2016;3(1):43–48.

107. Roy P, Dutta RK. Electrospun PVA-Pectin-Magnetite nanofiber as a novel drug carrier matrix. *International Journal of Applied Engineering Research.* 2014;9(6):629–635.

108. Cui S, Yao B, Gao M, Sun X, Gou D, Hu J, Zhou Y, Liu Y. Effects of pectin structure and crosslinking method on the properties of crosslinked pectin nanofibers. *Carbohydrate Polymers.* 2017;157:766–774.

109. Ye X, Zhan Y, Li T, Shi X, Deng H, Du Y. Pectin based composite nanofabrics incorporated with layered silicate and their cytotoxicity. *International Journal of Biological Macromolecules.* 2016;93:123–130.

110. Patra N, Salerno M, Cernik M. Electrospun polyvinyl alcohol/pectin composite nanofibers. *Electrospun Nanofibers.* 2017:599–608.

111. Echegoyen Y, Fabra MJ, Castro-Mayorga JL, Cherpinski A, Lagaron JM. High throughput electro-hydrodynamic processing in food encapsulation and food packaging applications: Viewpoint. *Trends in Food Science and Technology.* 2017;60:71–79.

112. Cherpinski A, Torres-Giner S, Cabedo L, Lagaron JM. Post-processing optimization of electrospun submicron poly(3-hydroxybutyrate) fibers to obtain continuous films of interest in food packaging applications. *Food Additives and Contaminants - Part A.* 2017;34(10):1817–1830.

113. Melendez-Rodriguez B, Castro-Mayorga JL, Reis MAM, Sammon C, Cabedo L, Torres-Giner S, Lagaron JM. Preparation and characterization of electrospun food biopackaging films of poly(3-hydroxybutyrate-co-3-hydroxyvalerate) derived from fruit pulp biowaste. *Frontiers in Sustainable Food System.* 2018;2(38):1–16.

114. Melendez-Rodriguez B, Figueroa-Lopez KJ, Bernardos A, Martínez-Máñez R, Cabedo L, Torres-Giner S, Lagaron JM. Electrospun antimicrobial films of poly(3-hydroxybutyrate-co-3-hydroxyvalerate) containing eugenol essential oil encapsulated in mesoporous silica nanoparticles. *Nanomaterials.* 2019;9(2):227.

115. Quiles-Carrillo L, Montanes N, Lagaron J, Balart R, Torres-Giner S. Bioactive multilayer polylactide films with controlled release capacity of gallic acid accomplished by incorporating electrospun nanostructured coatings and interlayers. *Applied Sciences.* 2019;9(3):533.

116. Steffe JF. *Rheological methods in food process engineering.* MI: Freeman Press; 1996.

117. Tadros TF. *Rheology of dispersions: principles and applications.* Weinheim: Wiley VCH; 2010.

118. Alborzi S, Lim LT, Kakuda Y. Electrospinning of sodium alginate-pectin ultrafine fibers. *Journal of Food Sciences.* 2010;75(1):100–107.

119. Fleer G, Stuart MC, Scheutjens JM, Cosgrove T, Vincent B. *Polymers at interfaces.* Netherlands:Springer; 1993.

120. Gilányi T, Varga I, Gilányi M, Mészáros R. Adsorption of poly (ethylene oxide) at the air/water interface: A dynamic and static surface tension study. *Journal of Colloid and Interface Science.* 2006;201(2):428–435.

121. Kim MW. Surface activity and property of polyethyleneoxide (PEO) in water. *Colloids Surfaces A: Physicochemical and Engineering Aspects.* 1997;128(1–3):145–154.

122. Karlström G. A new model for upper and lower critical solution temperatures in poly (ethylene oxide) solutions. *The Journal of Physical Chemistry.* 1985;89(23):4962–4964.

123. Bieze TWN. Barnes AC, Huige CJM, Enderby JE, Leyte JC. Distribution of water around poly (ethylene oxide): A neutron diffraction study. *The Journal of Physical Chemistry.* 1994;98(26):6568–6576.

124. Walter RH. *The chemistry and technology of pectin.* London: Academic Press Limited; 1991.

125. Liu SC, Li R, Tomasula PM, Sousa AMM, Liu L. Electrospun food-grade ultrafine fibers from pectin and pullulan blends. *Food and Nutrition Sciences.* 2016;7(07):636–646.

126. Jun Z, Hou H, Schaper A, Wendorff JH, Greiner A. Poly-L-lactide nanofibers by electrospinning - Influence of solution viscosity and electrical conductivity on fiber diameter and fiber morphology. *E-Polymers.* 2003;3(1):1–9.

127. Uyar T, Besenbacher F. Electrospinning of uniform polystyrene fibers: The effect of solvent conductivity. *Polymer.* 2008;49(24):5336–5343.

128. Gupta D, Jassal M, Agrawal AK. Electrospinning of poly(vinyl alcohol)-based boger fluids to understand the role of elasticity on morphology of nanofibers. *Industrial & Engineering Chemistry Research.* 2015;54(5):1547–1554.

129. Nie H, He A, Wu W, Zheng J, Xu S, Li J, Han CC. Effect of poly(ethylene oxide) with different molecular weights on the electrospinnability of sodium alginate. *Polymer.* 2009;50(20):4926–4934.

130. Zhao H, Chi H. Electrospun bead-on-string nanofibers: Useless or something of Value? *Novel aspects of nanofibers.* 2018: 87-102.

131. Reneker DH, Yarin AL, Fong H, Koombhongse S. Bending instability of electrically charged liquid jets of polymer solutions in electrospinning. *Journal of Applied Physics.* 2000;87(9):4531–4547.

132. Subbiah T, Bhat GS, Tock RW, Parameswaran, S., Ramkumar SS. Electrospinning of nanofibers. *Journal of Applied Polymer Science.* 2005;96(2):557–569.

133. Li T, Ding X, Tian L, Hu J, Yang X, Ramakrishna S. The control of beads diameter of bead-on-string electrospun nanofibers and the corresponding release behaviors of

embedded drugs. *Materials Science and Engineering: C.* 2017;74:471–477.

134. Fong H, Chun I, Reneker DH. Beaded fibers formed during electrospinning. *Polymer.* 1999;40(16):4585–4592.

135. Zhang C, Yuan X, Wu L, Han Y, Sheng J. Study on morphology of electrospun poly (vinyl alcohol) mats. *European Polymer Journal.* 2005;41(3):423–432.

136. Ralet MC, Crépeau MJ, Buchholt HC, Thibault JF. Polyelectrolyte behaviour and calcium binding properties of sugar beet pectins differing in their degrees of methylation and acetylation. *Biochemical Engineering Journal.* 2003;16(2):191–201.

137. Torres-Giner S, Wilkanowicz S, Melendez-Rodriguez B, Lagaron JM. Nanoencapsulation of aloe vera in synthetic and naturally occurring polymers by electrohydrodynamic processing of interest in food technology and bioactive packaging. *Journal of Agricultural and Food Chemistry.* 2017;65(22):4439–4448.

138. Cui SS, Sun X, Yao B, Peng XX, Zhang XT, Zhou YF, Hu JL, Liu YC. Size-tunable low molecular weight pectin-based electrospun nanofibers blended with low content of poly(ethylene oxide). *Journal of Nanoscience and Nanotechnology.* 2017;17(1):681–689.

139. Gloyna D, Kunzek H. Thermal solid phase degradation of plant cell wall polysaccharides. *Polish Journal of Food and Nutrition Sciences.* 1998;7(2).

140. Kastner H, Einhorn-Stoll U, Senge B. Structure formation in sugar containing pectin gels - Influence of Ca^{2+} on the gelation of low-methoxylated pectin at acidic pH. *Food Hydrocolloids.* 2012;27(1):42–49.

141. Nisar T, Wang ZC, Yang X, Tian Y, Iqbal M, Guo Y. Characterization of citrus pectin films integrated with clove bud essential oil: Physical, thermal, barrier, antioxidant and antibacterial properties. *International Journal of Biological Macromolecules.* 2018;106:670–680.

142. Dick M, Costa TMH, Gomaa A, Subirade M, de Oliveira Rios A, Flôres SH. Edible film production from chia seed mucilage: Effect of glycerol concentration on its physicochemical and mechanical properties. *Carbohydrate Polymers.*

2015;130:198–205.

143. Villanova JCO, Ayres E, Oréfice RL. Design, characterization and preliminary in vitro evaluation of a mucoadhesive polymer based on modified pectin and acrylic monomers with potential use as a pharmaceutical excipient. *Carbohydrate Polymers.* 2015;121:372–381.

144. Basiak E, Lenart A, Debeaufort F. How glycerol and water contents affect the structural and functional properties of starch-based edible films. *Polymers.* 2018;10(4):412.

145. Gondaliya N, Kanchan DK, Sharma P, Joge P. Structural and conductivity studies of poly(ethylene oxide) – silver triflate polymer electrolyte system. *Materials Sciences and Applications.* 2011;02(11):1639–1643.

146. Fabra MJ, Lopez-Rubio A, Lagaron JM. Nanostructured interlayers of zein to improve the barrier properties of high barrier polyhydroxyalkanoates and other polyesters. *Journal of Food Engineering.* 2014;127:1–9.

147. Donhowe G, Fennema O. Edible films and coatings:Characteristics, formation, definitions, and testing methods. *Edible Coatings and Films to Improve Food Quality.* 1994:1–24.

148. Cherpinski A, Torres-Giner S, Cabedo L, Méndez JA, Lagaron JM. Multilayer structures based on annealed electrospun biopolymer coatings of interest in water and aroma barrier fiber-based food packaging applications. *Journal of Applied Polymer Science.* 2018;135(24):1–11.

149. Einhorn-Stoll U, Kunzek H, Dongowski, G. Thermal analysis of chemically and mechanically modified pectins. *Food Hydrocolloids.* 2007;21(7):1101-1112.

150. Bizarria MTM, d'Ávila MA, Mei LHI. Non-woven nanofiber chitosan/PEO membranes obtained by electrospinning. *Brazilian Journal of Chemical Engineering.* 2014; 31(1):57-68.

151. Gerasimov AV, Ziganshin MA, Gorbatchuk VV, Usmanova LS. Low molecular weight polyethylene glycols as matrix to obtain solid dispersions of sulfanilamide. *International Journal of Pharmaceutical Science.* 2014; 6:372-377.

152. Godeck R, Kunzek H, Kabbert R. Thermal analysis of plant cell wall materials depending on the chemical structure and pre-treatment prior to drying. *European Food Research and Technology*. 2001; 213(4):395-404.

153. Cherpinski A, Torres-Giner S, Vartiainen J, Peresin MS, Lahtinen P, Lagaron JM. Improving the water resistance of nanocellulose-based films with polyhydroxyalkanoates processed by the electrospinning coating technique. *Cellulose*. 2018; 25(2):1291-1307.

154. Figueroa-Lopez KJ, Vicente, AA, Reis, MA, Torres-Giner S, Lagaron JM. (2019). Antimicrobial and antioxidant performance of various essential oils and natural extracts and their incorporation into biowaste derived poly (3-hydroxybutyrate-co-3-hydroxyvalerate) layers made from electrospun ultrathin fibers. *Nanomaterials*. 2019; 9(2):144.

155. Radusin T, Torres-Giner S, Stupar A, Ristic I, Miletic A, Novakovic A, Lagaron JM. Preparation, characterization and antimicrobial properties of electrospun polylactide films containing *Allium ursinum L.* extract. *Food Packaging and Shelf Life.* 2019; 21:357.

156. Sila DN, Smout C, Elliot F, Loey AV, Hendrickx M. Non-enzymatic depolymerization of carrot pectin: toward a better understanding of carrot texture during thermal processing. *Journal of Food Science*. 2006; 71(1):E1-E9.

157. Van Buren, JP. The chemistry of texture in fruits and vegetables. *Journal of Texture Studies*. 1979; 10(1):1-23.

158. Einhorn-Stoll U, Kastner H, Urbisch A, Kroh LW, Drusch S. Thermal degradation of citrus pectin in low-moisture environment-Influence of acidic and alkaline pre-treatment. *Food Hydrocolloids*. 2019; 86:104-115.

159. Fraeye I, De Roeck A, Duvetter T, Verlent I, Hendrickx M, Van Loey A. Influence of pectin properties and processing conditions on thermal pectin degradation. *Food Chemistry*. 2007; 105(2):555-563.

160. Diaz, JV, Anthon GE, Barrett DM. Nonenzymatic degradation of citrus pectin and pectate during prolonged heating: Effects of pH, temperature, and degree of methyl esterification. *Journal of Agricultural and Food Chemistry.* 2007; 55:5131-5136.

161. Krall SM, McFeeters RF. Pectin hydrolysis: effect of temperature, degree of methylation, pH, and calcium on hydrolysis rates. *Journal of Agricultural and Food Chemistry*. 1998; 46(4):1311-1315.

162. Aburto J, Moran M, Galano A, Torres-García E. Non-isothermal pyrolysis of pectin: a thermochemical and kinetic approach. *Journal of Analytical and Applied Pyrolysis*. 2015; 112:94-104.